The Astbury Centre for
Structural Molecular Biology

UNIVERSITY OF LEEDS

# ANNUAL REPORT 2016

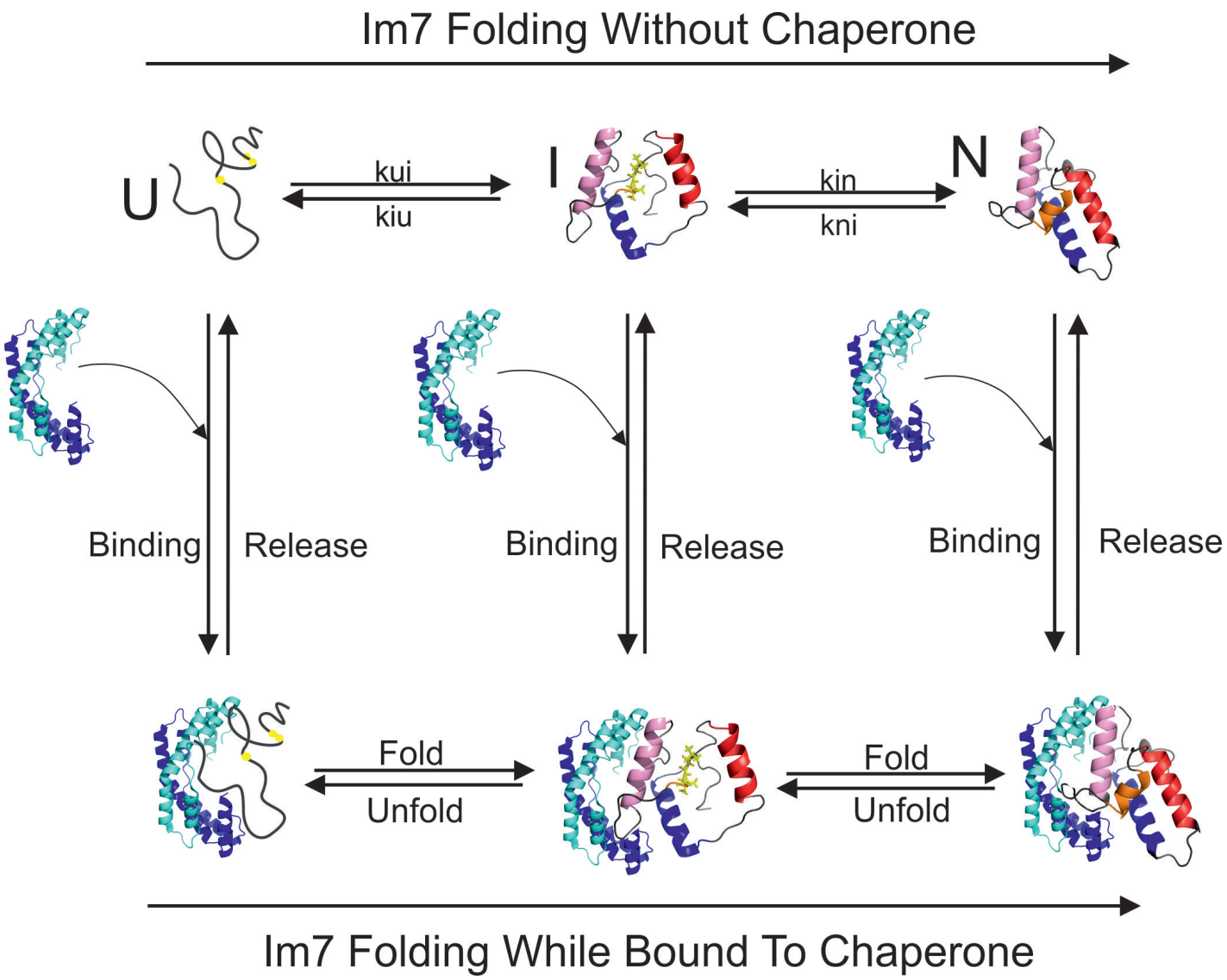

## Front cover illustration

Folding of the protein Im7 in the presence or absence of the small, periplasmic ATP-independent chaperone Spy from *E. coli*. Im7 is shown as a multi-coloured protein that is helical in both the folding intermediate (I) and in the native folded state (N) and lacks any persistent secondary structure in the unfolded state (U). Spy is shown as a blue cradle-shaped homodimer. The kinetic mechanism of Im7 folding in the presence of Spy was investigated as part of a collaboration between the Radford (Leeds) and Bardwell (Michigan) groups and published in *Nat. Struct. Mol. Biol.* in 2016. More details can be found on p58 of this report.

## Acknowledgement

The Astbury Centre for Structural Molecular Biology thanks its many sponsors for support of the work and its members for writing these reports. The report is edited by David Brockwell. This report is also available electronically at **www.astbury.leeds.ac.uk**

## Mission Statement

The Astbury Centre for Structural Molecular Biology will promote interdisciplinary research of the highest standard on the structure and function of biological molecules, biomolecular assemblies and complexes using physico-chemical, molecular biological and computational approaches.

## Introduction

Welcome to the Annual Report of the Astbury Centre for 2016. We have had another very busy and successful year and this letter highlights a few of our many successes. The Astbury Report is a shining example of the buoyancy of our science, the strength of our community and our collaborations that go hand in hand with the contributions our members make to others through engagement in public-facing events. I would like to thank every member of the Centre for their hard work over the year: our Support staff, Technicians, Facility Managers, Students, Post-docs, Fellows and Academic staff. And, of course, Lucy Gray for wonderful organisation and her excellent administrative support. Our success comes from our strong multidisciplinary science, as well as our collegiality and teamwork. Thank you all!

During 2016 the Centre continued in its quest of "Understanding Life in Molecular Detail" through multiple different activities, including seminars, publications, public lectures and other events. We continued to enjoy an excellent seminar series (organised by Joe Cockburn), hosting 10 lectures during the year with speakers from the UK and Europe. A wonderful tenth Annual Astbury Lecture was given by Sir Venki Ramakrishnan, FRS, (MRC Laboratory of Molecular Biology) on the 24th June, entitled "The use of recent advances in electron microscopy to study ribosome structure". This annual event was traditionally followed by (a rainy!) sports day and a much enjoyed barbecue hosted by the Astbury Society (see http://www.astbury.leeds.ac.uk/about/society.php). 139 members attended the Centre's Biennial Away Day, held on September 16th at The Thackray Medical Museum where students, post-docs and PIs shared their recent exciting scientific discoveries, through talks, posters and the ever-popular "Flash Poster" presentations.

A particular highlight of the year was launching the first ever Astbury Conversation that was held on 11th & 12th April 2016. More than 250 eminent researchers from around the world attended the Astbury Conversation – the first international event of its kind at the University dedicated to the subject of structural molecular biology. The two-day event began with an academic research symposium which was followed by a public exhibition showcasing the research and technologies used in the University's Astbury Centre for Structural Molecular Biology. The final highlight was a lecture by Nobel Laureate Professor Michael Levitt, FRS, during which he explained how computer modelling has advanced our knowledge of the molecular processes underpinning life, health and disease and what the future holds for this area of science. You can watch his lecture again on YouTube (https://www.youtube.com/watch?v=wtQY9IfBqPc) and see http://www.astburyconversation.leeds.ac.uk/ for photos of the Conversation event itself. He also talked about how his career developed from a childhood in South Africa, through research in the UK, Israel and the USA, to his Nobel Prize in 2013. The Astbury Conversation will run biennially and plans are now underway for the 2018 Astbury Conversation that will be held on 16th & 17th April 2018 – please add these dates to your diary now and we look forward to seeing you there!

The Centre welcomed Richard Bayliss, Juan Fontana, Elton Zeqiraj, Glyn Hemsworth and Megan Wright to the membership in 2016. As a result of generous funding from Leeds alumnus, Peter Cheney, we welcomed visits from Professors Carol Hall (North Carolina State University, USA), Herbert Waldman (Max Planck, Germany) and Harry Takagi (NIH, USA) and several events/activities were held to provide the opportunity for Fellows and Astbury members to meet and plan collaborations. We have received funding for three more Cheney Fellows in 2017 and look forward to welcoming Kelly Chibale University of Cape Town, (South Africa), Steve Polyak (University of Washington, Seattle, USA) and Preben Morth (University of Oslo, Norway) (see http://www.astbury.leeds.ac.uk/people/fellows.php). We were delighted to welcome many PhD students and postdocs to the Centre this year, bringing our total numbers to >300, including 69 academic staff, 208 PhD students, 93 postdoctoral researchers and 9 Research Fellows.

Astbury Centre members published their research in a wide range of journals in 2016 and a full list can be found at the end of this report. In terms of grant income, Astbury members also enjoyed many successes in 2016. Together with £9.3M of new project and programme grants, this brings the Astbury grant portfolio to a striking £52M share of £85M of grants: an impressive figure that is testament to the hard work and success of our members. Some of the larger awards included a £1.25M EPSRC Established Career Fellowship to Adam Nelson; a £1.5M Cancer Research UK Programme grant to Richard Bayliss and Wellcome Trust investigator award (£1.8M) to Sheena Radford. Lars Jeuken, Michael McPherson and Darren Tomlinson were part of a successful University of Leeds consortium bid ("Accelerating Development of Infection Diagnostics for Patient Management and Reduction of Antibiotic Misuse" (£3.8M) from the MRC-coordinated AMR2 initiative. We are much indebted to the funding agencies that support our science, including BBSRC, EPSRC, MRC, the Wellcome Trust, charities, ERC, EU and Industry. We also acknowledge, with thanks, the support of the University of Leeds; the Faculties of Biological Sciences and Maths and Physical Sciences and the Schools of Chemistry, Molecular and Cellular Biology, Biomedical Sciences and Physics and Astronomy for their support of the Centre and our research.

There was continued success in 2016 for several members of the Astbury Centre in terms of peer recognition. Alison Ashcroft was awarded Life-Membership of the British Mass Spectrometry Society and Andy Wilson was announced as the 2016 recipient of the RSC Norman Heatley Award for the development of methods to interrogate and manipulate protein-protein interactions using biomimetic approaches. Our students and post-docs also were awarded many prizes for their contributions at conferences and meetings that span the globe: Ethan Morgan (Wellcome Trust funded) was awarded third place in the national Young Microbiologist of the Year competition; Emma Pool (Zhou group) won the best poster price for her poster at the RSC Northern Dalton Meeting, Patrick Knight (BBSRC DTP student) won a poster prize at the 2016 BMSS meeting, Sarah Hewitt (Wilson group) was awarded a poster prize at the MSMLG meeting in Bath for her work on ruthenium based protein surface mimetics. Well done all.

The Astbury Society, led by the president Matt Jackson played a spectacular role in Astbury activities in 2016. Events included the famous Christmas quiz night, and a hugely successful fourth May Ball. With continued fund raising through cake bakes and coffee mornings, the Society continues to support the "Leeds Children's Charity" with donations reaching an impressive £2884.15 to date.

I hope that you enjoy reading this Annual Report and its new look. Thank you to David Brockwell and Lucy Gray for editing this report, everyone who contributed to it, and all who participated in the Astbury Centre's activities in 2016. I look forward to continuing our successes in the year ahead.

Sheena E. Radford, FMedSci, FRS

*Director, Astbury Centre for Structural Molecular Biology,*
*Leeds, March 2016*

Please note that this report (as well as those from previous years) is also available as a PDF document which can be downloaded from our website (www.astbury.leeds.ac.uk).

**CONTENTS**

## Contributions indexed by Astbury Centre Principal Investigator

## Efficiency of energy trapping by Light-Harvesting proteins

Peter Adams

### Introduction

We understand much about the fundamentals of photosynthesis from model organisms, such as purple phototrophic bacteria (e.g. *Rhodobacter* species) including the structure, function and organisation of their LH membranes. In natural photosynthetic membranes, an antenna system of light-harvesting (LH) membrane protein complexes absorb photons via embedded pigment cofactors and channel that energy downhill to the Reaction Center (RC) where energy trapping occurs via photochemical charge separation. In *Rhodobacter sphaeroides*, there are two types LH complex: (i) the 'core complex', comprised of Light-Harvesting complex 1 (LH1) encircling the RC and (ii) the peripheral Light-Harvesting complex 2 (LH2). The core complex structure is quite variable between different species and it is still not understood how this relates to the efficiency of energy trapping by the RC. The native dimeric form of core complexes is found in wild-type strains, comprised of two RC subunits surrounded by an S-shaped arrangement of 28 LH1 subunits (Fig. 1, upper, *blue*). Whereas, a monomeric form of core complexes, comprised of only one RC enclosed by a ring-shaped enclosure of 15 LH1 subunits is found in PufX-truncation mutant strains (Fig. 1, lower, *red*).

### Results

We investigated the effect of core complex structure on its energy trapping by investigation of a series of different compositions of photosynthetic membranes using various spectroscopies and analyses. Membranes containing either (i) dimeric or (ii) monomeric core complexes and a matched content of LH2 antenna complexes were extracted. LH protein content was measured by absorption spectroscopy and graphical analysis. Time-resolved fluorescence spectroscopy (Fig. 1, *right*) revealed that samples with monomeric cores have consistently longer the fluorescence lifetime than those of dimeric cores, irrespective of their LH2 content or the state of the RC (active or saturated). A kinetic model of exciton transfer produced good agreement between experimental and calculated fluorescence yield. This correlates with the finding of a higher quantum efficiency for energy trapping in core complex dimers. We propose that the shorter lifetime for dimeric complexes is due to excitation sharing across a larger LH1 antenna with access to two traps (RCs), resulting in increased efficiency of trapping or quenching LH1 excitons.

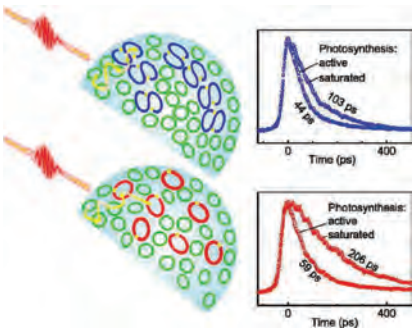


**Figure 1:** *schematic (left):* Energy transfer in photosynthetic vesicles containing either dimeric (blue) or monomeric (red) core complexes and LH2 (green). *Graphs (right)*: Picosecond time-resolved fluorescence spectra from corresponding samples (same colour-coding). Fluorescence lifetime fit is displayed in ps next to the corresponding curve.

### Publications

Chenchiliyan M., Timpmann K., Jalviste E., Adams P.G., Hunter C.N. & Freiberg A. (2016) Dimerization of core complexes as an efficient strategy for energy trapping in *Rhodobacter sphaeroides*. *Biochim. Biophys. Acta-Bioenerg.* **1857**:634-642.

### Funding

This work was funded by the BBSRC.

### Collaborators

*External:* C. Hunter (University of Sheffield), A. Freiberg (University of Tartu, Estonia).

## Biomolecular mass spectrometry and structural proteomics

James Ault, Samuel Bunce, Antonio Calabrese, Owen Cornwell, Paul Devine, Rachel George, Kate Groves, Patrick Knight, Esther Martin, Tom Watkinson, Leon Willis, Lydia Young and Alison Ashcroft

### Introduction

Our research is focussed on the development and application of mass spectrometry (MS) to investigate the structure and function of biomolecules. We use non-covalent electrospray ionisation (ESI)-MS, tandem mass spectrometry (MS/MS) and ion mobility spectrometry (IMS)-MS to determine the mass, conformational properties, stoichiometry, stability, and binding characteristics of biomolecules and their complexes. Specifically, we study protein folding, function and self-aggregation, protein-ligand interactions and biomolecular complex assembly. We also use chemical labelling methods in conjunction with ESI-MS and ESI-MS/MS to map protein folding and aggregation pathways and to characterise non-covalently bound biomolecular complexes (Figure 1).

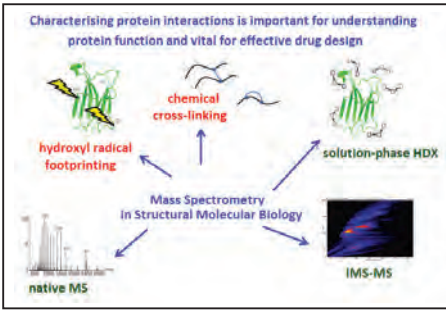


**Figure 1:** chemical labelling methods used with MS for structural proteomics to study protein structure and identify protein:protein and protein:ligand interactions include: hydrogen-deuterium exchange (HDX), hydroxyl radical foot-printing (FPOP) and chemical crosslinking.

### Results

Our major projects are aimed at characterising amyloid protein aggregation and inhibition, for which we have developed a high-throughput screening method to evaluate potential small molecule amyloid inhibitors, determining membrane protein structure and function (Figure 2), and developing new biomolecular MS methodologies.

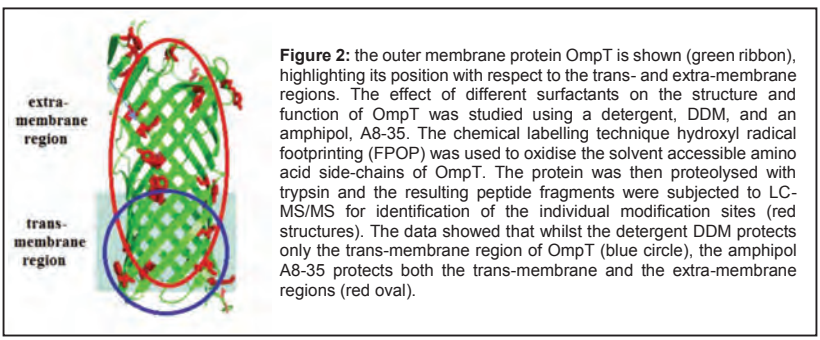


**Figure 2:** the outer membrane protein OmpT is shown (green ribbon), highlighting its position with respect to the trans- and extra-membrane regions. The effect of different surfactants on the structure and function of OmpT was studied using a detergent, DDM, and an amphipol, A8-35. The chemical labelling technique hydroxyl radical footprinting (FPOP) was used to oxidise the solvent accessible amino acid side-chains of OmpT. The protein was then proteolysed with trypsin and the resulting peptide fragments were subjected to LC-MS/MS for identification of the individual modification sites (red structures). The data showed that whilst the detergent DDM protects only the trans-membrane region of OmpT (blue circle), the amphipol A8-35 protects both the trans-membrane and the extra-membrane regions (red oval).

**Publications**

Saunders J.C., Young L.M., Mahood R.A., Jackson M.P., Revill C.H., Foster R.J., Smith D.A., Ashcroft A.E., Brockwell D.J. & Radford S.E. (2016) An *in vivo* platform for identifying inhibitors of protein aggregation. *Nat. Chem. Biol.* **12**:94-101.

Scarff C.A., Ashcroft A.E. & Radford S.E. (2016) Characterization of amyloid oligomers by electrospray ionization-ion mobility spectrometry-mass spectrometry (ESI-IMS-MS). *Methods Mol. Biol.* 1345:115-132.

Young L.M., Saunders J.C., Mahood R.A., Revill C.H., Foster R.J., Ashcroft A.E. & Radford S.E. (2016) ESI-IMS-MS: A method for rapid analysis of protein aggregation and its inhibition by small molecules. *Methods* **95**:62-69.

Schiffrin B., Calabrese A.N., Devine P.W.A., Harris S.A., Ashcroft A.E., Brockwell D.J. & Radford S.E. (2016) Skp is a multivalent chaperone of outer-membrane proteins. *Nat. Struct. Mol. Biol.* **23**:786-793.

Iadanza M.G., Higgins A.J., Schiffrin B., Calabrese A.N., Brockwell D.J., Ashcroft A.E., Radford S.E. & Ranson N.A. (2016) Lateral opening in the intact β-barrel assembly machinery captured by cryo-EM. *Nat. Commun.* **7**:12865.

Dobson C.L., Devine P.W.A., Phillips J.J., Higazi D.R., Lloyd C., Popovic B., Arnold J., Buchanan A., Lewis A., Goodman J.*, et al.* (2016) Engineering the surface properties of a human monoclonal antibody prevents self-association and rapid clearance *in vivo*. *Sci Rep* **6:**38644.

**Funding**

Our research is funded by the BBSRC, the EPSRC, the Wellcome Trust, Waters UK Ltd., LGC, AZ, UCB, & Medimmune. We thank the BMSS for student travel grants.

**Collaborators**

*University of Leeds:* D. Brockwell, R. Foster, S. Harris, P. Henderson, P. Kay, S. Radford, D. Rowlands, P. Stockley, N. Stonehouse, A. Wilson.

*External:* M. Quaglia (LGC, UK), M. Morris & K. Giles (Waters UK Ltd.), S. Macedo-Ribeiro (IBMC, Portugal), D. Raleigh (Stonybrook, NY, USA), J-L. Popot & M. Zoonens (CNRS Paris, France) and E. Duerling (Konstanz, Germany).

## Host-cell interactions of Risk Group 4 viruses

Rebecca Surtees, Amelia Shaw, Jamel Mankouri, Thomas Edwards and John Barr

### Introduction

Identification of interactions between host and virus components is important as it holds the potential to develop novel disease prevention strategies that focus on either host or viral targets. Therapeutic strategies that target host cell components possibly reduce the likelihood of resistance developing due to the relatively slow rate of cellular DNA genetic change compared to the more rapid time frame of virus evolution. This is especially pertinent in the case of RNA viruses such as Crimean-Congo hemorrhagic fever virus (CCHFV), which have high mutation rates due to their error prone RNA polymerases. CCHFV is classified within the *Bunyaviridae* family of tri-segmented negative sense RNA viruses, which comprises five genera namely *Orthobunyavirus*, *Hantavirus*, *Nairovirus*, *Phlebovirus* and *Tospovirus*. The *Nairovirus* genus contains several serogroups, one of which is the Crimean-Congo hemorrhagic fever virus (CCHFV) serogroup with sole members CCHFV and the genetically-distinct Hazara virus (HAZV) that are formally grouped under the same species name of CCHFV. CCHFV is a Risk Group 4 human pathogen, responsible for a devastating disease for which preventative or therapeutic measures do not exist. Transmission of CCHFV to humans is often by the bite of infected ixodid ticks of the *Hyalomma* genus, and the human case-fatality rate can exceed 60%. In recent years, incidence of CCHFV-mediated disease has been newly-reported in many Mediterranean countries, likely as a consequence of the increasingly broad habitat and population size of its tick vector, possibly in response to climate change. CCHFV is now recognized as a potential threat to human health in the densely populated regions of Northern Europe, with recent fatal cases in Northern Spain causing concern. In contrast, HAZV has not been associated with serious human disease, and is classified as a Risk Group 2 pathogen. HAZV is a useful surrogate that can be used to study the molecular, cellular and disease biology of the highly pathogenic CCHFV, as well as other nairoviruses responsible for serious human and animal diseases.

### Results

In order to better understand the interaction between the nairovirus N protein and the host cell, we performed a mass spectrometry-based analysis of its co-precipitating cellular proteins. Independent validation by immunological means with infectious HAZV and CCHFV revealed that cellular chaperones were abundant interactors, particularly those of the HSP70 family and its dnaJ cofactors. We showed these interactions were maintained within both intracellular and extracellular virions, suggesting the interactions were required at multiple stages within the virus life cycle. Ablation of HSP70 activity using characterized small molecule inhibitors

resulted in a 1000-fold reduction of infectious HAZV production, with no evidence of virus escape. This suggests HSP70 family members provide an important role within the nairovirus replication cycle, and that inhibition of HSP70 function maybe an important therapeutic

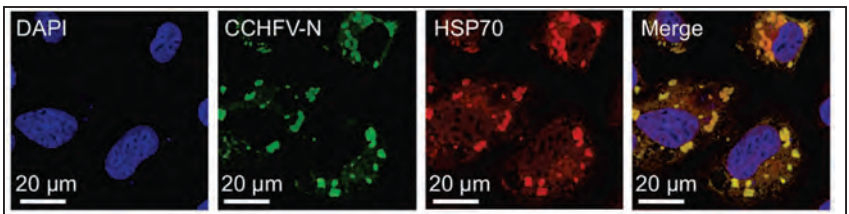


**Figure 1:** indirect confocal immunofluorescence analysis of SW13 cells transiently expressing native CCHFV-N protein. Cells were co-stained using antibodies specific for CCHFV N (green) and anti-HSP70 (red) and DAPI (blue).

strategy for currently untreatable viral diseases. We postulate that negative stranded RNA viruses are highly susceptible to errors in protein folding that may arise due to the high error rate of their polymerase. Such viruses possess RNP complexes built from multiple copies of N protein in association with the RNA genome, as well as an associated polymerase. The nairovirus L segment is over 12,000 nucleotides long, and is likely encapsidated by over 1000 N protein monomers that enwrap the long L segment RNA. It is feasible that the nairoviruses have developed a strategy involving cellular chaperones to protect this significant metabolic investment in the face of frequent polymerase error.

**Publications**

Surtees R., Dowall S.D., Shaw A., Armstrong S., Hewson R., Carroll M.W., Mankouri J., Edwards T.A., Hiscox J.A. & Barr J.N. (2016) Heat shock protein 70 family members interact with Crimean-Congo hemorrhagic fever virus and Hazara virus nucleocapsid proteins and perform a functional role in the nairovirus replication cycle. *J. Virol.* **90**:9305-9316.

**Funding**

This work was funded by a Public Health England/BBSRC CASE studentship.

**Collaborators**

*External:* S. Dowall, R. Hewson, M. Carroll (Public Health England) and S. Armstrong, J. Hiscox (University of Liverpool).

## The many (interacting) faces of Aurora-A kinase

Selena Burgess, Mark Richards and Richard Bayliss

### Introduction

Aurora-A kinase is best known for its role in the regulation of mitosis, specifically through the coordination of protein-protein interactions that govern the timing and robustness of the assembling mitotic spindle. The catalytic activity of Aurora-A is stimulated upon interaction with the microtubule-associated protein TPX2, which promotes kinase autophosphorylation Crystal structures of Aurora-A show how this activation process converts the kinase from an inactive to an active conformation. Indeed, unlike many kinases that are regulated by phosphorylation, formation of a fully-active kinase requires both phosphorylation and binding of a protein partner such as TPX2. This is because the activation loop of Aurora-A is remarkably dynamic, and both phosphorylation and TPX2 binding are required to lock it into a conformation that is compatible with the binding of substrates.

More recently, Aurora-A was found to moonlight as a regulator of Myc oncoproteins, a function that is apparently independent of its kinase activity. Myc proteins are transcription factors that markedly alter gene expression through both activation and repression. The three human Myc proteins, c-Myc, N-Myc and L-Myc, have regions of sequence homology that mediate interactions with critical partner proteins. Myc proteins are turned over rapidly, with a short half-life of ~20 minutes in non-transformed cells. Aurora-A stabilises N-Myc in neuroblastoma and c-Myc in liver cancer, most likely by interfering with the degradation of Myc through the ubiquitin-proteasome pathway.

### Results

Myc proteins are intrinsically disordered and, consequently, there are very few published structural studies on them. We determined the crystal structure of the catalytic domain of Aurora-A bound to N-Myc to 1.7 Å resolution (Figure 1). Residues 61-89 of N-Myc are ordered, forming an extended region of contacts that span across the surface of Aurora-A. Based on the structure, we propose that Aurora-A must alter the way in which N-Myc is recognised by the ubiquitination machinery.

**Figure 1:** crystal structure of the complex between Aurora-A (aa122-403) and N-Myc (aa61-89). N-Myc protein (red) interacts with the region of Aurora-A (teal) that changes conformation between a more dynamic, inactive state and a less dynamic, active state. Here, Aurora-A is in an active conformation, the binding site for N-Myc is disrupted by ligands that stabilize an inactive conformation. Figure is based on PDB entry 5G1X.

The Aurora-A inhibitor alistertib is currently under investigation in clinical trials to treat patients with neuroblastoma. The binding of alisterib promotes the inactive conformation of Aurora-A, which destabilises the interaction with N-Myc. The structure of the Aurora-A/N-Myc complex explains why the interaction is sensitive to Alisertib. Moreover, the structure provides a template for structure-guided design of small molecules that disrupt the interaction. This is an alternative, attractive strategy for the therapeutic targeting of Myc because alisertib is a very potent inhibitor of Aurora-A kinase activity, but is not particularly effective at disrupting the interaction with Myc.

The structural mechanism by which TPX2 activates Aurora-A has been studied for more than ten years. However, we have only recently made progress in using this information in the development of Aurora-A inhibitors. Through phage display screening of a library of single domain antibody (sdAb) scaffolds based on a shark IgNARV, we identified vNAR-D01, a sdAb that inhibits Aurora-A through an allosteric mechanism that is antagonistic to that of TPX2 (Figure 2). The crystal structure of the Aurora-A/vNAR-D01 complex shows that the sdAb stabilises an inactive conformation of Aurora-A in which the Lys-Glu salt-bridge, critical for activity, is broken. We are now exploring the development of allosteric kinase inhibitors based on the mechanism of action of vNAR-D01.

TPX2, like Myc, is an intrinsically disordered protein that becomes structured upon binding to Aurora-A. We generated a synthetic version of TPX2 that incorporated a hydrocarbon-stapled helix. Stapled TPX2 retained the ability to activate Aurora-A, but bound to the kinase with 10-fold enhanced affinity. This strategy could be used to develop peptide inhibitors of the various protein-protein interactions of Aurora-A.

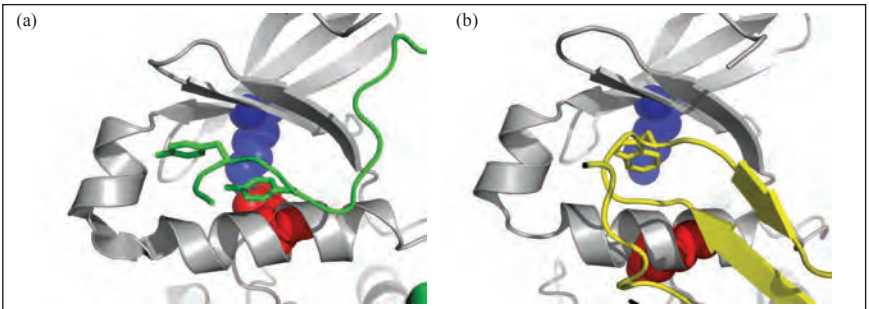


**Figure 2:** Aurora-A can be positively and negatively regulated through interactions at the same pocket. **(a)** Crystal structure of Aurora-A (grey) in complex with TPX2 (green). TPX2 inserts a pair of Tyr side chains into a pocket on the surface of Aurora-A. This stabilises the active conformation, as indicated by the formation of a Lys-Glu salt-bridge (blue-red spheres). **(b)** Crystal structure of Aurora-A in complex with a synthetic sdAb, vNAR-D01 (yellow). The sdAb inserts a Trp side chain into the pocket on the surface of Aurora-A. This stabilises a conformation in which the Lys-Glu salt-bridge is broken.

**Publications**

Richards M.W., Burgess S.G., Poon E., Carstensen A., Eilers M., Chesler L., & Bayliss R. (2016) Structural basis of N-Myc binding by Aurora-A and its destabilization by kinase inhibitors. *Proc. Natl. Acad. Sci. USA.* **113**:13726-13731.

Burgess S.G., Oleksy A., Cavazza T., Richards M.W., Vernos I., Matthews D., Bayliss R. (2016) Allosteric inhibition of Aurora-A kinase by a synthetic vNAR domain. *Open Biol.* **6**: 160089.

Rennie Y.K., McIntyre P.J., Akindele T., Bayliss R., Jamieson A.G. (2016) A TPX2 Proteomimetic Has Enhanced Affinity for Aurora-A Due to Hydrocarbon Stapling of a Helix. *ACS Chem. Biol*. **11**: 3383-3390.

**Funding**

This work was funded by Cancer Research UK, ERC, MRC and MRC-T.

**Collaborators**

*External:* M. Eilers (Würzburg), L. Chesler (ICR, London), I. Vernos (CRG, Barcelona), D. Matthews (MRC-T), A. Jamieson (Glasgow), P. McIntyre (Leicester).

## Bio-inspired model membranes and light-harvesting nanomaterials

Sanobar Khan, Mengqiu Li, Stephen Muench, Lars Jeuken and Paul Beales

### Introduction

Hybrid materials aim to synergistically combine components in ways that compensate for their individual weaknesses while maintaining and combining their advantageous properties. Our aim is to make vesicle compartments with enhanced functionality and stability for *in vitro* formulation and exploitation in biotechnologies. Lipid vesicles, the most native-like reconstitution system, have inherent biocompatibility and biofunctionality yet lack long term stability and versatility in a wide range of environments. Conversely, polymersomes, vesicles that self-assemble from amphiphilic block copolymers, while lacking biocompatibility have vastly superior mechanical toughness and durability. Therefore hybrid vesicles composed of lipids and block copolymers might synergistically combine biocompatibility and durability into a single material (Figure 1). This work develops and characterises hybrid vesicle formulations of the redox-driven proton pump cytochrome $bo_3$ ubiquinol oxidase (cyt $bo_3$) as a model system. Successful enhancement of in vitro membrane protein systems will facilitate their application in wide-ranging applications, including biosensors, pharmaceutical assays, environmental remediation and artificial cells and organelles.

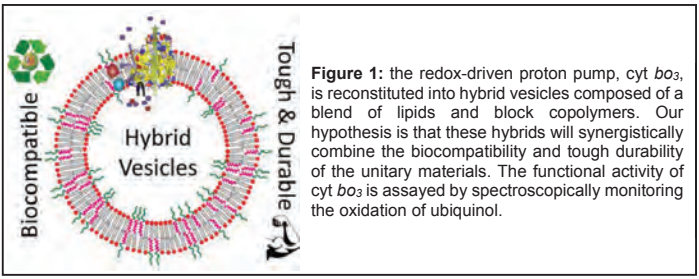


**Figure 1:** the redox-driven proton pump, cyt $bo_3$, is reconstituted into hybrid vesicles composed of a blend of lipids and block copolymers. Our hypothesis is that these hybrids will synergistically combine the biocompatibility and tough durability of the unitary materials. The functional activity of cyt $bo_3$ is assayed by spectroscopically monitoring the oxidation of ubiquinol.

### Results

We developed an *in vitro* reconstitutional protocol for cyt $bo_3$ in hybrid vesicles. The lipid used in this study for POPC and the polymer was a polybutadiene-block-polyethyleneoxide ($PBd_{22}$-*b*-$PEO_{14}$). Initial micellisation of lipids and block copolymers using detergents followed by detergent removal in the presence of the membrane protein proved unsuccessful due to the slow, viscous dynamics of the block copolymers frustrating the micelle to vesicle transition. Success was found in starting from preformed hybrid vesicles that were destabilised with detergemt to facilitate membrane protein insertion before removal of detergent by biobeads. Proteo-hybrid vesicles were created across the full compositional parameter space from 100% lipid to 100% copolymer in 25% degrees of increment. Initial activity assays were conducted on the day the samples were made. Proteo-liposomes showed the greatest initial activity (biofunctionality), while proteo-polymersomes were inactive. Significantly, there was less than 20% decrease in activity between pure lipid systems and 50% copolymer vesicles. However formulations containing >50% copolymer saw a rapid drop in initial activity. The advantage of the hybrid systems became evident when looking at the longer term functional activity of these proteo-vesicles over a period of 6 weeks. The decay rate of the initial activity of these vesicles significantly decreased with increasing polymer content. The best combination of high initial activity and long term functional durability was seen in the 50% copolymer formulations.

However, an important detail in the characterisation of these vesicles was that dynamic light scattering suggested the presence of a population of ~20nm diameter micelles coexisting with the hybrid vesicles in the 50% and 75% copolymer samples. Further investigation by cryo-

TEM revealed that there were in fact worm-like micelles multi-microns in length; the DLS appeared to be probing relaxation times of internal modes in these worm-like micelles that were consistent with the diffusion of 20 nm diameter Brownian spheres.

Hybrid vesicles were purified from these mixed samples by size exclusion chromatography on a Sephadex G-50 column, Analysis of eluted fractions proved the separation of hybrid vesicle fractions and that the functional activity of these samples was contained within these vesicles. Long term activity studies were then repeated on purified 50% and 75% hybrid vesicles (Figure 2). 75% copolymer hybrids had similar functional decay rates before or after purification. However purified 50% copolymer hybrids appear to be more stable than the initial mixture. These purified 50% hybrids have an initial activity drop of ~25% in week one, likely due to a less stable fraction forming in the initial reconstitution; the activity then stabilises with a much slower decay rate with 40% activity retained 6 months after initial reconstitution. This 4-6 month half-life compares with a 1-2 week half-life in the current gold standard of proteo-liposomes. Stored hybrid vesicle samples will allow us to continue to monitor functional activity of these samples over a 12-18 month period.

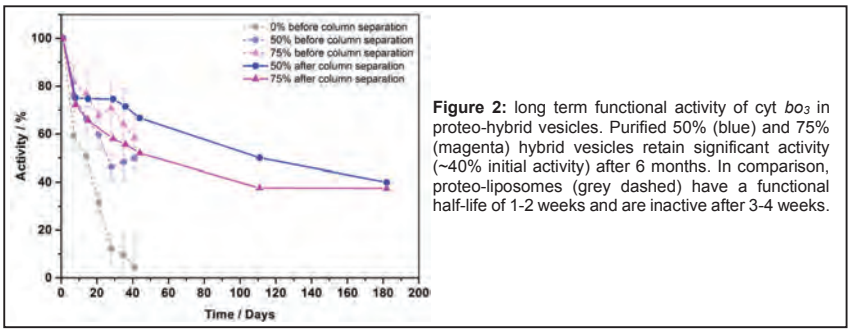


**Figure 2:** long term functional activity of cyt $bo_3$ in proteo-hybrid vesicles. Purified 50% (blue) and 75% (magenta) hybrid vesicles retain significant activity (~40% initial activity) after 6 months. In comparison, proteo-liposomes (grey dashed) have a functional half-life of 1-2 weeks and are inactive after 3-4 weeks.

We have shown that hybrid vesicles can increase the functional half-life of a membrane protein by in excess of an order of magnitude. This highly significant enhancement in membrane protein functional durability has the potential to revolutionise their use in nascent biotechnologies. In particular, applications that were previously not viable due to poor shelf-life or longevity of functional efficacy may now become feasible.

**Publications**

Khan S., Li M.Q., Muench S.P., Jeuken L.J.C. & Beales P.A. (2016) Durable proteo-hybrid vesicles for the extended functional lifetime of membrane proteins in bionanotechnology. *Chem. Commun.* **52**:11020-11023.

**Funding**

This work was funded by the European Union Marie Curie Actions and ERC.

## Protein engineering of aldolases

Claire Windle, Robert Smith, Alex Moloney, Naim Stiti, Adam Nelson and Alan Berry

### Introduction

Aldolases are attractive candidates for use in biocatalysis. They catalyse the aldol reaction and form new carbon-carbon bonds with high specificity, high yields and under mild conditions. We are interested in re-engineering the substrate and stereochemical specificity of these enzymes, using both traditional protein engineering techniques and methods which utilise non-canonical amino acids.

### A threonine aldolase as a tool for stereoselective synthesis

Threonine aldolases have emerged as important tools in the synthesis of β-hydroxy-α-amino acids. These compounds are often found in natural products such as antibiotics and immunosuppressants. Recently, we have developed a high throughput screen to target libraries of *E.coli* threonine aldolase (ItaE) mutants created using CASTing (combinatorial active site saturation testing). This approach has thus far been successful in identifying enzymes with switched specificities and enhanced selectivity for the cleavage reaction of phenylserine (PS); although still in the early stages of screening (Figure 1). A high resolution crystal structure of the wild type enzyme has been solved to help with identification of important active site residues.

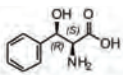


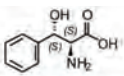


| Enzyme | 2S 3R PS $k_{cat}$ $min^{-1}$ | $K_M$ mM | $k_{cat}/K_M$ $min^{-1}$ mM | 2S 3S PS $k_{cat}$ $min^{-1}$ | $K_M$ mM | $k_{cat}/K_M$ $min^{-1}$ mM | SFR 3* (R/S) (S/R) |
|---|---|---|---|---|---|---|---|
| WT ItaE | 1400 ± 1 | 1.0 ± 0.07 | 1400 | 280 ± 15 | 0.3 ± 0.05 | 930 | 1.5 (R) |
| 3 B10 | 113 ± 8 | 0.31 ± 0.07 | 365 | 92 ± 5 | 0.21 ± 0.04 | 438 | **1.2 (S)** |
| 3 G6 | 113 ± 5 | 0.33 ± 0.04 | 342 | 136 ± 4 | 0.17 ± 0.02 | 800 | **2.34 (S)** |

**Figure 1:** steady-state kinetic parameters of the wild-type and mutant enzymes for the cleavage reaction of 2S3R and 2S3S phenylserine.

### Modifying substrate specificity using non-canonical amino acids

Until recently protein engineering methods were restricted to using the 20 proteogenic amino acids to alter enzyme activities. Our recent work has focused on using non-canonical amino acids (ncAAs) to alter the substrate specificity of the aldolase N-acetylneuraminic acid lyase (NAL). ncAAs are incorporated at a variety of positions throughout the enzyme, using a method which works via a dehydroalanine intermediate and a subsequent addition of a thiol compound to form novel side chains. These ncAA containing enzymes have then been screened for altered activity.

When a 2,3-dihydroxypropyl cysteine was positioned at the residue 190, the activity of the enzyme for the reaction between pyruvate and erythrose increased above that of the wild-type enzyme for this reaction. This increase in activity could not be replicated by using any of the canonical 20 amino acids at this position, and using *in silico* modelling it was discovered that the non-canonical residue forms a unique hydrogen bonding network that would not be possible using canonical residues (Figure 2).

We are expanding these methods to new enzymes, such as trans-O-hydroxybenzylidenepyruvate hydratase-aldolase. We aim to generate highly efficient enzymes that catalyze fundamentally different reactions to the native enzyme and/or which exhibit

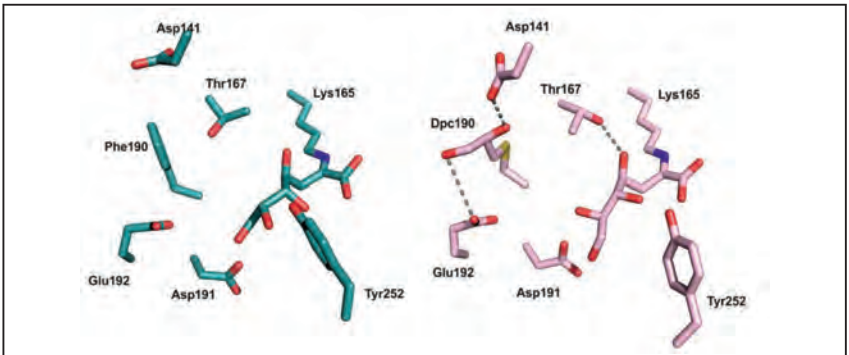


**Figure 2:** left shows the result of in silico modelling for the architecture of the active site with substrate bound. Right shows the results of the same modelling for the ncAA containing enzyme, with the hydrogen bonding network highlighted.

modified substrate specificities. Combinations of such enzymes might be exploited in one-pot, multistep transformations, analogous to metabolic pathways that yield high value fine chemicals which are coveted for their biological activities.

With these computational and biochemical methods at hand, coupled with the enormous variety of side chains and chemistries possible with ncAAs, the way is now open to engineer enzymes with catalytic functions that are not found in Nature.

**Publications**

Howard J.K., Muller M., Berry A. & Nelson A. (2016) An enantio- and diastereoselective chemoenzymatic synthesis of $\alpha$-fluoro $\beta$-hydroxy carboxylic esters. *Angew. Chem.-Int. Edit.* **55**:6766-6769.

**Funding**

Our work is funded by BBSRC, GlaxoSmithKline and Dr Reddy's-Chirotech.

**Collaborators**

*External:* J. Adams (GSK) and M. Bycroft (Dr Reddy's-Chirotech).

## Engineering novel natural products and binding motifs

Ieva Drulyte, Emily Turri, Adam Nelson and Alan Berry

### Introduction

Natural products belong to an extensive family of diverse organic molecules: in excess of 200,000 discovered and extracted from various sources. Of particular interest are the polyketide, non-ribosomal peptide and isoprenoid classes, contributing to the pharmaceutical, cosmetic and biofuel industries. These classes of natural products are synthesised by polyketide synthases, non-ribosomal peptide synthases and terpene synthases, respectively; and our interest lies in understanding the structure-function relationship of these enzymes; facilitating our engineering efforts to synthesise existing and novel natural products.

### Structural studies in indanomycin biosynthesis

Polyketides represent a broad class of natural products which often possess important biological and pharmacological activities. In nature, polyketides are produced by multi-enzyme proteins known as polyketide synthases (PKS). Indanomycin, an antibiotic active against Gram-positive bacteria, is produced by a hybrid nonribosomal peptide synthetase-polyketide synthase (NRPS/PKS) from *Streptomyces antibioticus* NRRL 81673. The aim of this project is to structurally characterise the indanomycin PKS to gain a better understanding of the interfaces between the functional domains, the assembly of the full complex and the chemistry involved in the generation of mature polyketide (Figure 1).

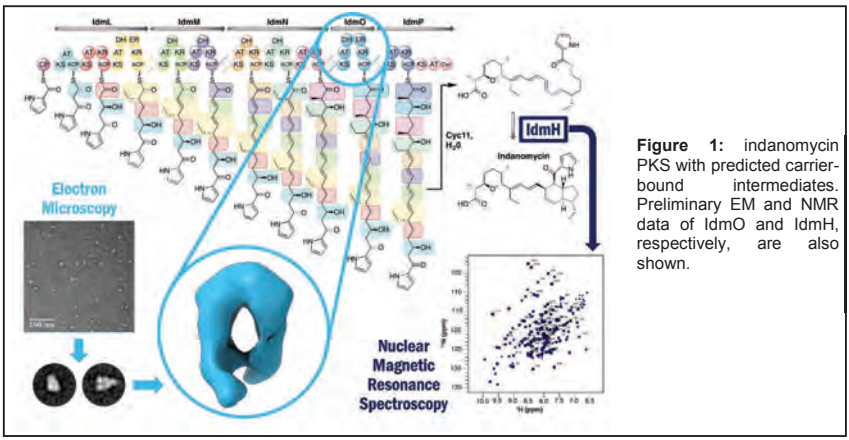


**Figure 1:** indanomycin PKS with predicted carrier-bound intermediates. Preliminary EM and NMR data of IdmO and IdmH, respectively, are also shown.

We have taken an interest in determining the structure of IdmO, the fourth subunit of indanomycin PKS. IdmO has been successfully produced and visualized by negative stain electron microscopy. A low-resolution model of IdmO was produced, which suggested a dimeric architecture. Going forward, a large cryoEM dataset will be collected and processed to produce a high resolution 3D structure of IdmO. We also study IdmH, a putative post-PKS cyclase enzyme thought to catalyze the indane ring formation via a Diels-Alder [4+2] cycloaddition reaction. IdmH was cloned, heterologously expressed and purified. Biochemical analysis suggested IdmH also acts as a dimer. 3D nuclear magnetic resonance spectra were collected which allowed the assignment of approximately 65% of backbone resonances. These data will help to probe binding of IdmH to potential substrates and further characterize this enzyme.

**Engineering bisabolene synthase for novel activities**

Bisabolene is a sesquiterpene found to have properties important for a biofuel in hydrogenated form (bisabolane). Bisabolene synthase produces bisabolene from farnesyl pyrophosphate bisaboyl cation. Initial work has been focused on redesigning the enzyme active site (Figure 2) to produce novel activities and novel terpenes. So far 75 enzyme mutants have been designed and produced using site-directed mutagenesis and screened for novel activities. Screening is carried out using gas chromatography, mass spectrometry and any novel terpenes will be characterised using 2D NMR. The malachite green assay is being adapted from the work of Vardakou to screen the mutants for pyrophosphate cleavage. This assay utilises an inorganic pyrophosphatase, converting pyrophosphate into two inorganic phosphate ions, which consequently form the malachite green complex (Figure 3). Pyrophosphate cleavage is the first step in the reaction mechanism, therefore this assay can be used to test both active and inactive mutants. Testing the inactive mutants can tell us whether the cleavage of pyrophosphate is the inhibited step inactivating the enzyme. From these 75 mutants potential catalytically important residues have been identified along with inactive mutants and mutations increasing the native product profile up to double the wild-type production level.

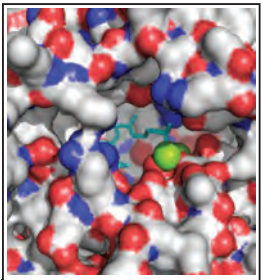

**Figure 2:** crystal structure of the active site of *Abies grandis* bisabolene synthase (3SAE) with farnesyl thio-pyrophosphate (cyan) and catalytically important magnesium ions (green) bound.

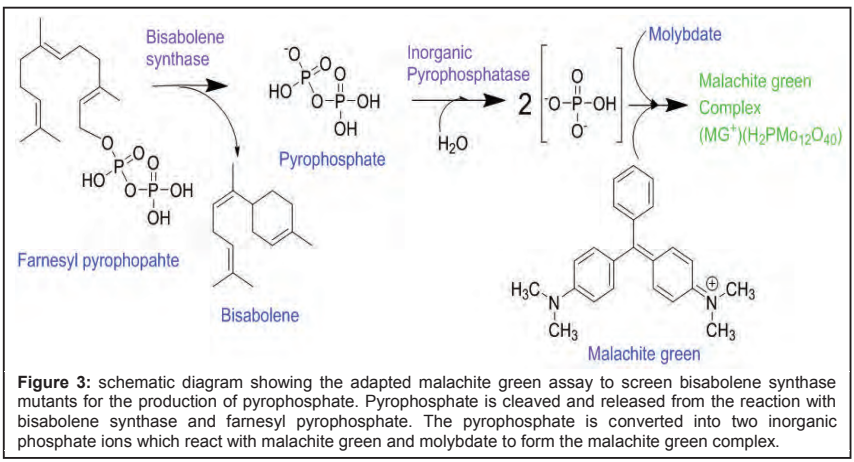


**Figure 3:** schematic diagram showing the adapted malachite green assay to screen bisabolene synthase mutants for the production of pyrophosphate. Pyrophosphate is cleaved and released from the reaction with bisabolene synthase and farnesyl pyrophosphate. The pyrophosphate is converted into two inorganic phosphate ions which react with malachite green and molybdate to form the malachite green complex.

**Funding**

Our work is funded by BBSRC and The Wellcome Trust.

## Economical and scalable synthesis of 6-amino-2-cyanobenzothiazole

Jacob Hauser, Hester Beard, Stuart Warriner and Robin Bon

### Introduction

2-Cyanobenzothiazoles (CBTs) are useful building blocks for both luciferin derivatives for bioluminescent imaging (BLI) and handles for fast (k ~ 10 $M^{-1}s^{-1}$) biorthogonal ligations (Figure 1). A particularly versatile CBT is 6-amino-2-cyanobenzothiazole (ACBT, **9**), which has an amine handle for straight-forward derivatisation. Previously reported routes to ACBT are low-yielding, difficult to scale up, and/or use costly and highly toxic (combinations of) reagents. We developed a safe, economical and scalable synthesis of ACBT.

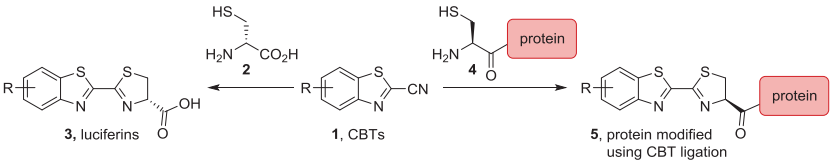


**Figure 1:** functionalised CBTs **1** can be used for the synthesis of luciferins **3** and for bio-orthogonal ligations such as the site-specific labelling/immobilisation of proteins **4**.

### Results

After variation of reagents, catalyst, solvent and reaction temperature, we found that the 2-cyano group of ACBT can be installed under mild conditions through the DABCO-catalysed cyanation of 2-chloro-6-nitro-benzothiazole **7** (Figure 2). Any unreacted cyanide in the reaction mixture was safely quenched by the addition of an $FeCl_3$ solution, and calorimetric analysis showed that the rate and energetic profile of the cyanation reaction could be controlled by the slow addition of a dilute aqueous NaCN solution to the reaction mixture, preventing potential thermal runaway upon scale-up. We also developed an improved procedure for the reduction of 2-cyano-6-nitro-benzothiazole **8** using iron powder. Our route allowed the safe synthesis of ACBT on multi-gram scale and in high purity. In addition, the sole use of filtrations and crystallisations for purification of all intermediates and products, in combination with the endothermic nature of the controlled cyanation procedure, will enable straight-forward further scale up if required.

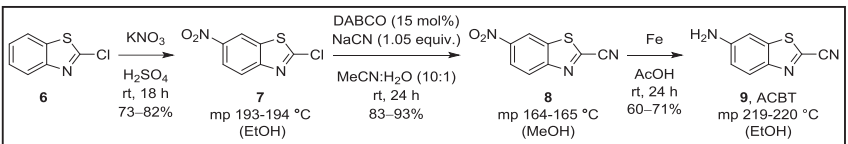


**Figure 2:** optimised procedure for ACBT synthesis.

### Publications

Hauser J.R., Beard H.A., Bayana M.E., Jolley K.E., Warriner S.L. & Bon R.S. (2016) Economical and scalable synthesis of 6-amino-2-cyanobenzothiazole. *Beilstein J. Org. Chem.* **12**:2019-2025.

### Funding

We thank EPSRC for funding (DTA studentship to HAB).

### Collaborators

*University of Leeds*: Mary Bayana and Katherine Jolley (School of Chemistry).

## Structural studies of auto-inhibition and mutational activation in fibroblast growth-factor receptors

Brendan Farrell, Gary Thompson, Arnout Kalverda and Alex Breeze

### Introduction

Fibroblast growth factor receptors (FGFRs) are receptor tyrosine kinases that play key roles in embryogenesis, tissue development and wound healing, but are also key drivers of a number of human cancers. We are using NMR, alongside other structural and biophysical techniques, to understand disease-associated mutational activation of FGFRs at the molecular level, and how this knowledge may be used to develop new-generation drugs against FGFR-mediated cancers.

### Results

Together with our collaborators at UCL (Prof Matilda Katan) and AstraZeneca, we have explored the structural and functional consequences of activating mutations in FGFR3 kinase domain in terms of the effects on drug responses of clinical FGFR kinase inhibitors. We included in this comparison a mutation, R669G, that lies close to, but outside, the activation loop.

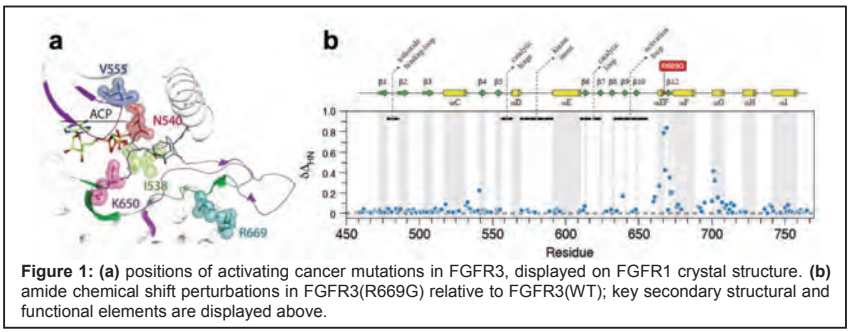


**Figure 1: (a)** positions of activating cancer mutations in FGFR3, displayed on FGFR1 crystal structure. **(b)** amide chemical shift perturbations in FGFR3(R669G) relative to FGFR3(WT); key secondary structural and functional elements are displayed above.

The mechanism whereby R669G activates the kinase has not previously been characterised, and our studies using X-ray crystallography and NMR have established that, like the well-known K650E activation loop mutation, R669G stabilises an active-like conformation of the kinase activation loop, and induces characteristic amide chemical shift perturbations. Furthermore, our NMR-based analysis of the conformational and dynamic effects of the R669G mutation demonstrate that there is 'cross-talk' between the sites of the R669G mutation and that of another 'hot-spot' mutation, N540S, located 30 Å away in the so-called 'molecular brake' region (Figure 1). This demonstrates that spatially distant mutation sites are able to communicate structural and dynamic changes that affect the activation state of the kinase in similar ways via allosteric structural networks.

### Publications

Patani H., Bunney T.D., Thiyagarajan N., Norman R.A., Ogg D., Breed J., Ashford P., Potterton A., Edwards M., Williams S.V., *et al.* (2016) Landscape of activating cancer mutations in FGFR kinases and their differential responses to inhibitors in clinical use. *Oncotarget* **7**:24252-24268.

### Funding

This work was funded by CRUK and AstraZeneca UK.

## Structural biology of the microtubule cytoskeleton

Joe Cockburn

**How cellular cargo molecules recruit molecular motors and regulate their activities**
The cytoplasm is a highly crowded environment containing tens of thousands of different protein species, mRNA molecules, ribosomes, vesicles and organelles. Cellular function is critically dependent on the correct localisation of these components in space and time.

The movement of cellular cargoes over long distances requires dedicated motor proteins (kinesins and cytoplasmic dynein) that use ATP hydrolysis to power movement along a dynamic network of tracks called microtubules. How these motors couple ATP hydrolysis to movement is now fairly well understood, and attention in the field is now turning towards the questions of how cellular cargoes recruit molecular motors and regulate their motility. The combined action of all the kinesin and dynein motors inside your body is very powerful – if all the kinesin motors in your cells were working at full tilt all the time, they would use up somewhere in the region of 8000 kcal of energy per day! Molecular motors must therefore be carefully regulated by their cargoes to ensure that they only consume energy then they are needed.

The main focus of our activity at present is on kinesin-1, which mediates the long-range transport of diverse cellular cargoes (proteins, mRNPs, vesicles, organelles and viruses). We use structural biology, biophysical and cell biology techniques to understand how kinesin-1 switches itself off when not in use, how cargo molecules bind to kinesin, and how this “switches on” kinesin-1.

**Towards a molecular-level understanding of the ciliary transition zone**
Cilia are the antennae of eukaryotic cells, sensing a wide variety of environmental signals (e.g light, molecules, proteins, and fluid flow). The cilium possesses a distinct protein and lipid composition relative to the rest of the cell. This is maintained by the transition zone, a large complex of over 20 proteins at the base of the cilium that controls the exchange of material between the cilium and the rest of the cell. Mutations in transition zone genes result in a range of autosomal recessive inherited disorders, such as nephronophthisis, Joubert Syndrome and Meckel-Gruber syndrome. Around 1% of the population are genetic carriers for these conditions.

Funded by a Wellcome Trust Seed Award, and in collaboration with Prof Colin Johnson at the Faculty of Medicine and Health (University of Leeds), we will use a combination of structural and cell biology approaches to begin to obtain a unified, molecular-level understanding of the function of transition zone proteins, and how mutations in transition zone genes cause diseases. This will aid in the development of gene therapies against these conditions.

**Funding**
Funding from the Wellcome Trust, the Royal Society and startup funding from the University of Leeds is gratefuly acknowledged.

**Collaborators**
*University of Leeds:* C. Johnson, F. Sobot, M. Peckham.

## The physics of life in extreme environments

Kasia Tych, Matthew Batchelor, Toni Hoffmann, Michael Wilson, Megan Hughes, Samuel Lenton, Danielle Walsh, Natasha Rhys, James Towey, Emanuele Paci, David Brockwell and Lorna Dougan

### Introduction

We are developing single molecule manipulation techniques and neutron diffraction to explore the physics of living systems. These powerful techniques are used to study biomolecular self-assembly and the structure and dynamics of molecules in aqueous solutions, in both simple and complex systems. We are particularly interested in the physics of life under extreme environmental conditions including high and low temperatures, high salt concentrations and high and low pH.

### Results

Extremophiles are organisms which survive and thrive in extreme environments. The proteins from extremophilic single-celled organisms are structurally stable and functionally active under extreme physical and chemical conditions. These proteins provide excellent model systems to determine the role of non-covalent interactions in defining protein stability and dynamics as well as being attractive targets for the development of robust biomaterials. Hyperthermophilic proteins have a prevalence of salt bridges, relative to their mesophilic homologues, which are thought to be important for enhanced thermal stability. However, the impact of salt bridges on the mechanical properties of proteins is far from understood. We have used a combination of protein engineering, biophysical characterisation, single molecule force spectroscopy (SMFS) and molecular dynamics (MD) simulations to directly investigate the role of salt bridges in the mechanical stability of two cold shock proteins; *Bs*CSP from the mesophilic organism *Bacillus subtilis* and *Tm*CSP from the hyperthermophilic organism *Thermotoga maritima* (Figure 1). We show that a grafted ionic cluster from a hyperthermophilic protein can increase the mechanical softness of a mesophilic protein. We speculate that mechanical softness could provide a mechanical recovery mechanism and that it may be a design feature applicable to other proteins.

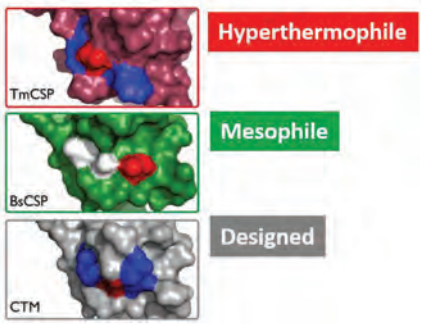


**Figure 1:** SMFS shows that *Tm*CSP is mechanically stronger yet its native state can withstand greater deformation before unfolding compared with *Bs*CSP. MD simulations were used to identify the location and quantify the populations of salt bridges, and revealed that *Tm*CSP contains a larger number of highly occupied salt bridges. We tested the hypothesis that salt bridges endow these mechanical properties by grafting an ionic cluster from *Tm*CSP into *Bs*CSP to design a charged triple mutant (CTM). As expected CTM is thermodynamically more stable and mechanically softer than *Bs*CSP.

As well as proteins, we are interested in understanding the molecular mechanisms by which the solvent environment can stabilise and protect molecules and cells. Cryoprotectant molecules are widely used in basic molecular research through to industrial and biomedical applications. The molecular mechanisms by which cryoprotectants stabilise and protect molecules and cells, along with suppressing the formation of ice, are incompletely understood. To gain greater insight, we completed experiments to determine the structure of cryoprotectant solutions at low temperatures. Our investigations combine neutron diffraction

experiments with isotopic substitution and computational modelling to determine the atomistic level structure of the mixtures. We examine the local structure of the system including the water structure (Figure 2).

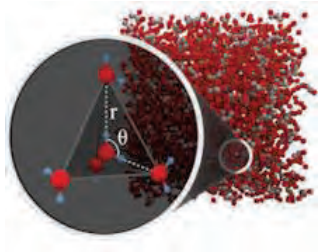


**Figure 2:** we use a combination of neutron diffraction and computational modelling to examine the structure of water in glycerol-water liquid mixtures at low temperatures from 285 to 238 K. We show that the mixtures are nanosegregated into regions of glycerol-rich and water-rich clusters. We examine the water structure and reveal that water forms a low density water structure that is more tetrahedral than the structure at room temperature. We postulate that nanosegregation allows water to forms a low density structure that is protected by an extensive and encapsulating glycerol interface.

**Publications**

Tych K.M., Batchelor M., Hoffmann T., Wilson M.C., Hughes M.L., Paci E., Brockwell D.J. & Dougan L. (2016) Differential effects of hydrophobic core packing residues for thermodynamic and mechanical stability of a hyperthermophilic protein. *Langmuir* **32**:7392-7402.

Lenton S., Walsh D.L., Rhys N.H., Soper A.K. & Dougan L. (2016) Structural evidence for solvent-stabilisation by aspartic acid as a mechanism for halophilic protein stability in high salt concentrations. *Phys. Chem. Chem. Phys.* **18**:18054-18062.

Hughes M.L. & Dougan L. (2016) The physics of pulling polyproteins: A review of single molecule force spectroscopy using the AFM to study protein unfolding. *Rep. Prog. Phys.* **79**:076601.

Towey J.J., Soper A.K. & Dougan L. (2016) Low-density water structure observed in a nanosegregated cryoprotectant solution at low temperatures from 285 to 238 K. *J. Phys. Chem. B* **120**:4439-4448.

Tych K.M., Batchelor M., Hoffmann T., Wilson M.C., Paci E., Brockwell D.J. & Dougan L. (2016) Tuning protein mechanics through an ionic cluster graft from an extremophilic protein. *Soft Matter* **12**:2688-2699.

**Funding**

This work was funded by the European Research Council

**Collaborators**

*External:* A. Soper (ISIS Facility, Rutherford Appleton Laboratories).

## Ferroptosis as a new cell death pathway involved in neurodegeneration

Andrew Tsatsanis, Bruce Wong and James Duce

### Introduction

Iron is required as a cofactor in metabolic processes throughout the body and specifically in tissues of high oxygen consumption, such as the central nervous system. The ability of iron to freely receive and donate electrons is critical for neurotransmitter regulation as well as oxidative phosphorylation, nitric oxide metabolism and oxygen transport. An iron imbalance can lead to metabolic stress on these processes. High levels of unbound iron also detrimentally catalyze the production of toxic reactive oxygen species. Increased cellular susceptibility to oxidative stress associated with iron accumulation leads to neurodegeneration within patients and animal models of dementia related disorders.

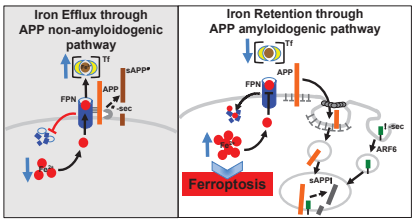


**Figure 1:** schematic of APP processing and iron homeostasis. Non-amyloidogenic processing of APP leading to increased efflux of iron through elevated APP and FPN retention on the cell surface. However amyloidogenic processing of APP through the endocytic pathway leads to intracellular retention through decrease FPN on the cell surface. Inhibition of endocytic internalisation through lipid rafts and β-secretase trafficking to the early endosome has also been found to increase APP and FPN levels on the neuronal surface.

Cellular iron efflux is tightly controlled to maintain iron homeostasis. We discovered a new endogenous regulatory mechanism for AD-implicated amyloid precursor protein (APP) in controlling neuronal iron export. APP facilitates the movement of iron across the plasma membrane by binding to the iron exporter ferroportin (FPN) and promoting its functional retention on the cell surface. APP loss causes iron elevation and iron mediated cell death.

Restoring or replacing neuronal iron export could be a novel mechanism of action for new therapeutics targeting oxidative stress in a range of neurodegenerative diseases. Ferroptosis is a non-apoptotic form of cell death that can be triggered by conditions that inhibit glutathione biosynthesis. This lethal process is defined by the iron-dependent accumulation of lipid reactive oxygen species and a number of small molecule inhibitors of ferroptosis have been identified (e.g. ferrostatin-1) which block pathological cell death in the brain.

### Results

More recent developments in our line of research have resulted in another route for APP-dependent regulation of neuronal iron that is highly relevant to AD pathology (Fig. 1). Secretase cleavage of APP is essential for APP maintenance on the membrane surface. Data currently in preparation for submission indicates that altering the proteolytic processing of APP at the cell surface causes consequential changes in neuronal iron homeostasis. Changing the expression, activity and cellular trafficking of endogenous secretase activity to enhance the amyloidogenic pathway of APP processing (Fig. 2A&B), or overexpressing APP carrying familial AD mutations (Fig. 2C), leads to intracellular iron accumulation via cell surface FPN changes. With increased amyloidogenic processing of APP being a major contributor to AD, these studies increase our understanding as to why iron accumulation in dementia patients and transgenic models could facilitate susceptibility to reactive oxygen species neurotoxicity. Persistent processing of APP by β-secretase to elevate neuronal iron retention leads to lipid peroxidation and ferroptosis inhibition by Ferrostatin-1 is able to protect against cell death induced by altered APP processing (Fig. 2D). Combined, this evidence provides an intriguing

therapeutic target for dementia associated with abnormal proteolytic processing of APP.

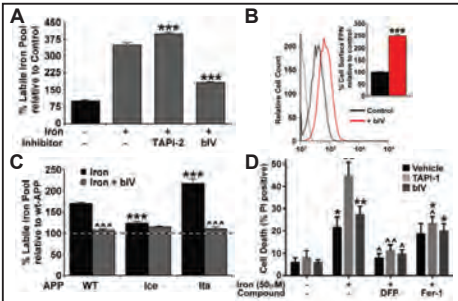


**Figure 2:** APP proteolysis alters neuronal iron homeostasis with ferroptosis induced by amyloidogenic processing of APP being rescued by chelation and ferrostatin-1. **(A, B)** Altering proteolytic cleavage of APP causes a response to intraneuronal iron levels (**A**) and ferroportin (FPN) cell surface location (flow cytometry) (**B**). α-Secretase inhibition (TAPI-2) increases amyloidogenic processing of APP and iron retention whereas by β-secretase inhibition (bIV) induces non-amyloidogenic processing of APP, reduces iron and increases cell surface retention of FPN. (**C**) Similar to (A) amyloidogenic processing of APP caused by the AD familial Italian mutation increased intraneuronal iron levels whereas the longevity Icelandic (Ice) mutation associated with impaired β-secretase processing retained iron at control levels. β-secretase inhibition (bIV) only reduced iron from cell lines overexpressing wild-type APP or Ita-APP. (**D**) All iron induced cell death was prevented by addition of deferiprone (DFP), whereas ferroptosis inhibition (ferrostatin-1; Fer-1) rescued cell toxicity only induced through amyloidogenic processing of APP (TAPI-1). ***, p<0.001; **, p<0.01; *, p<0.05 compared to control. For C and D ^^^, p<0.001; ^^, p<0.01; ^, p<0.05 compared to iron treated.

**Outlook**

By continuing to support a novel candidate function for APP we now begin to explain the diverse trophic and morpho-regulatory activities of the protein and elucidate the vulnerability the body to age-associated iron accumulation.

Modulatory factors that can increase the processing of APP through the amyloidogenic pathway may have additional affects on iron regulation and oxidative stress. We have identified that ferroptosis may be an instrumental consequence of chronic altered amyloidogenic processing of APP. Similar to a range of neurodegenerative models identified by collaborators, we have now identified ferroptosis as a key player in disease progression and the use of feroptotic inhibition as a promising future therapeutic target for these diseases.

**Publications**

Poujois A., Devedjian J.C., Moreau C., Devos D., Chaine P., Woimant F. & Duce J.A. (2016) Bioavailable trace metals in neurological diseases. *Curr. Treat. Options Neurol.* **18**:46.

Gunn A.P., Wong B.X., Johanssen T., Griffith J.C., Masters C.L., Bush A.I., Barnham K.J., Duce J.A. & Cherny R.A. (2016) Amyloid- peptide A3PE-42 induces lipid peroxidation, membrane permeabilization, and calcium influx in neurons. *J. Biol. Chem.* **291**:6134-6145.

**Funding**

This work was supported in the UK by a PhD Studentship from Alzhiemer's Society and a Marie Curie Integration Grant from the European Commission. International support is also provided by the NHMRC and AADRF Project Grant from Australia.

**Collaborators**

***External:*** A. Bush (University of Melbourne, Australia); D. Devos and Dr. J.-C. Devedjian (Universite de Lille, France); R. Evans (Brunel University, London); D. Tetard and F. Lewis (Northumbria University) and D. Smith (Sheffield Hallam University).

## Structure-based design of inhibitors of metallo β-lactamases: rescuing our current antibiotics

Ricky Cain and Colin Fishwick

### Introduction

The β-lactam antibiotics such as the penicillins and cephalosporins, remain the most important drug class for the treatment of bacterial infections. However, their continued use is jeopardized by the increasing spread of resistance mechanisms, including that mediated by β-lactamases, which, cumulatively, can hydrolyse all classes of β-lactam antibiotics. The serine-β-lactamases (SBLs), classes A, C, and D, likely evolved from the penicillin-binding protein (PBP) targets of β-lactam antibiotics. Inhibitors of the SBLs include clavulanic acid, sulbactam, and tazobactam, which are active against class A β-lactamases, and the recently introduced non-β-lactam β-lactamase inhibitor avibactam, which has a broader spectrum of SBL inhibition activity. These inhibitors have increased the efficacy of β-lactam antibiotics against SBL-mediated resistance in bacteria, but they are inactive against the Zn(II)-dependent class B metallo-β-lactamases (MBLs), which constitute a structural and mechanistically distinct family of enzymes and exhibit considerable heterogeneity, even among themselves. The MBLs are able to hydrolyse all classes of β-lactam except for monobactams. The ability of the MBLs to hydrolyse SBL inhibitors, including avibactam, is a growing problem in the treatment of infections where both SBL- and MBL-mediated cephalosporin and carbapenem resistance have been acquired. To date there are no clinically approved MBL inhibitors. Our work aims to use structure-guided molecular design and organic synthesis in order to identify small molecule inhibitors of β-lactamases that in the form of a co-therapy, have the potential to render resistant bacteria open to the effects of β-lactam antibiotics.

### Results

We applied the de novo molecular design programe SPROUT to a crystal structure of NDM-1 (4RAM.pdb) followed by subsequent synthesis, to produce a smal library of cyclic boronate-based inhibitors. Using a fluorogenic assay for MBLs, these were then screened against a representative panel of clinically relevant B1 subfamily MBLs, including IMP-1 (Imipenemase-1), VIM-2 (Verona-Integron-Encoded MBL-2), NDM-1 (New Delhi MBL-1), SPM-1 (São Paulo MBL-1), and the model MBL, BcII from *Bacillus cereus* (Table 1).

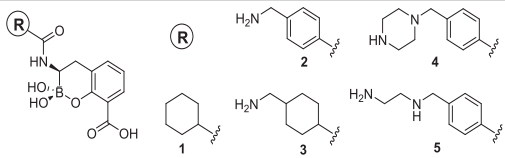

| | $IC_{50}$ [μM] | | | | |
|---|---|---|---|---|---|
| | **1** | **2** | **3** | **4** | **5** |
| BcII | 7.27 | 0.30 | 0.96 | 0.52 | 1.14 |
| VIM-2 | 0.051 | 0.003 | 0.011 | 0.014 | 0.002 |
| IMP-1 | 1.44 | 1.00 | 1.50 | 1.21 | 1.41 |
| NDM-1 | 2.04 | 0.029 | 0.687 | 0.04 | 0.004 |
| SPM-1 | 24.1 | 16.7 | 16.0 | 13.9 | 36.3 |
| TEM-1 | 0.001 | 0.003 | 0.002 | 0.0003 | 0.006 |
| OXA-10 | 0.33 | 5.1 | 0.83 | 2.26 | 12.7 |

**Figure 1:** X-ray crystal structures of 2 bound to the VIM-2 (left) and OXa-10 (right).

The results imply that cyclic boronates with an aromatic sidechain, positioned analogously to the 6β/7β sidechains of the penicillins/cephalosporins, are potent inhibitors of B1 MBLs. In vitro inhibition of MBLs by the tested cyclic boronates yielded the following rank order of

potency: VIM-2 > NDM-1 > BcII > IMP-1 > SPM-1. Overall, these data identify **2** and **5** as highly potent inhibitors of VIM-2 and NDM-1, the most widely distributed members of the clinically important B1 subfamily. We then used fluorogenic assays to measure the potency of the cyclic boronates against clinically relevant Class A and Class D SBLs, including TEM-1 (Class A) and OXA-10 (Class D). All of the compounds tested were potent TEM-1 inhibitors ($IC_{50}$ 6 →0.3 nM) and compounds with saturated sidechains (**1** and **3**) manifested $IC_{50}$ values < 1 μM against OXA-10.

We were able to verify the mode of binding of these inhibitors to both classes of enzymes via X-ray crystallography (Figure 1).

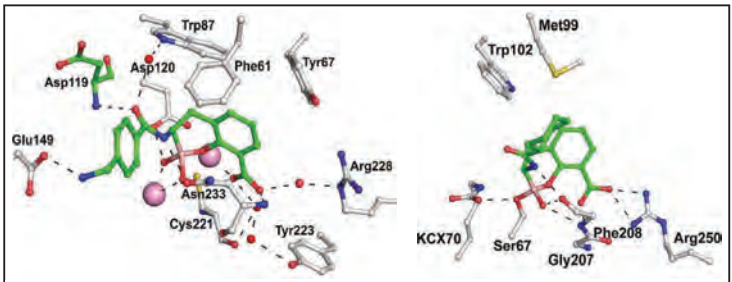


**Figure 2:** X-ray crystal structures of 2 bound to the VIM-2 (left) and OXa-10 (right).

Since **2** was a potent inhibitor of both enzyme classes in vitro, we next tested its activity against highly resistant Gram-negative bacterial cells (strains of *E. coli* and *Klebsiella pneumoniae,* both carrying the NDM-1 MBL together with multiple SBLs of different classes), alone and in combination with the carbapenem meropenem, Compound **2** alone did not display antibacterial activity against any of the strains tested. However, for all strains carrying the MBL NDM-1, co-administration with **2** reduced the minimal inhibitory concentration (MIC) of meropenem. Clear reductions in meropenem MIC were observed at 10 μg / mL inhibitor, while increasing the concentration of 2 to 25 μg / mL brought the meropenem MIC into the susceptible range (MIC < 8 μg / mL). Strikingly, for the clinical strain *K. pneumoniae* IR16, compound **2**, even at 10 μg / mL, was able to reduce the meropenem MIC from resistant (32 μg / mL) to fully susceptible (MIC ≤ 0.25 μg / mL). Neither compounds **1**, nor **2** showed cytotoxicity in human HEK293 cells when administered at concentrations up to 100 μM.

**Publications**

Adams P.G., Collins A.M., Sahin T., Subramanian V., Urban V.S., Vairaprakash P., Tian Y., Evans D.G., Shreve A.P. & Montano G.A. (2015) Diblock copolymer micelles and supported films with noncovalently incorporated chromophores: A modular platform for efficient energy transfer. *Nano Lett.* **15**:2422-2428.

Adams P.G., Swingle K.L., Paxton W.F., Nogan J.J., Stromberg L.R., Firestone M.A., Mukundan H. & Montano G.A. (2015) Exploiting lipopolysaccharide-induced deformation of lipid bilayers to modify membrane composition and generate two-dimensional geometric membrane array patterns. *Sci. Rep.* **5:**10331.

**Funding**

This work was funded by the MRC.

**Collaborators**

*External:* C. Schofield (Oxford), J. Spencer (Bristol).

## New small molecule inhibitors of *T. gondii* $bc_1$: towards a cure for toxoplasmosis

Martin McPhillie, James Gordon, Stephen Muench and Colin Fishwick

### Introduction

*Toxoplasma gondii*, the causative agent of toxoplasmosis, is responsible for the most common parasitic infection of human brain and eye, persists across lifetimes, can progressively damage sight, and is currently incurable. *T. gondii* infections can cause systemic symptoms, damage and destroy tissues especially eye and brain, and cause fatalities. Primary infections may be asymptomatic, or cause fever, headache, malaise, lymphadenopathy, and rarely meningoencephalitis, myocarditis, or pericarditis. Retinochoroiditis and retinal scars develop in up to 30% of infected persons, and epilepsy may occur. Furthermore, expression of the essential mitochondrial electron transport complex cytochrome $bc_1$, is markedly increased in infective forms of the parasite, suggesting cytochrome $bc_1$ might be a viable drug target for the development of agents to combat toxoplasmosis.

We wished to use a structure-guided approach to produce potent small molecule inhibitors of *T. gondii* $bc_1$ that may represent starting points for development into anti-infective drug leads.

### Results

We applied a range of structure-guided methods to a homology model of *T. gondii* $bc_1$ complex derived from the crystal structure of $bc_1$ from *S. cerevisiae* (1KB9.pdb, Figure 1), and used structure-based methods followed by synthesis to produce a series of putative $bc_1$ inhibitors.

One of these inhibitors, MJM170, was found to be a potent inhibitor ($IC_{50}$ = 30 nM of the growth of *T. gondii* tachyzoites *ex vivo* (Figure 2).

Furthermore, we found that MJM170 was highly efficacious against *T. gondii* tachyzoites in mice at 25 mg/kg without toxicity for 5 days (Figure 3).

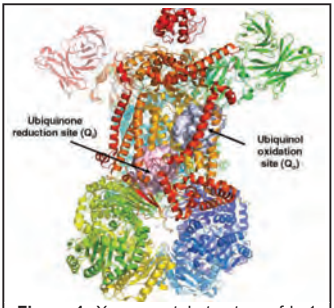


**Figure 1:** X-ray crystal structure of bc1 from *S. cerevisiae* (1KB9.pdb)

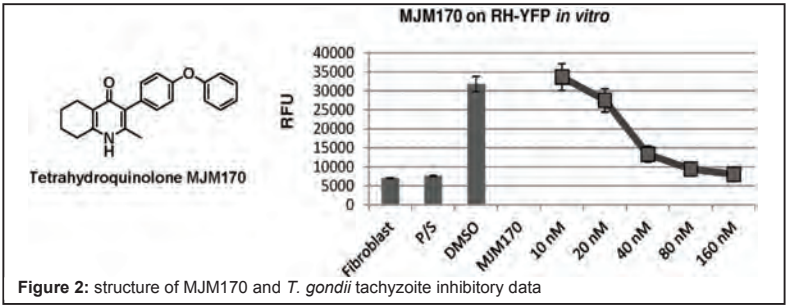


**Figure 2:** structure of MJM170 and *T. gondii* tachyzoite inhibitory data

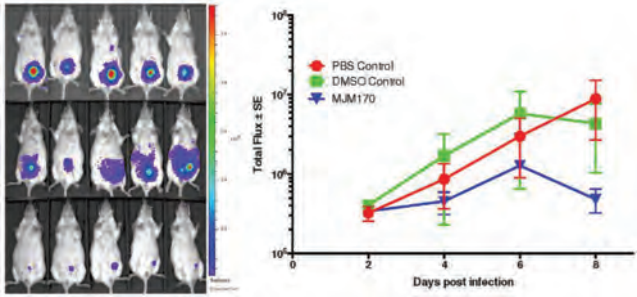


**Figure 3:** *in vivo* effect of MJM170. MJM 170 25 mg/kg daily reduces type 2 parasites.

We also used X-ray crystallography to establish that MJM170 binds into the Qi site of $bc_1$ (Figure 4).

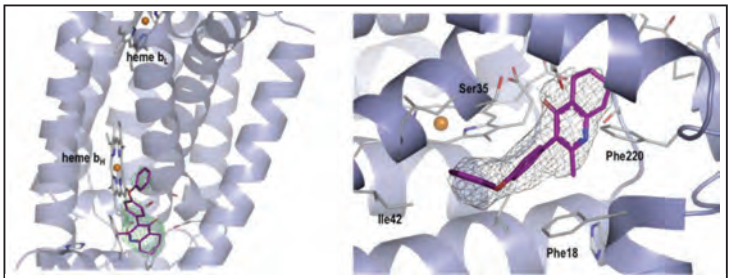


**Figure 4:** crystal structure of MJM170 bound into the Qi site of $bc_1$ (bovine enzyme)

**Publications**

McPhillie, M., Zhou, Y., El Bissati, K., Dubey, J., Lorenzi, H., Capper, M., Lukens, A., Hickman, M., Muench, S., Kumar Verma, S., *et al*. (2016) New paradigms for understanding and step changes in treating active and chronic, persistent apicomplexan infections. *Sci. Rep.* **6**:29179.

**Funding**

This work was funded by the NIH.

**Collaborators**

*External:* R. McLeod (Chicago).

## Understanding how the fusion protein of Herpes Simplex Virus-1, gB, drives fusion between the virus and the host cell membranes

Lauren Brown and Juan Fontana

### Introduction

Herpes Simplex Virus (HSV) is a model system for the Herpesvirus family, which includes human viruses that cause life-long infections and a variety of diseases, including skin lesions, encephalitis and cancers. Antivirals that reduce the severity and frequency of HSV symptoms exist. However, these drugs cannot cure infection, and there is no HSV vaccine available.
A key step of viral infection is entry into the host cell, a process that for enveloped viruses like HSV involves fusion of viral and cellular membranes, allowing the viral genome to access the interior of the cell. In HSV, this process is mediated by the fusion protein gB, for which a structure in its post-fusion conformation is available. While this structure has significantly advanced our understanding of the fusion process of HSV, it is the structure of pre-fusion gB that is essential to complete our knowledge of how gB undergoes the pre- to post-fusion transition. However, solving this structure has been hampered by the fact that all of the purified forms of gB are post-fusion.

### Results

We have set-up a system that generates vesicles displaying full-length gB from HSV type 1 on their envelope and analysed them by cryo-electron tomography (cryo-ET), which allows direct 3D imaging of unique objects, combined with subtomogram averaging, which further improves the signal to noise ratio of repeated structures within a tomogram, like fusion proteins within a virion. To elucidate the rearrangement of gB during fusion, we have labelled gB's domains by inserting fluorescent proteins (which are readily visible in the subtomogram averages) in specific positions and we have co-expressed gB with neutralising antibodies (whose size is comparable to that of the fluorescent proteins) for which the binding sites are known. These experiments have provided a working hypothesis for the structure of pre-fusion gB and the conformations rearrangements of gB during fusion.

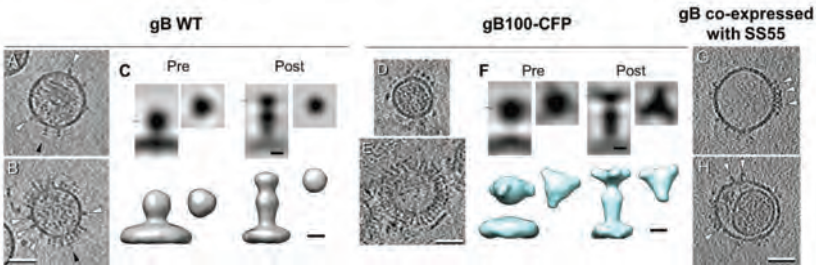


**Figure 1:** Cryo-ET (A, B, D, E, G & H; scale bars 50 nm) & subtomogram averaging (C & F; scale bars, 5 nm) of full-length gB expressed in vesicles. A-C, gB WT. D-F, gB tagged with cyan fluorescent protein at residue 100. G & H, gB co-expressed with the neutralising antibody SS55.

### Funding

This work was funded by the University of Leeds and the Royal Society.

### Collaborators

*External:* D. Atanasiu, W.-T. Saw, R. J. Eisenberg and G. Cohen (University of Pennsylvania).

## Development of a novel small molecule anticoagulant with minimal bleeding risk

Roger Taylor, Colin Fishwick, Charlotte Revill, Emma Hethershaw and Richard Foster

**Introduction:**
The underlying focus of our research is small molecule drug discovery. We are interested in the synthesis and development of small molecules as therapeutics as well as the design of chemical probes to support validation of novel biological targets in areas of unmet medical need. A priority area of research is development of new approaches to the generation of small molecule anti-coagulants with minimal bleeding risk.

**Results:**
We have identified potent, novel small molecule inhibitors of the coagulation cascade with exceptional *in vivo* efficacy. The inhibitors have been identified by a number of parallel approaches incorporating virtual drug design, chemical synthesis and high-throughput screening of drug-like small molecule libraries and fragment screening. Presently, we are optimising the inhibitors for target potency, specificity and drug-like physicochemical properties using iterative rounds of medicinal chemistry development and screening using a panel of orthogonal bioassays. The compounds have been optimised for drug-likeness and demonstrate high aqueous solubility, metabolic stability, plasma stability and low levels of plasma protein binding and cardiotoxicity, including hERG inhbition. The compounds are >300x selective for 10 structurally (and functionally) related targets and the compounds demonstrate no toxicity on high concentration dosing in mice. The aim of the on-going work is to further develop the leads to generate a candidate compound with suitable pharmaceutical properties consistent with an optimised lead ready for progression to out-licensing and eventually clinical trials. A second series of inhibitors identified by fragment-based screening (NMR and SPR) is undergoing optimisation for potency driven by structural guided design. The second series of ligands bind in a different manner to the primary series and offer a possibility to generate inhibitors with a complementary selectivity and property profile to the current leads.

**Publication**
Patent: 15217111

**Funding:**
Our work is funded by the Wellcome Trust, MRC and BHF.

**Collaborators**
*University of Leeds:* R. Ariens and H. Philippou.

## Structural and functional studies of membrane pyrophosphatases

Craig Wilkinson, Nita Shah, Steven Harborne and Adrian Goldman

### Introduction

Membrane pyrophosphatases (M-PPases) occur in plants, protozoan parasites and prokaryotes. They are associated with low-energy stress: overcoming saline or drought conditions in plants or rapid changes in pH or osmotic pressure in protozoan parasites. M-PPases couple pyrophosphate hydrolysis to the pumping of sodium ions and/or protons across the inner membrane of prokaryotes or the vacuole/acidocalcisome membranes of plants/parasites. These proteins are important in the lifecycle of several pathogenic species of parasites, including *Plasmodium falciparum*, which causes malaria, and in several species of pathogenic bacteria, such as *Clostridium botulinum* and species of *Bacteroides* that can cause severe opportunistic infections. There are no analogues in mammals, so M-PPases are an important potential drug target. Continuing from our M-PPase structure, we are completing a model of the catalytic cycle using additional structural and biochemical data and are using this in drug design.

### Results

We have solved two new structures of the M-PPase of the thermophilic bacteria: *Thermotoga maritima* (TmPPase) in different catalytic states[2]. Combining this data with previously solved structures of this and a related protein from *Vigna radiata* (VrPPase) we have generated a model of the complete catalytic cycle covering all of the major catalytic states (Fig. 1).

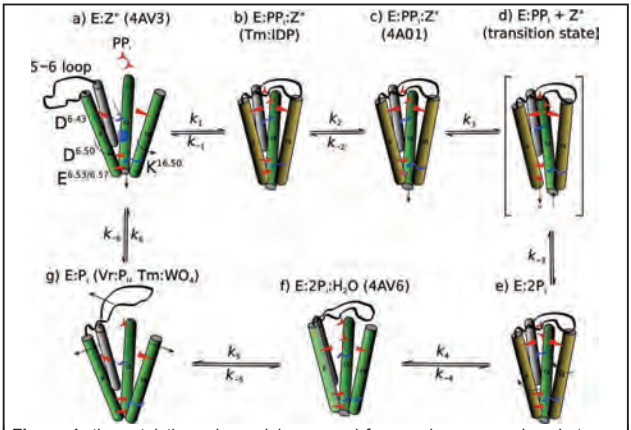


**Figure 1:** the catalytic cycle model proposed for membrane pyrophosphatases based on structural information from X-ray crystallography. Only key helices and residues are shown for the sake of clarity.

New structural information confirmed that there is a "downwards" motion of helix 12 upon substrate binding that severs an important ion pair at the base of the active site. This allows the active site residues to alter conformation, leading to the complete coordination of a nucleophilic water by two aspartate residues, setting up the mechanism for hydrolysis. The new structure also shows a bound $Na^+$ at the ion gate, however, from the structures alone it is not possible to tell whether ion pumping or hydrolysis occurs first during this high-energy transition state. Understanding this state would provide information on this final, important step of the catalytic cycle. To try to solve this problem, electrometric measurements were taken of VrPPase proteoliposomes using the Nanion SURFE$^2$R N1[2], which can measure differences in charge across a membrane. Experiments involving the substrate (pyrophosphate) (Fig. 2) generated a strong and repeatable signal attributed to proton pumping that was absent in phosphate-only, and empty liposome controls (Fig.2A). Further experiments used non-hydrolysable inhibitors in place of pyrophosphate (Fig.2B) and produced an above-background signal that could be dissipated by protonophores. This

suggests that the signal seen with the inhibitors is due to a single-turnover event upon inhibitor binding and that ion pumping occurs after substrate binding and before substrate hydrolysis.

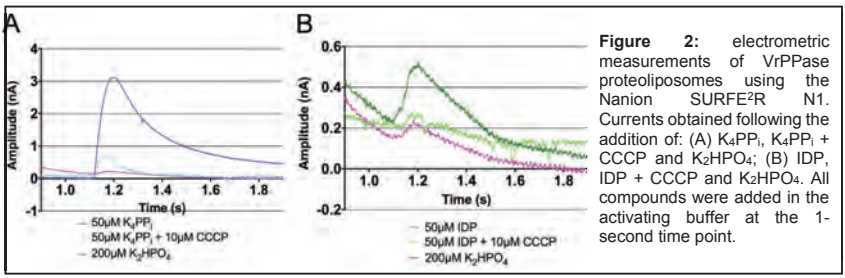


**Figure 2:** electrometric measurements of VrPPase proteoliposomes using the Nanion SURFE$^2$R N1. Currents obtained following the addition of: (A) $K_4PP_i$, $K_4PP_i$ + CCCP and $K_2HPO_4$; (B) IDP, IDP + CCCP and $K_2HPO_4$. All compounds were added in the activating buffer at the 1-second time point.

We are currently studying other classes of M-PPases such as the $K^+$-independent $H^+$-PPases and the dual-pumping PPases from *Bacteroides vulgatus*, using cryoEM to solve these structures and those of other membrane proteins. Biochemical and fluorescence studies, alongside molecular dynamics simulations, are being used to understand the mechanisms involved in each stage of the catalytic cycle. Finally, we are starting to develop potential lead molecules that kill protozoan parasites in collaboration with labs in Leeds and Helsinki.

**Publications**

Shah N.R., Vidilaseris K., Xhaard H. & Goldman A. (2016) Integral membrane pyrophosphatases: A novel drug target for human pathogens? *AIMS Biophys.* **3**:171-194.

Li K.M., Wilkinson C., Kellosalo J., Tsai J.Y., Kajander T., Jeuken L.J.C., Sun Y.J. & Goldman A. (2016) Membrane pyrophosphatases from *Thermotoga maritima* and *Vigna radiata* suggest a conserved coupling mechanism. *Nat. Commun.* **7**:13596.

Goldman, A., Boije af Gennis G., Xhaard H., Meri S. & Yli-Kauhaluoma J. (2016) Pyrofosfaatti lääketieteessä. *Duodecim* **132**:1111–1117 (In Finnish).

Ji Y.R., Postis V.L.G., Wang Y.Y., Bartlam M. & Goldman A. (2016) Transport mechanism of a glutamate transporter homologue Glt(Ph). *Biochem. Soc. Trans.* **44**:898-904.

Lee S.C., Knowles T.J., Postis V.L.G., Jamshad M., Parslow R.A., Lin Y.P., Goldman A., Sridhar P., Overduin M., Muench S.P., *et al.* (2016) A method for detergent-free isolation of membrane proteins in their local lipid environment. *Nat. Protoc.* **11**:1149-1162.

Parmar M.J., Lousa C.D., Muench S.P., Goldman A. & Postis V.L.G. (2016) Artificial membranes for membrane protein purification, functionality and structure studies. *Biochem. Soc. Trans.* **44**:877-882.

**Funding**

BBSRC (ALERT-13 and BB/M021610/1), Royal Society (Wolfson award), Wellcome Trust (091322/2/10/2), EDICT (201924), Academy of Finland (12522061 and 256049), Sigrid Juselius foundation and Leeds 110th Anniversary scholarship

**Collaborators**

*University of Leeds:* L. Jeuken, R. Tuma, S. Harris, C. Fishwick; on other projects A. Morgan. *External:* J. Kellosalo, T. Kajander, G. Boije af Gennäs and J. Yliakauhaluoma (Helsinki), Y.-J. Sun (Taiwan), D. Linke (Oslo) and R. Lahti (Turku).

## Causative and curative viruses in human cancer

Abigail Bloy, Matthew Bentham, Claire Scott, Hannah Beaumont, Emma Brown, Elizabeth Appleton, Mohamed Madkour, Adel Samson and Stephen Griffin

**Introduction**

Virus infections are associated with 20-30% of human cancer, with evidence of their further involvement arising through the genomics era. However, whilst certain well-established oncogenic DNA viruses cause cancer via expression of dominant oncogenes or integration of the viral genome within host DNA, the mechanisms by which some other viruses do so are less apparent, despite clear associations with malignant change.

Hepatitis C virus (HCV) infects over 150 million individuals and is associated with approx. 30% of primary liver cancer, predominantly hepatocellular carcinoma (HCC). However, as an RNA virus that replicates within the cytoplasm, its direct oncogenic mechanism is unclear, and dogma attributes HCV-associated HCC to a consequence of chronic inflammation. Nevertheless, growing evidence supports that HCV directly drives transformation and that treating both the cancer and virus concomitantly may be beneficial for patients.

Our research in this area comprises two parallel themes: firstly, we are investigating the mechanisms by which HCV drives oncogenic change. Secondly, by contrast, we are investigating the use of benign viruses as an immunotherapy targeting virus-associated cancer – so-called “oncolytic” virus immunotherapy.

**Results**

**1. Mechanisms of HCV-induced carcinogenesis.** Difficulties in culturing HCV in the laboratory have prevented researchers from conducting classical assays whereby prolonged virus infection of primary cells leads to immortalisation and transformation. Nevertheless, evidence from transgenic systems shows that HCV proteins can transform cells. It is often assumed that HCV induces the formation of a cancer-initiating cell following infection of terminally differentiated hepatocytes. However, the majority of cells within a chronically inflamed liver are in fact being constantly repopulated through the proliferation of the resident hepatic progenitor cell (HPC) compartment.

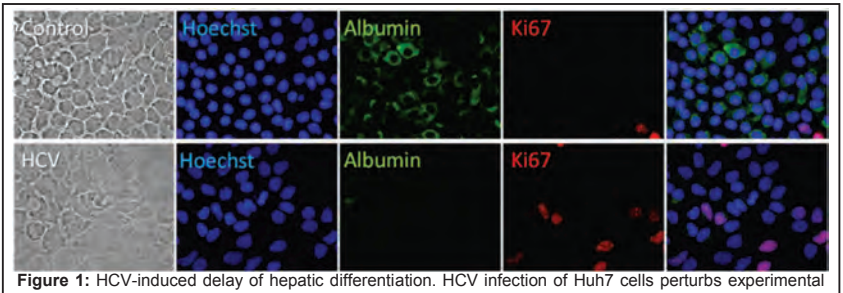


**Figure 1:** HCV-induced delay of hepatic differentiation. HCV infection of Huh7 cells perturbs experimental differentiation, leading to altered morphology (phase), lowered expression of terminal differentiation markers (albumin) and increased numbers of cells in cycle (Ki67).

We hypothesised that HCV might infect HPC, perturbing their proliferation and differentiation programmes and so increasing the likelihood of transformation. In agreement with this notion, we have shown that primary human HPC isolated from healthy liver are susceptible to HCV infection *ex vivo*, setting a precedent for these representing an alternative source of cancer initiating cells. Moreover, HCV significantly delays and perturbs hepatic differentiation in cell

culture models, maintaining cells in cycle despite strong differentiation stimuli (Figure 1). Ongoing work implicates HIPPO signalling as a pathway hijacked by the virus in order to achieve this effect. We are currently exploring the precise mechanisms at play during this phenomenon, including assessing such virus-induced effects upon primary HPC.

**2. Oncolytic virus immunotherapy in virus-associated liver cancer.** It is clear that hyper-activation of our immune systems, or "immunotherapy", represents a potent new way of improving cancer treatment. This could be particularly important for virus-associated tumours where inflammatory responses should concomitantly target both the underlying oncogenic virus infection, as well as mediating immune lysis of cancerous cells. Ironically, one potent means of achieving this objective is through therapeutic administration of otherwise benign "oncolytic" viruses (OV). Classically, OV were thought to act principally via preferential replication within immune-compromised cancerous cells, leading to direct tumour lysis. However, it is now increasingly recognised that these instead act primarily via immune stimulation.

We showed that clinical grade oncolytic human *Orthoreovirus* (Type 3, Dearing, "Reo") elicited potent type 1 interferon responses using *in vivo* preclinical models of HCC. These responses simultaneously activated natural killer cells to directly lyse tumours, whilst suppressing the replication of HCV. This translated to significant survival benefits, and was also applicable to other models of virus-associated cancer (hepatitis B virus HCC, Epstein Barr virus lymphoma). The efficacy of *uv*-inactivated virus confirmed this process to be principally immune-mediated rather than cytopathic. We have since developed synergistic regimens based upon modified Reo combined with targeted HCC therapies, which dramatically enhance survival in preclinical models, and we are investigating the innate immune activation associated with beneficial outcomes.

**Publications**

Samson A., Bentham M.J., Scott K., Nuovo G., Bloy A., Appleton E., Adair R.A., Dave R., Peckham-Cooper A., Toogood G., Nagamori S., Coffey M., Vile R., Harrington K., Selby P., Errington-Mais F., Melcher A.A. & Griffin S. (2016) Oncolytic viruses as combined anti-viral and anti-tumour agents for the treatment of liver cancer**.** *Gut* **doi:** 10.1136/gutjnl-2016-312009.

Mankouri J., Walter C., Stewart H., Bentham M., Park W.S., Heo W.D., Fukuda M., Griffin S. & Harris M. (2016) Release of infectious hepatitis c virus from huh7 cells occurs via a trans-golgi network-to-endosome pathway independent of very-low-density lipoprotein secretion. *J. Virol.* **90**:7159-7170.

**Funding**

This work has been funded by CRUK, MRC, ERC and the University of Leeds

**Collaborators**

*University of Leeds:* A. Macdonald (SMCB), R. Foster (Chemistry), G. Cook (LICAP), G. Toogood (SJUH).
*External:* A. Melcher (ICR), W. Barclay (Imperial), W. Fischer (Taipei).

## Fluctuating Finite Element Analysis - A Simulation Package for Biomolecular Simulation of Electron Microscopy Data Base (EMDB) Structures

Albert Solernou, Ben Hanson, Glenn Carrington, Rob Welch and Sarah Harris

**Overview**

We have developed a new software tool for biomolecular simulation known as Fluctuating Finite Element Analysis (FFEA), which is specifically designed to take advantage of the current explosion in the quantity and quality of structural data from cryo-Electron Microscopy (cryoEM) being deposited in the Electron Microscopy Data Base (EMDB). At the atomistic level, Molecular Dynamics (MD) simulations have been widely adopted by the biomolecular sciences community to calculate protein dynamics trajectories from the structural information available in the Protein Data Base (PDB). FFEA aims to provide an equivalent tool for protein simulation but using structures from the EMDB, rather than the PDB.

FFEA simulates the dynamic behaviour of collections of proteins or large protein complexes. It provides access to the elusive mesoscale regime (between 10 and 500nm) that is too computationally expensive for atomistic MD, but too small for conventional macroscopic simulation techniques. FFEA produces a trajectory that is analogous to a conventional atomistic (or coarse-grained) MD simulation, only the dynamics of the macromolecule are calculated on a mesh using stochastic partial differential equations derived from continuum mechanics. FFEA treats a soft macromolecule as a continuum viscoelastic solid that is subject to thermal noise, which must be chosen so as to satisfy the fluctuation-dissipation theorem. The material properties of the protein are determined by the density, Young's modulus and internal viscosity. The motion of the continuum is governed by the stochastic partial differential equation:

$$\rho \frac{D\mathbf{u}}{Dt} = \nabla \cdot \boldsymbol{\sigma} + \mathbf{f} + \nabla \cdot \boldsymbol{\pi}$$

where **u** is the velocity, ρ is the density, **σ** is the continuum stress, **f** are the body forces arising from the material deformation and external interactions; and **π** is the stochastic stress arising from thermal noise.

This equation, together with the material constitutive equation for the continuum stress, is discretised using the finite element method by subdividing the protein into a set of tetrahedral elements (see Fig 1). This yields a system of Langevin equations describing the motion of the element nodes. The method has no upper length-scale (and converges smoothly to the athermal limit at large lengths), however the continuum approximation breaks down for mesh element sizes < 5Å. The flexibility of the simulated proteins is determined by the Young's modulus, which is usually obtained by comparing the range of conformers obtained in the FFEA simulations with negative stain EM images.

To describe ensembles of interacting proteins, FFEA uses short-range van der Waals forces. These prevent steric overlap, and can also include a reversible attractive interaction over longer length-scales. Separate biomolecules can also be permanently tethered by harmonic springs, and external forces can be applied to individual nodes of the FE mesh. The viscosity of the surrounding solvent in FFEA is represented as simple Brownian noise, and we are currently implementing the ability to represent solvent flow.

FFEA is shortly to be released as open-source software for mesoscale biomolecular simulation. The software is stored in the BitBucket repository, which facilitates version control during development. It has users' and developers' manuals, a tutorial guide for new users, a documented visualisation tool which is a plugin for the established PyMol program, and a robust test suite to ensure that the physics within FFEA is working correctly. The software is available from the Bitbucket software repository on request.

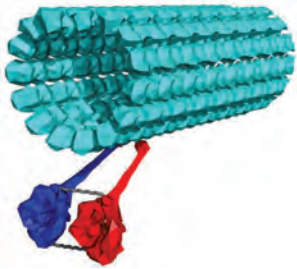

**Figure 1:** FFEA simulations cytoplasmic dynein on a microtubule track. To investigate the importance of the interaction between the two monomers during walking, in our models they are connected together by springs (shown in grey) of varying lengths and stiffness.

We are currently using FFEA to model the mechanism of action of flagellar and cytoplasmic dyneins, fibrinogen aggregation during blood clotting, myosin, and the inner kinetochore. With the Institute for Protein Research in Osaka, Japan, we are developing methods to parameterise FFEA simulations from atomistic models, and experimental data on biomolecular flexibility. By developing a new mesoscale model of soft macromolecules, we aim to open up new regimes of soft matter physics and molecular biology to computer simulation. Our goal is that the FFEA methodology will become a standard tool for *in silico* design and investigation at the mesoscale in both the commercial and academic sectors. Since FFEA bridges the gap between atomistic and conventional Finite Element models of biological organs, blood flow and tumour growth, and therefore facilitates the future development of multi-scale simulation schemes that operate from the atomistic through to the macroscale.

**Collaborators**
*University of Leeds:* D. Read and O. Harlen (School of Mathematics).

## Towards a better understanding of oxidative biomass deconstruction

Glyn Hemsworth

### Introduction

The breakdown of waste plant material, in the form of lignocellulose, for subsequent fermentation into biofuels holds tremendous promise for securing humankind's future energy needs. Though research over several decades has provided many details of how fungi and microbes are able to degrade these materials, the industrial production of lignocellulosic biofuels has remained too costly to compete with fossil fuels. The discovery of lytic polysaccharide monooxygenases (LPMOs) in 2010/11 was, therefore, a key breakthrough. These enzymes oxidatively induce chain breaks into the crystalline region of hard to degrade polysaccharides such as cellulose and chitin, thereby augmenting the ability of other enzymes to degrade biomass. Indeed, the inclusion of LPMOs in enzymatic cocktails for cellulose degradation provides considerable improvements in the efficiency of saccharification, so there is now a worldwide drive to ensure that these enzymes are used effectively in industry. Our research is focused on the electron transfer processes that might be used to activate LPMOs.

### Results

CAZy (www.CAZy.org) is a comprehensive database of structurally-related, catalytic and non-catalytic modules from enzymes involved in the degradation, modification or synthesis of carbohydrates. Using this resource we have identified a range of target proteins that contain domains of unknown funtion, denoted X-domains, appended to carbohydrate binding modules. Sequence analysis of these X-domains suggests that they may well play an electron transfer function and so we have selected a subset of targets to be characterised (Figure 1A).

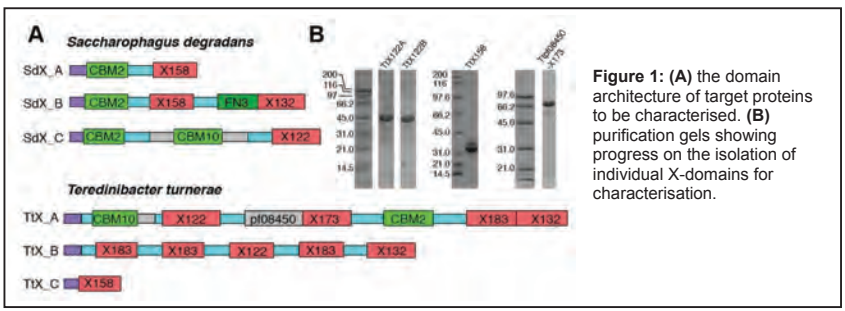


**Figure 1: (A)** the domain architecture of target proteins to be characterised. **(B)** purification gels showing progress on the isolation of individual X-domains for characterisation.

We are currently working on expressing and purifying these domains (Figure 1B) with the aim of combining structural studies together with biochemical, spectroscopic and redox analyses to gain a thorough understanding of X-domain function. We will then seek to exploit the knowledge gained through enzyme engineering to ensure maximal enzyme turnover during biomass degradation whilst also investigating other potential applications for these domains.

### Funding

This work is funded by the BBSRC.

### Collaborators

*University of Leeds:* A. Berry
*External:* B. Henrissat (AIX Marseille Université), P. Walton (University of York), A. Parkin (University of York).

## Production, purification and characterization of proteins of the proteobacterial acinetobacter chlorhexidine efflux, PACE family involved in antimicrobial resistance

Irshad Ahmad, Karl Hassan, Scott Jackson, Ian Paulsen and Peter Henderson

### Introduction

Drug resistance is an increasing problem in clinical settings with some bacterial pathogens now resistant to virtually all available drugs. Chlorhexidine is a bisbiguanide antimicrobial agent that is extensively used in antiseptics ranging through soaps, mouthwashes and preservatives. Increasing resistance to chlorhexidine is seen in some pathogens such as *Acinetobacter baumannii*, in which a novel efflux resistance was associated with a gene designated *acel* (for Acinetobacter chlorhexidine efflux I). We have cloned genes encoding proteins that are homologues of AceI, with a view to their amplified expression, purification and characterization as a preliminary towards structural studies.

### Results

Genes encoding AceI homologues from 23 species of bacteria were transferred to the pTTQ18 plasmid vector, and transformed into *Escherichia coli* BL21(DE3) host cells, where the expression of each cloned gene in membrane fractions was detected in Coomassie stained SDS gels comparing preparations from induced with uninduced cells (nine examples are shown in Figure 1). Western blots detecting the $His_6$-terminus of each protein were used to verify the extent of expression (Figure 1).

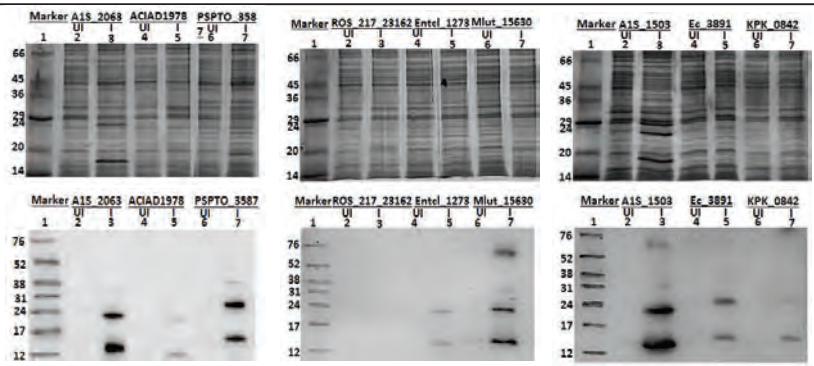


**Figure 1:** expression screening of PACE family proteins. SDS-PAGE (top) and Western blot (bottom) analysis of membrane preparations from small-scale cultures of *E. coli* expressing each indicated protein. Lane 1 shows molecular weight markers for un-induced (UI) and induced (I) preparations as shown.

Out of twenty three investigated, seven genes were expressed at levels sufficient for production at a 30 litre fermentation scale. Each of these was then purified in mg quantities by IMAC. The appearance of more than one band (cf Figure 2) does not necessarily represent degradation or multimers, but an effect of SDS in partially unfolding the molecules in a preparation. The integrity of the purified proteins was also assessed by assaying binding to known or putative substrates (Figure 3a). Several of the highly expressed AceI homologues conferred resistance to acriflavine, a nucleic acid intercalating biocide. Acriflavine fluorescence is reduced when it is intercalated in nucleic acids, allowing real time measurements of acriflavine transport in *E. coli* cells (Figure 3b), showing activity of the over-expressed proteins.

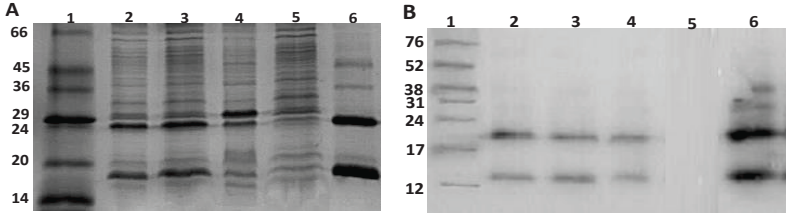


**Figure 2:** purification of Fbal3166 protein. Fbal_3166 protein was purified from the inner membrane of *E. coli* BL21(DE3) pTTQ18 (Fbal_3166)-$His_6$. The inner membranes were solubilised in 1% DDM. (A). Coomassie blue stained 15% SDS-PAGE of Fbal_3166 protein (B). Western blot. Samples loaded as follows: (1) mol. Wt. markers (kDa); (2) membranes; (3) supernatant; (4) membrane pellet; (5) unbound flow; (6) purified protein.

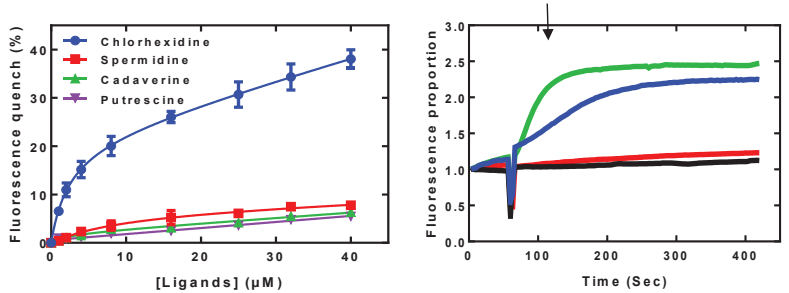


**Figure 3:** activities of the Fbal_3166 protein. (**A**) (Fbal3166)-$His_6$ protein was purified from the inner membrane of 30L cultures of induced *E. coli* BL21(DE3) pTTQ18-Fbal3166)-$His_6$, and solubilised in 1% DDM. The fluorescence change (quench) of tryptophan residues in the protein was monitored at increasing concentrations of the potential ligands: chlorhexidine (blue); spermidine (red); cadaverine (green); putrescine (mauve). (**B**) Small volume cultures were grown of cells expressing the Amva chlorhexidine efflux protein (green), induced cells expressing Fba-His6 protein (blue), uninduced cells not expressing the Fba3166 protein (black), and cells containing pTTQ18 plasmid without the gene insert (red). D-glucose was added at the point indicated by an arrow in order to energise efflux of fluorescent acriflavine. Cells expressing FbaHis6 are competent for efflux of acriflavine.

Current work continues with the seven homologues of the PACE efflux transporter family that have been purified and their ability to bind and transport ligands tested. Structural studies are under way.

**Funding**
This work is funded by Project Grants GNT1060895 and GNT1120298 from the NHMRC (Australia) to IP, KAH and PJFH. PJFH thanks the Leverhulme Trust for an Emeritus Research Fellowship and KAH thanks the EU for a Marie Slowdoska Curie Research Fellowship.

## An integrated approach to the study of cellular interactions with amyloid

Matthew Jackson, Clare Pashley, Sheena Radford and Eric Hewitt

### Introduction

The formation of insoluble amyloid fibrils is associated with a spectrum of human disorders, the amyloidoses, which include Alzheimer's, Parkinson's, type 2 diabetes and dialysis related amyloidosis (DRA). In these disorders the formation of amyloid fibrils is associated with cellular dysfunction and tissue destruction. Yet despite decades of research the culprit species and mechanisms of amyloid toxicity remain poorly understood.

Our goal is to determine how the structure and physical properties of amyloid affects cellular physiology and viability. This involves a multidisciplinary approach in which information obtained by NMR, atomic force microscopy, electron microscopy, photo-crosslinking, mass spectrometry and fluorescence based spectroscopic techniques is integrated with analyses of cell function and viability. We are studying the oligomeric assembly intermediates, fibrils and fibril-derived oligomers formed by an array of amyloidogenic precursors, including α-synuclein (Parkinson's), amyloid-β (Alzheimer's) and $\beta_2$-microglobulin (DRA). Experimental approaches used to analyse the interactions and effects of these amyloid species on cells include plate-based assays for cell viability and metabolism, live cell confocal microscopy microscopy, flow cytometry, subcellular fractionation and proteomics. In addition, we are exploring approaches for the delivery of amyloid aggregates into the cytoplasm of single cells with colleagues in the Schools of Biomedical Sciences and Electrical and Electronic Engineering.

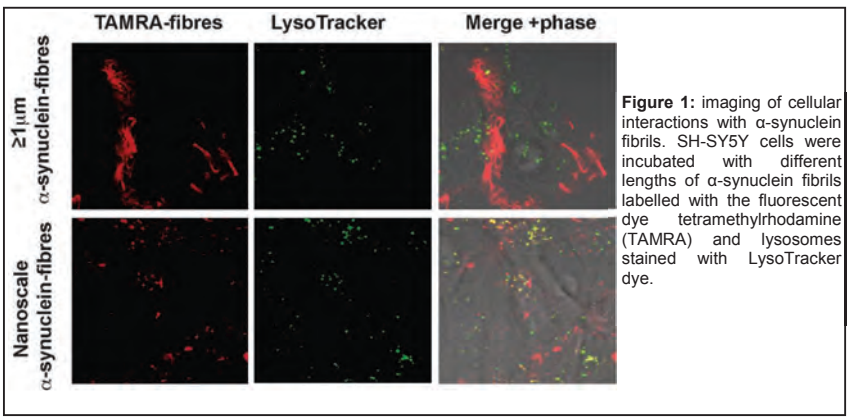


**Figure 1:** imaging of cellular interactions with α-synuclein fibrils. SH-SY5Y cells were incubated with different lengths of α-synuclein fibrils labelled with the fluorescent dye tetramethylrhodamine (TAMRA) and lysosomes stained with LysoTracker dye.

### Publications

Jackson M.P. & Hewitt E.W. (2016) Cellular proteostasis: degradation of misfolded proteins by lysosomes. *Essays Biochem.* **60**:173-180.

Pashley C.L., Hewitt E.W. & Radford S.E. (2016) Comparison of the aggregation of homologous beta(2)-microglobulin variants reveals protein solubility as a key determinant of amyloid formation. *J. Mol. Biol.* **428**:631-643.

### Funding

This work was funded by the Wellcome Trust, EPSRC and ERC.

## A model membrane system to mimic folded cristae of mitochondria and thylakoid stacks of chloroplast

George Heath, Mengqiu Li and Lars Jeuken

### Introduction

Multilayered lipid membrane assemblies are utilized throughout nature and are involved in a wide range of energy producing pathways, from the double membranes surrounding mitochondria and gram-negative bacteria to the stacked thylakoid membranes of photosynthetic plant chloroplasts. The benefits of multiple membrane stacks lie with the ability to amplify and compartmentalize single membrane functions in series. This presents significant technological potential for mimicking and harnessing a diverse range of energy production machinery. Such applications range from producing fuels from organic matter, to converting organic matter into electricity and exploiting photosynthesis for solar power. In addition to energy production it has been thought that multilayered membranes may allow the serial coupling of membrane proteins that could lead to new applications in photonics, biosensing and the 3D crystallization of membrane proteins. Accompanying the functionality, the multilayered structures also offer increased mechanical robustness, a trait that can hinder single membrane systems. To utilise the power of multimembrane stacks in biotechnology, methodologies are required to create these systems in a simple, stable and scalable manner. The formation of multiple lipid membrane stacks has been previously demonstrated by a number of groups, but their constructions either does not allow the incorporation of membrane proteins or the systems require laborious procedures or even custom-synthesised lipid analogues. Here we describe a technique using poly-l-lysine (PLL) as an electrostatic linking polymer layer between membranes. PLL is a widely used biocompatible cationic polypeptide that is inexpensive, biocompatable and readily available.

### Results

Assembly of the PLL multilayered lipid bilayers is schematically shown in Figure 1 (Top). PLL is allowed to bind to a negatively charged 'base' SLB (supported lipid bilayer) (POPC/POPG 1:1) until saturation. Excess PLL is then rinsed away and a second membrane is formed on top via a solution of negatively charged vesicles (POPC/POPG 3:1). This process is then repeated for each additional layer: binding of PLL followed by rupturing vesicles in a layer-by-layer fashion. Whilst the formation of the first 'base' bilayer requires calcium in solution as 'fusagen', all subsequent lipid bilayers do not, since they bind to the positively charged PLL layer. The formation of the multilayer stack was confirmed by fluorescence microscopy, quartz-crystal microballance with dissipation (QCM-D) and atomic formce microscopy (AFM). The AFM results indicates that when the stacks get more than three membrane layers, they become very heterogeneous with patches of membranes in the tens of nanometer range. The 'patchy' nature of the membranes in the multilayer stacks was consistent with the QCM-D data, which showed the dissipation increasing with each additional membrane layer.

To study fundamental biological interactions and for future potential technological applications in multiple membrane systems, the ability to incorporate membrane proteins is vital. Thus we followed the same method to

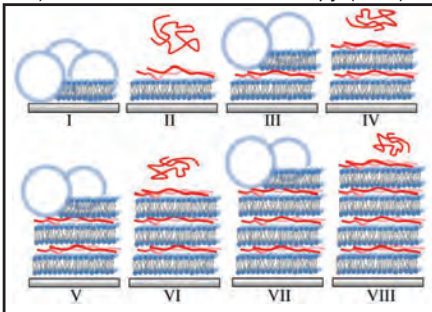


**Figure 1:** a schematic representation of the formation of a multilayer membrane stack using layer-by-layer assembly of negatively charged lipid vesicles that rupture on the surface to form planar membranes and positively charged PLL.

form a membrane stack, but formed the second lipid bilayer with proteoliposomes (POPC/POPG 3:1) containing a transmembrane protein. In total three membrane proteins were investigated: two different drug-metabolizing mono-oxygenases, human flavin-containing monooxygenase 3 (hFMO3) and cytochrome P450 2D6 (CYP2D6). The third protein studied was the heterotrimeric outer membrane protein complex MtrCAB which plays a central role in the metal reducing ability of *Shewanella oneidensis* MR-1. We typically used proteoliposomes with 1-2% protein to lipid ratio (w/w). For each protein, AFM images were obtained of the base bilayer (1:1 POPC/POPG) before incubation with PLL and subsequent secondary bilayer formation with proteoliposomes. AFM images showed almost complete 2nd bilayer coverage with many small protrusions corresponding to extra-membranous regions of the proteins

By labeling each protein with a fluorescent dye, the diffusion properties were investigated firstly in a single base bilayer alone and then in the second bilayer of a double membrane. Figure 3, A-C show double bilayers containing each labeled protein in the second bilayer immediately after bleaching a central region. The recovery of the photobleached area (Figure D-F) indicates that all three membrane proteins freely diffuse within the membrane stack.

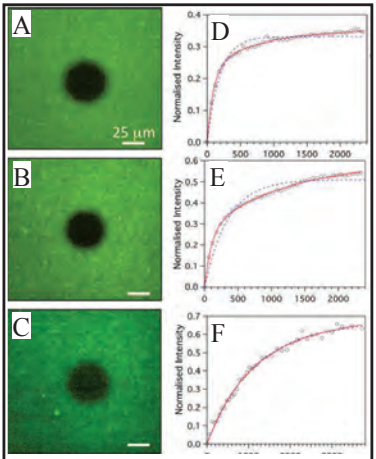


**Figure 2:** the three protein double bilayer assemblies were investigated using fluorescence recovery after photobleaching (FRAP). (**A**-**C**) shows fluorescent microscopy images after labelling proteins (hFMO3, CYP2D6 and MtrCAB, resp.) with Texas red (MtrCAB) and fluorescein (hFMO3 and CYP2D6) dyes. Plots (**D**-**F**) show fluorescence recovery after bleaching for the three proteins in double bilayers with fits to single (blue dashed line) and double (red solid line) exponentials.

This new multilayer membrane model system opens up possibilities for recreating and amplifying some of nature's most useful machineries. This work is also a key component in the development of artificial gram-negative bacterial double membranes with the intension of understanding electron transport across multiple membranes via a number of metalloproteins. As such it not only provides a system for future possible technologies but also for understanding fundamental biological processes at membrane-membrane interfaces.

**Publications**

Heath G.R., Li M., Polignano I.L., Richens J.L., Catucci G., O'Shea P., Sadeghi S.J., Gilardi G., Butt J.N. & Jeuken L.J.C. (2016) Layer-by-layer assembly of supported lipid bilayer poly-L-lysine multilayers. *Biomacromolecules* **17**:324-335.

**Funding**

This work was funded by the BBSRC.

**Collaborators**

*External*: I. Polignano, G. Catucci, S. Sadeghi, G. Gilardi (University of Torino, Italy);J. Richens, P. O'Shea (University of Nottingham, UK; now in the University of British Columbia, Vancouver, Canada); J. Butt (Universtiy of East Anglia, Norwich, UK).

## Optimal reaction coordinates

Polina Banushkina and Sergei Krivov

**Introduction**

Advances in computer hardware and simulation methodology have made realistic simulations of complex biological systems possible. Nonetheless, because of the high-dimensionality of the resulting time series, the generation of many trajectories *per se* is not sufficient to provide full scientific insight. Eventually it becomes necessary to synthesize the data into as faithful as possible a picture of the process of interest. Given the growing size and complexity of simulations, analysis and interpretation of such data are widely recognized as fundamental bottlenecks in the application of atomistic simulations. A common way to analyze a simulation is to determine the free energy landscape, i.e., the free energy as a function of one or more reaction coordinates. In spite of its fundamental importance the systematic research into how properly select such reaction coordinates is still in its early stages. Here we suggest the definition of the optimal reaction coordinates and derive their important properties.

**Results**

The dynamics of complex molecular systems (e.g., proteins) is often analyzed by projection onto a reaction coordinate (RC). The dynamics is then described in a simple and intuitive way as diffusion on the associated free-energy profile. However, this simple diffusive description is not correct becouse the dynamics projected on a coordinate is generally non-Markovian and subdiffusive. While, in principle, the generalized Langevin equation can be used to describe the non-Markovian dynamics exactly, however determination of its kernel is very difficult.

The framework of optimal RCs employs an alternative strategy. It selects RCs in an optimal way, i.e., to make the projected dynamics more diffusive, to minimize non-Markovian effects, or to compute exactly a particular dynamic property. While, in general, the non-Markovian effects cannot be eliminated completely, the projected dynamics could be modeled with good accuracy as diffusive or Markovian. In particular, some quantities can be computed exactly for the original dynamics on a multidimensional free-energy landscape of any complexity.

In a description of reaction dynamics (i.e., the dynamics between two end states), the following quantities are of particular interest: the reaction flux, the mean first passage times (mfpt), and the mean transition path times (mtpt). While, in principle, one may expect a different optimal RC for each of the quantities, the committor RC can be used to compute all of them exactly. Also, the equilibrium mean squared displacement grows linearly with time as for simple diffusion. The committor equals the probability for the trajectory to reach one boundary state (e.g., the native state in the analysis of protein folding) before it reaches another (e.g., the denatured state) starting from any given configuration.

The equilibrium flux J between the boundary states of the committor can be computed *exactly* as $J = \int_0^1 e^{-F(q)/kT} dq \int_0^1 \frac{dq}{e^{-F(q)/kT} D(q)}$, where *F(q)* and *D(q)* are the free energy and the diffusion coefficient as functions of the committor *(q)*. Corrspodingly, the mfpt, can be computed *exactly* as $mfpt = 1/J \int_0^1 P_{eq}(q)(1-q)dq = \langle 1-q \rangle / J$ .The mtpt, can be computed *exactly* as $mtpt = 1/J \int_0^1 P_{eq}(q)q(1-q)dq = \langle q(1-q) \rangle / J$ . One can take any two points on the committor ($q_0$ and $q_1$) and use them as boundaries that define two new end states: $q<q_0$ and $q_1<q$, respectively. The new committor function $q'$ between these two end states can be obtained

by simple rescaling, $q' = (q - q_0)/(q_1 - q_0)$, which means that the above quantities can be computed exactly between any two points on the committor, not just the boundary nodes. For the mean squared displacement of the committor one finds $\langle \Delta q(\Delta t)^2 \rangle = 2J\Delta t$, i.e., the diffusive behavior.

Thus, while generally the dynamics projected on the committor is not exactly diffusive and Markovian, in many respects it behaves as it is diffusive. One may compute some important properties exactly by using the simple diffusive model with the free energy profile and the diffusion coefficient as functions of this optimal RC. Consequently, these free energy profile and diffusion coefficient can be used, in particular, to rigorously define the free-energy barrier and preexponential factor - other major descriptors of reaction dynamics, and in general, to make possible a rigorous analysis of complex biological dynamics.

To apply these results in practice, one needs efficient and robust methods to determine the optimal RC from atomistic simulations, which is currently a work in progress. A number of approaches have been suggested, which can be used to determine an optimized RC, which is a significant improvement over conventionally employed simple RCs, but is still less optimal

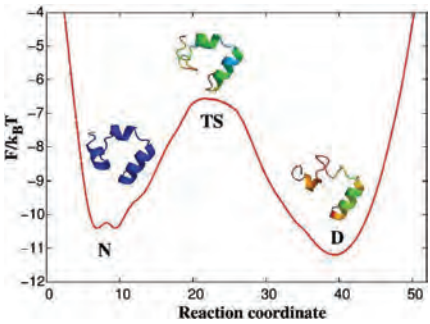


**Figure 1:** free energy landscape of HP35 Nle/Nle mutant as a function of a putative optimal reaction coordinate, rescaled so that the diffusion coefficient is D(x) = 1. The mean first passage time, computed from the diffusive model is two times shorter than that computed directly from the simulation trajectories, meaning that the coordinate is close to the committor but not yet equal to it. The representative structures for the regions of the landscape show a trajectory snapshot closest to the average structure of the region. Colour code the root-mean-square (rms) fluctuations of atomic positions around the average structure.

than the committor (Fig. 1). In our lab, we are currently developing an approach which, given a long trajectory, will determine with high accuracy the optimal RCs and the associated free energy landscape with minimal input from the user.

**Publications**

Banushkina P.V. & Krivov S.V. (2016) Optimal reaction coordinates. *Wiley Interdiscip. Rev.-Comput. Mol. Sci.* **6**:748-763.

**Funding**

This work was funded by the BBSRC.

## Receptor tyrosine kinase signalling in the absence of growth factor stimulation

Eleanor Cawthorne, Janne Darell, Christopher Jones, Sabine Knapp,
Chi-Chuan Lin, Dovile Milonaityte, Arndt Rohwedder, Caroline Seiler and John Ladbury

**Introduction**

In the absence of extracellular stimulation or genetic mutation, an oncogenic response can be driven by the competitive binding of SH3 domain-containing downstream effector proteins to proline-rich sequences on growth factor receptors. Of the approximately 50 plasma membrane receptor tyrosine kinases (RTKs) the majority have proline-rich sequences in their C-termini. These have a propensity to bind to the >300 proteins expressed in human cells which contain SH3 domains. These interactions occur in the absence of any extracellular stimulation (e.g. growth factors, cytokines). Proline-rich sequence binding to SH3 domains are promiscuous and the observed interactions with RTKs are dependent on the relative concentrations of the proteins involved.

We previously established that under non-stimulatory conditions the fibroblast growth factor receptor 2 (FGFR2) recruits the adaptor protein, growth factor receptor binding protein 2 (Grb2) through its C-terminal SH3 domain. In cells depleted of Grb2 other proteins can access the proline-rich motif on FGFR2. One of these proteins, phospholipase C(gamma)1 (Plcγ1) is activated on binding and through turnover of plasma membrane phospholipids to produce second messengers, raises cellular calcium levels which are responsible for increased cell motility and invasive behaviour. In ovarian and lung adenocarcinoma patients with low levels of Grb2 and increased expression of Plcγ1higher incidence of metastasis leads to greatly reduced survival outcomes.

**Results**

We have extended our studies in this area to explore other RTK-SH3 domain-containing protein interactions to establish whether the up-regulation of signal transduction through these interactions is a general phenomenon. This leads to the hypothesis that two tiers of intracellular signalling can be derived from receptors with intrinsic protein kinase activity:
1) Ligand-induced elevation in kinase activity resulting in tyrosylphosphate-mediated effector protein recruitment and committal to a defined cellular outcome (e.g. proliferation).
2) Receptor phosphorylation-independent activation of downstream effectors through SH3 domain/proline-rich sequence interactions, which appear to be required for cell homeostasis/metabolic control.

Hyperactivity of the tier 1 signalling is a feature of receptor tyrosine kinase-related cancers arising from genetic mutation. Although the tier 2 signalling mechanism occurs under basal conditions, and is thus likely to be associated with cellular maintenance, we have shown that fluctuations in expression levels of SH3-containing proteins can drive cells into pathological phenotypes including proliferation and metastasis.

We are testing this hypothesis with a range of methods extending from cell-based assays (including fluorescence lifetime imaging microscopy) through to structural and in vitro biophysical analysis.

Focusing primarily on gastro-intestinal cancers we have begun to explore the effects of stress on intracellular protein expression and the outcomes on tier 2 signalling. We have shown that by mimicking conditions experienced in the GI tract we can affect expression of receptor tyrosine kinases.

In addition to identifying the signalling pathways which are initiated as a result of fluctuations in protein concentrations in cell-based assays, we are exploring the interactions associated with up-regulation of Tier 2 signalling using both biophysical and structural biological methods.

High resolution structural detail on the receptor-ligand interactions are providing invaluable detail on the mode of recruitment of signalling proteins as well as information towards potential inhibition of aberrant pathways that lead to pathogenic outcome.

**Publications**

Kim J.Y., Kinoshita M., Kume S., Hanke G.T., Sugiki T., Ladbury J.E., Kojima C., Ikegami T., Kurisu G., Goto Y.*, et al.* (2016) Non-covalent forces tune the electron transfer complex between ferredoxin and sulfite reductase to optimize enzymatic activity. *Biochem. J.* **473**:3837-3854.

Belousova N., Mikheeva G., Xiong C.Y., Stagg L.J., Gagea M., Fox P.S., Bassett R.L., Ladbury J.E., Braun M.B., Stehle T.*, et al.* (2016) Native and engineered tropism of vectors derived from a rare species D adenovirus serotype 43. *Oncotarget* **7**:53414-53429.

Timsah Z., Ahmed Z., Ivan C., Berrout J., Gagea M., Zhou Y., Pena G.N.A., Hu X., Vallien C., Kingsley C.V.*, et al.* (2016) Grb2 depletion under non-stimulated conditions inhibits PTEN, promotes Akt-induced tumor formation and contributes to poor prognosis in ovarian cancer. *Oncogene* **35**:2186-2196.

Campbell J.C., Kim J.J., Li K.Y., Huang G.Y., Reger A.S., Matsuda S., Sankaran B., Link T.M., Yuasa K., Ladbury J.E.*, et al.* (2016) Structural basis of cyclic nucleotide selectivity in cGMP-dependent protein kinase ii. *J. Biol. Chem.* **291**:5623-5633.

Carter B. Z., Mak P. Y., Chen Y., Mak D. H., Mu H., Jacamo R., Ruvolo V., Arold S. T., Ladbury J. E., Burks, J. K., *et al.* (2016) Anti-apoptotic ARC protein confers chemoresistance by controlling leukemia-microenvironment interactions through an NFκB/IL1β signaling network. *Oncotarget* **7**:20054-20067.

**Funding**

This work was funded by the Mathers Foundation, USA and the NIH, USA.

**Collaborators**

*University of Leeds:* P. Quirke, S. Short, A. Breeze and D. Tomlinson.
*External:* Z. Ahmed; M.-C. Hung, S. Arur (University of Texas MD Anderson Cancer Center, USA); M. Bogdanov (University of Texas, USA) and R. Grose (Barts Cancer Institute, London).

## Understanding the requirement for ion channel activity during virus infection

Samantha Hover, Becky Foster, Eleanor Todd, John Barr and Jamel Mankouri

**Overview**

Segmented negative stranded RNA viruses comprise several hundred species that are classified into Orthomyxoviridae, Arenaviridae and Bunyaviridae families. These families contain a disproportionate number of serious human pathogens including influenza, Lassa and Crimean-Congo hemorrhagic fever viruses. While these viruses are genetically diverse, all have common structural features including an outer host-cell derived envelope with inserted glycoprotein spikes, and segmented RNA genomes that are associated with multiple viral proteins into ribonucleocapsid (RNP) complexes. These RNPs must escape from the viral envelope in order to initiate infection of susceptible cells. We have previously demonstrated that Bunyamwera virus (BUNV), a model virus for the *Bunyaviridae* family, requires cellular potassium ($K^+$) channel activity during virus infection of mammalian and arthropod cell lines. Subsequent analysis identified that $K^+$ channel inhibition was detrimental to BUNV infection during the early post-entry stages of the virus lifecycle, implicating a role in virus-host membrane fusion and RNP release. We are now using BUNV to understand why $K^+$ channel activity would be required during virus lifecycles. We have produced dual-labelled fluorescent BUNV virions to visualise BUNV host cell entry processes and found that it traffics through endosomal vesicles containing a high [$K^+$], which is required for efficient virus infection. Blocking $K^+$ channels was found to shift endosomal [$K^+$] within endocytic vesicles from late endosomes into lysosomes indicating $K^+$ channels may have functions within endosomal compartments, a previously undescribed role. We believe that $K^+$ channels are therefore acting in endosomal processes to usurp the $K^+$ endosomal balance required for BUNV RNP release.

**Publications**

Hover S., King B., Hall B., Loundras E.A., Taqi H., Daly J., Dallas M., Peers C., Schnettler E., Mckimmie C.*, et al.* (2016) Modulation of potassium channels inhibits bunyavirus infection. *J. Biol. Chem.* **291**:3411-3422.

Mankouri J., Walter C., Stewart H., Bentham M., Park W.S., Heo W.D., Fukuda M., Griffin S. & Harris M. (2016) Release of infectious hepatitis c virus from huh7 cells occurs via a trans-golgi network-to-endosome pathway independent of very-low-density lipoprotein secretion. *J. Virol.* **90**:7159-7170.

Mohl B.P., Bartlett C., Mankouri J. & Harris M. (2016) Early events in the generation of autophagosomes are required for the formation of membrane structures involved in hepatitis c virus genome replication. *J. Gen. Virol.* **97**:680-693.

Surtees R., Dowall S.D., Shaw A., Armstrong S., Hewson R., Carroll M.W., Mankouri J., Edwards T.A., Hiscox J.A. & Barr J.N. (2016) Heat shock protein 70 family members interact with Crimean-Congo hemorrhagic fever virus and Hazara virus nucleocapsid proteins and perform a functional role in the nairovirus replication cycle. *J. Virol.* **90**:9305-9316.

**Funding**

This work was funded by the Royal Society and the British Lung foundation.

**Collaborators**

*University of Leeds:* A. Whitehouse, A. Macdonald, A.Tuplin and J. Lippiat.
*External:* A. Kohl, S.Goldstein and S.Finke.

## An improved binary cloning system for studying the mechanistic biology of plants

Michael Watson, Yu-fei Lin, Elizabeth Hollwey, Rachel Dodds, Peter Meyer and Kenneth McDowall

### Introduction

Central to the study and engineering of plants is their transformation, which is achieved most commonly using *Agrobacterium tumefaciens*, the causal agent of crown galls (or tumours) in dicotyledonous plants. The induction of crown galls is induced by the transfer of T-DNA, a segment of a tumour-inducing plasmid that is resident in *A. tumefaciens*, into the nucleus of infected plant cells, wherein it is stably integrated into the genome and expressed. The genes required for the transfer of T-DNA have been identified and are well characterised. Moreover, the segment between the borders of T-DNA can be engineered to contain heterologous DNA while maintaining the ability to be transferred efficiently into plant cells. Indeed, *A. tumefaciens* is used routinely to transform many plant species of academic, agronomical and horticultural importance. To our knowledge, all of the systems that have been developed for this purpose incorporated binary vectors that allow propagation in *Escherichia coli*, wherein DNA can be readily cloned and manipulated between the borders of the T-DNA, prior to transfer into *A. tumefaciens* and finally plants. For any functional study it is of course imperative that the integrity of constructs carrying inserts between the borders of the T-DNA is maintained.

### Results

Recently, as part of a structure-function study of *Arabidopsis thaliana* MET1, which encodes a cytosine-DNA-methyltransferase involved in epigenetic gene regulation, we observed that *E. coli* cells containing a construct encoding MET1 produced unusually small colonies on agar plates and were extremely difficult to passage, i.e. subculture, in liquid media (Figure 1). Moreover, this poor growth provided sufficient selective pressure for mutants, some of which had rearrangements of the plasmid, to dominate the population when dense cultures were eventually obtained. The adverse effect of pGreenII on *E. coli* growth was also evidenced by extensive filamentation (i.e. incomplete septation) of cells (Figure 1).

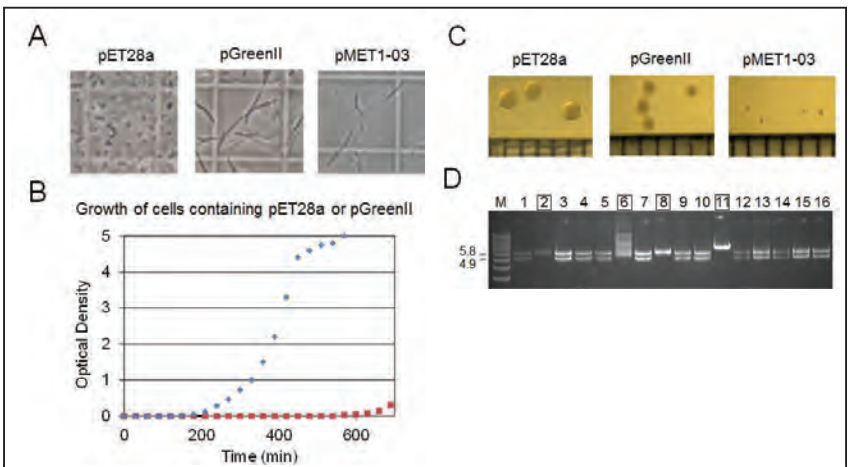


**Figure 1:** growth of DH5α cells containing pET28a (a standard expression vector), pGreenII and pMET1-03 (pGreenII with MET1 insert). **(A)** Cell morphology. **(B)** The growth of *E. coli* using overnight cultures as an inoculum. The data-points for pET28a and pGreenII are represented by blue diamonds and red squares, respectively. **(C)** Colony morphology. **(D)** RE analysis of a selection of plasmids isolated from spontaneous mutants that produce large colonies. Labels that are outlined indicate plasmids with obvious rearrangements.

The finding that a plasmid-based construct can affect the growth of *E. coli* was not in itself unusual. However, closer investigation revealed that the vector (pGreenII), one of the most widely used binary vectors in *Agrobacterium*-mediated transformation, was itself without any insert affecting the growth of *E. coli* substantially, which in turn placed pGreenII-based constructs under considerable selective pressure. To minimise the risk of constructs destined for plants being mutated, we have produced, through a series of genetic screens, a new version of pGreenII that does not affect the growth of *E. coli* (Figure 2).

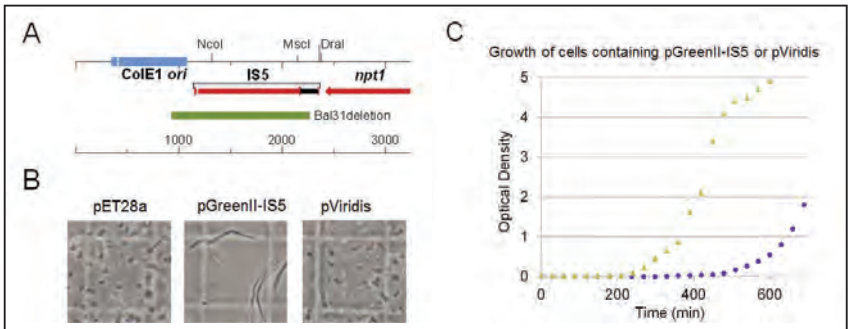


**Figure 2:** characterisation of pViridis and an intermediate in its production, pGreenII-IS5. **(A)** The region between the ColE1 origin of replication and the 3′ end of *npt1* (confers kanamycin resistance) in pGreenII-IS5. Shown are the positions of an IS5 element that was integrated into pGreenII and the "Bal31 deletion" that was final step in the production of pViridis. **(B)** Cell morphology. **(C)** Growth in liquid culture using overnight cultures as an inoculum. The triangles and circles correspond to data-points for cells containing pViridis and pGreenII-IS5, respectively. Compare with the diamonds and squares correspond to data-points for cells containing pET28a and pGreenII, respectively, in Fig. 1.

We have also selected a new strain of *E. coli* that better tolerates existing pGreenII-based constructs without reducing the yield of plasmid recovery (data not shown). The adoption of the new derivative of pGreenII and *E. coli* strain, which we have named pViridis and MW906 respectively, should minimise the mutation of genes destined for study in plants, while they are propagated and manipulated in *E. coli*. This is turn should minimise the possibility that unforeseen rearrangement cause the misinterpretation of mechanistic and other studies in plants.

**Publications**

Watson M.R., Lin Y.F., Hollwey E., Dodds R.E., Meyer P. & McDowall K.J. (2016) An improved binary vector and *Escherichia coli* strain for *Agrobacterium tumefaciens*-mediated plant transformation. *G3-Genes Genomes Genet.* **6**:2195-2201.

**Funding**

This work was funded by the Leverhulme Trust.

## Electron microscopy of membrane proteins to underpin structure guided inhibitor design

Shaun Rawson, Emily Caseley, Paul Beales, Lin-Hua Jiang, Colin Fishwick and Stephen Muench

### Introduction

Membrane proteins are ubiquitous in biology and are key targets for therapeutic development. Despite this, our structural understanding has lagged behind that of their soluble counterparts. This is primarily due to the complications of expressing, stabilising and crystallising membrane proteins. The recent resurgence of electron microscopy (EM) and its requirement for less homogenous protein and a highly ordered crystal lattice has made it a powerful technique for studying membrane proteins. Our group have been studying a range of membrane proteins through EM and homology modelling to drive structure based inhibitor design programs. However, a number of problems still remain, in-particular the ability to study membrane proteins in more native environments.

### Results

The group have been looking at new ways of studying membrane proteins in more “native” environments. The first approach has been through the use of styrene maleic acid (SMA) co polymers, which cut up the membrane into lipid particles (SMALPs). In doing so membrane proteins are enclosed by native lipid, and show higher activity than their detergent solubilized counterparts. Last year we published the first negative stain reconstruction of a SMALP extracted membrane protein and this year have been working on single particle cryo-EM studies in addition to developing new polymers. In parallel, we have worked with the Beales group to study new proteo-hybrid vesicles which offer extended functional lifetimes for membrane proteins.

The overall goal of our studies is to further our structural and mechanical understanding of proteins and protein complexes to drive the design of novel modulators of function. To this end we have a range of target proteins within the lab including, V-ATPase, bc1, Enoyl Reductase, P2X7 and IGPD. We are combining electron microscopy, X-ray crystallography molecular dynamics simulations and biochemical techniques to provide new insights into structure function and inhibitor development (Figure 1A). For those systems we have yet to resolve a high resolution structure for we are using a structure modelling approach with biochemical validation. This is exemplified by our work on P2X7, for which we have developed a series of novel and potent inhibitors that both block and open the central pore based on a model structure.

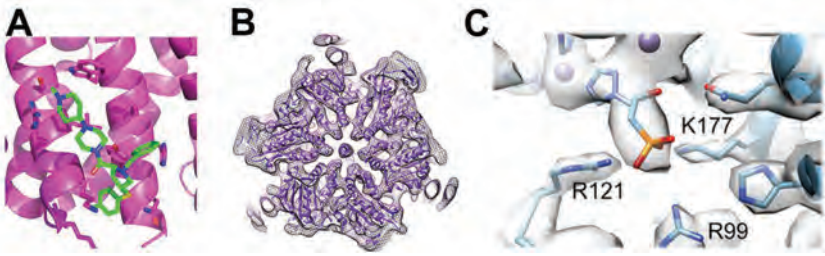


**Figure 1: (A)** *in silico* designed small molecule inhibitor based on modelled structure of the V-ATPase. **(B)** improvement in the V-ATPase EM reconstruction after taking into account the inherent flexibility in the system. **(C)** direct observation of a bound small molecule inhibitor within an EM reconstruction.

The group has been using EM in particular to study the inherent flexibility within large biological systems, for which it is well suited (Figure 1B). Moreover, using the advancements in EM we have been able to clearly resolve small molecule binding directly opening up the door for structure guided inhibitor design by EM methodologies (Figure 1C).

**Publications**

Rawson S., Harrison M.A. & Muench S.P. (2016) Rotating with the brakes on and other unresolved features of the vacuolar ATPase. *Biochem. Soc. Trans.* **44**:851-855.

Rawson S., Iadanza M.G., Ranson N.A. & Muench S.P. (2016) Methods to account for movement and flexibility in cryo-EM data processing. *Methods* **100**:35-41.

Lee S.C., Knowles T.J., Postis V.L.G., Jamshad M., Parslow R.A., Lin Y.P., Goldman A., Sridhar P., Overduin M., Muench S.P., *et al.* (2016) A method for detergent-free isolation of membrane proteins in their local lipid environment. *Nat. Protoc.* **11**:1149-1162.

Khan S., Li M.Q., Muench S.P., Jeuken L.J.C. & Beales P.A. (2016) Durable proteo-hybrid vesicles for the extended functional lifetime of membrane proteins in bionanotechnology. *Chem. Commun.* **52**:11020-11023.

Caseley E.A., Muench S.P., Fishwick C.W. & Jiang L.H. (2016) Structure-based identification and characterisation of structurally novel human P2X7 receptor antagonists. *Biochem. Pharmacol.* **116**:130-139.

Papachristos K., Muench S.P. & Paci E. (2016) Characterization of the flexibility of the peripheral stalk of prokaryotic rotary A-ATPases by atomistic simulations. *Proteins* **84**:1203-1212.

Muench S.P. (2016) Single particle cryo-EM, from sample to reconstruction introduction. *Methods* **100**:1-2.

Thompson R.F., Walker M., Siebert C.A., Muench S.P. & Ranson N.A. (2016) An introduction to sample preparation and imaging by cryo-electron microscopy for structural biology. *Methods* **100**:3-15.

**Funding**

This work was supported by the MRC, Wellcome Trust and NIH.

**Collaborators**

*External:* T. Dafforn (University of Birmingham) and R. McLeod (University of Chicago).

## Unified synthetic approaches to explore biologically-relevant chemical space

Ignacio Colomer, Philip Craven, Richard Doveston, Christopher Empson, James Firth, Daniel Foley, Matthew Lilburn, Zach Owen and Adam Nelson

**Introduction**

The discovery of biologically-active small molecules is an enduring theme in chemical biology and medicinal chemistry. However, the historical exploration of chemical space has been highly uneven and unsystematic: a sixth of known cyclic organic compounds are based on just 30 (of 2.5 million) known molecular scaffolds! This uneven exploration stems, in large part, from the narrow toolkit of reliable reactions that currently underpins molecular discovery. We have established a vibrant research programme focusing on the development of synthetic methods that have potential to explore novel regions within chemical space. To assist prioritisation of methods able to explore chemical space appropriate for specific discovery applications, we have recently launched the open-access computational tool, LLAMA (Lead Likeness And Molecular Analysis).

**A biosynthesis-inspired approach to natural product-like scaffolds**

A synthetic approach to diverse scaffolds was developed that was broadly inspired by terpene biosynthesis (Scheme). Diels–Alder reactions were exploited to convert $sp^2$-rich substrates into complex three-dimensional intermediates. These intermediates were then transformed into 25 diverse and novel scaffolds using cleavage, ring expansion, annulation and rearrangement reactions. It was shown virtual libraries (enumerated using LLAMA) based on the scaffolds had high natural product-likeness and had molecular properties suitable for application in drug discovery.

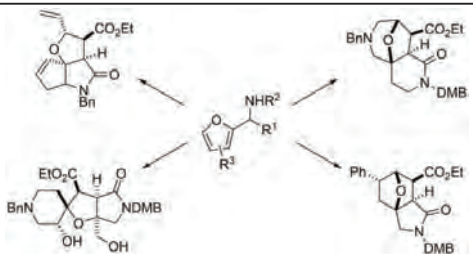


**Scheme:** synthetic approach to natural product-like molecular scaffolds.

**Summary**

The development of unified strategies that are able to deliver skeletally diverse compounds with defined molecular properties is demanding. We have translated many of our unified diversity-oriented synthetic approaches into the €196M European Lead Factory in which Leeds is a partner. Publications from this programme, and other programmes under active development in the group, are listed below. Further details of research within the Nelson group may be found at www.asn.leeds.ac.uk.

**Publications**

Stockwell J., Daniels A.D., Windle C.L., Harman T.A., Woodhall T., Lebl T., Trinh C.H., Mulholland K., Pearson A.R., Berry A., *et al.* (2016) Evaluation of fluoropyruvate as nucleophile in reactions catalysed by N-acetyl neuraminic acid lyase variants: Scope, limitations and stereoselectivity. *Org. Biomol. Chem.* **14**:105-112.

Burslem G.M., Kyle H.F., Breeze A.L., Edwards T.A., Nelson A., Warriner S.L. & Wilson A.J. (2016) Towards "bionic" proteins: replacement of continuous sequences from HIF-1$\alpha$ with

proteomimetics to create functional p300 binding HIF-1α mimics. *Chem. Commun.* **52**:5421-5424.

Burslem G.M., Kyle H.F., Prabhakaran P., Breeze A.L., Edwards T.A., Warriner S.L., Nelson A. & Wilson A.J. (2016) Synthesis of highly functionalized oligobenzamide proteomimetic foldamers by late stage introduction of sensitive groups. *Org. Biomol. Chem.* **14**:3782-3786.

Howard, J. K., Müller, M., Berry, A., Nelson, A. (2016) "An enantio- and diastereoselective chemoenzymatic synthesis of α-fluoro β-hydroxy carboxylic esters", *Angew. Chem. Int. Ed.* **55**, 6767-6770.

Colomer I., Empson C.J., Craven P., Owen Z., Doveston R.G., Churcher I., Marsden S.P. & Nelson A. (2016) A divergent synthetic approach to diverse molecular scaffolds: Assessment of lead-likeness using LLAMA, an open-access computational tool. *Chem. Commun.* **52**:7209-7212.

Firth J.D., Craven P.G.E., Lilburn M., Pahl A., Marsden S.P. & Nelson A. (2016) A biosynthesis-inspired approach to over twenty diverse natural product-like scaffolds. *Chem. Commun.* **52**:9837-9840.

Foley D.J., Nelson A. & Marsden S.P. (2016) Evaluating new chemistry to drive molecular discovery: Fit for purpose? *Angew. Chem.-Int. Edit.* **55**:13650-13657.

**Funding**
We thank EPSRC, BBSRC, the EU and GSK for support.

**Collaborators**
*University of Leeds:* S. Marsden
*External:* I. Churcher, GSK; and A. Pahl (Max Planck Institute for Molecular Physiology). We also acknowledge other scientific collaborators who have also contributed strongly to other aspects of our on-going research programme.

## ABC-F proteins mediate antibiotic resistance through ribosomal protection

Liam Sharkey, Thomas Edwards and Alex O'Neill

### Introduction

Elucidation of the mechanisms by which bacteria resist the inhibitory effects of antibiotics provides essential intelligence in the ongoing fight against antibiotic resistance. Whilst the majority of clinically important antibiotic resistance mechanisms are by now well characterised, some key gaps in our knowledge remain. One such gap concerns the mechanism by which ABC-F proteins mediate resistance to antibiotics that target protein synthesis in Gram-positive pathogens; although members of the ABC-F family collectively yield resistance to a broader range of clinically important antibiotic classes than any other family of resistance determinants, their mechanism of action has been the subject of controversy since their discovery at the University of Leeds 25 years ago.

ABC-F proteins comprise a single polypeptide containing two ATP-binding cassette (ABC) domains separated by a linker of ~80 amino acids. In contrast to canonical ABC transporters, the ABC portions of ABC-F proteins are not fused to transmembrane domains (TMDs), nor are they genetically associated with TMDs in operons. Two competing hypotheses have been proposed to explain how these proteins mediate resistance to antibiotics (Figure 1). The efflux hypothesis posits that ABC-F proteins associate with as-yet-unidentified TMDs to form a functional efflux complex capable of exporting antibiotics out of the cell, whilst the ribosomal protection hypothesis suggests that these resistance proteins act instead to reduce the accessibility or affinity of antibiotic binding sites on the 50S subunit of the ribosome, thereby directly protecting the translational machinery from antibiotic-mediated inhibition. This project was initiated with the intention of elucidating the mechanism of antibiotic resistance mediated by ABC-F proteins.

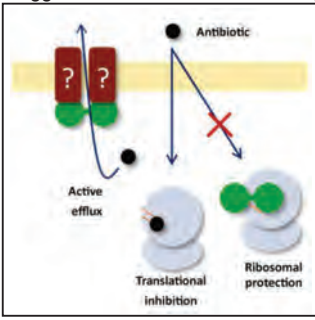


**Figure 1:** proposed mechanisms of ABC-F mediated antibiotic resistance. In an antibiotic-susceptible bacterium, translation is inhibited by the antibiotic, leading to growth arrest (centre). ABC-F proteins (green) are proposed to rescue translation from inhibition either by recruiting an unknown membrane-spanning protein to promote active efflux of the antibiotic (left), or, by displacing the antibiotic from its ribosomal binding site (right).

### Results

#### ABC-F proteins protect staphylococcal translation from antibiotic inhibition *in vitro*

We initially sought to determine whether ABC-F proteins could mediate antibiotic resistance *in vitro,* under conditions where efflux was not possible. To this end, staphylococcal S30 extracts were generated, and used to establish *in vitro* transcription-translation (T/T) assays. Two phylogenetically-distant ABC-F proteins, Vga(A) and Lsa(A), were heterologously expressed in *E. coli*, purified to homogeneity, and tested for their ability to protect T/T assays from antibiotic inhibition. Both proteins were shown to mediate dose-dependent restoration of translational activity (Figure 2A).

To provide confirmation that the observed ability of ABC-F proteins to protect *in vitro* translation from antibiotics reflected the activity of these proteins in whole cells, we

successfully recapitulated in the T/T assay three phenotypes that have been associated with these proteins in bacteria.

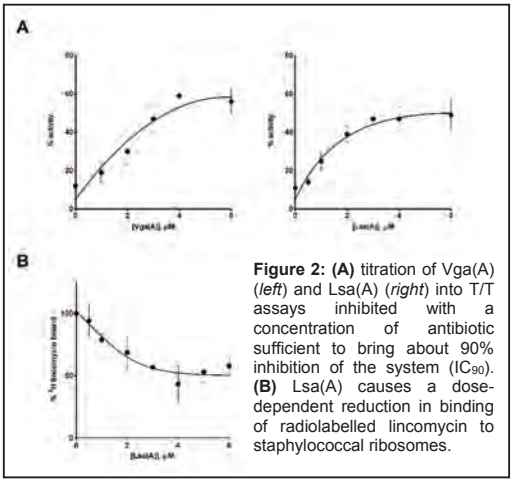


**Figure 2: (A)** titration of Vga(A) (*left*) and Lsa(A) (*right*) into T/T assays inhibited with a concentration of antibiotic sufficient to bring about 90% inhibition of the system ($IC_{90}$). **(B)** Lsa(A) causes a dose-dependent reduction in binding of radiolabelled lincomycin to staphylococcal ribosomes.

**ABC-F proteins directly displace antibiotics from the ribosome**

To assess whether ABC-F proteins protect the translation apparatus from antibiotic-mediated inhibition by directly interfering with the interaction between the antibiotic and the ribosome, we evaluated the ability of the Lsa(A) protein to prevent binding of radiolabeled ($^3$H) lincomycin to purified staphylococcal ribosomes. Pre-incubation of Lsa(A) with ribosomes prior to the addition of $^3$H-lincomycin resulted in a dose-dependent decrease in subsequent binding of the drug to ribosomes (Figure 2B). Subsequently, we also examined the ability of Lsa(A) to displace pre-bound $^3$H-lincomycin from ribosomes, establishing that addition of an 8-fold molar-excess of Lsa(A) to ribosomes pre-incubated with drug resulted in a substantial (~73%) reduction in ribosome-associated $^3$H lincomycin. Collectively, our results show that the ABCF-F proteins mediate antibiotic resistance through ribosomal protection.

**A model for ABC-F mediated ribosomal protection**

Although the molecular detail underlying this resistance mechanism is yet to be elucidated, we are able to propose a model by which ABC-F proteins may mediate ribosomal protection. This model is built upon the recent structural and functional characterisation of an innate *Escherichia coli* ABC-F protein that does not confer antibiotic resistance but instead acts as a translation factor that responds to the ATP/ADP ratio within the cell. This protein, EttA, binds the ribosome at the exit site and inserts its interdomain linker towards the peptidyl-transferase centre (PTC), inhibiting translation when cellular energy levels are low. We propose that ABC-F proteins mediate antibiotic resistance by binding to the ribosome in the same mode as EttA, thereby allowing their interdomain linker, which is extended by ~30aa in comparison to EttA, to contact the antibiotic binding sites at the PTC and cause either direct or allosteric displacement of the drug. Support for this model is found in the observation that mutations within the linker domain can alter the resistance phenotype of ABC-F proteins. Future studies will focus on gaining structural insights into the ABC-F: ribosome complex.

**Publications**

Sharkey L.K.R., Edwards T.A. & O'Neill A.J. (2016) ABC-F proteins mediate antibiotic resistance through ribosomal protection. *mBio* **7**:e01975-15.

**Funding**

This work was funded by the BBSRC.

## Transcellular stress signalling: How proteotoxic stress is communicated between different tissues in *C.elegans*

Daniel O'Brien, Rebecca Aston, Vijay Shanmugiah, David Westhead and Patricija van Oosten-Hawle

### Introduction

In all biological systems, cells throughout their lifetime are exposed to different physiological and environmental stress conditions that lead to protein damage and cellular dysfunction – and ultimately disease. Cumulative protein misfolding and aggregation is one of the hallmarks implicated in the pathologies of misfolding diseases associated with neurodegeneration, including Alzheimer's disease, amyotrophic lateral sclerosis, Huntington's disease and Parkinson's disease, as well as cancer, diabetes and several myopathies. Maintaining a healthy cellular proteome is crucial to cellular viability. This is achieved by the proteostasis network, which integrates protein biogenesis, protein folding by molecular chaperones, as well as clearance mechanisms and stress response pathways. The significance of cell protective stress response mechanisms is now widely appreciated to not just act at the level of single cells, but at the "multicellular" level, throughout an entire organism. Thus, evolutionary conserved stress responses such as the heat shock response initiate inter-cellular communication that allows protective chaperone expression to be signalled and spread from one tissue to another, a process known as transcellular chaperone signalling (TCS). One key observation of TCS is that an imbalance of proteostasis in only one tissue (e.g. neurons) through altered expression of the major chaperone hsp90, can lead to an upregulated hsp90 chaperone response in receiving tissues that is spread throughout the organism (Figure 1). How these transcellular chaperone response mechanisms function at the molecular level however remains an open question to date.

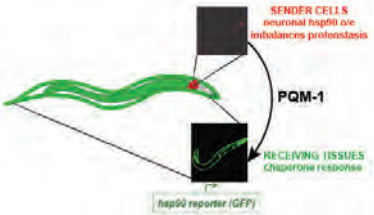


**Figure 1:** model explaining transcellular chaperone signalling (TSC) in *C. elegans*

### Results

This project aims to determine how transcellular chaperone signalling is mediated between different tissues. To address this question, we utilised a systems-wide approach using RNA-Seq and further genetic analysis of *C. elegans* strains where TCS is activated through increased hsp90 expression in either neurons, intestine or bodywall muscle. This approach allowed us to identify the GATA transcription factor PQM-1 as a mediator of transcellular chaperone signaling in *C. elegans.* Systemic depletion of *pqm-1* by RNAi in these strains where TCS is activated through increased hsp90 expression, leads to reduced TCS that is measured by the *hsp90p::GFP* reporter expression level (Figure 2). While PQM-1 is known to be required for life span extension in *C. elegans*, its precise role in the regulation of proteostasis is however unknown. Our data shows that *C. elegans* depleted for *pqm-1* exhibit increased sensitivity to heat stress, similar to animals expressing mutant *hsf-1*, the master regulator of stress

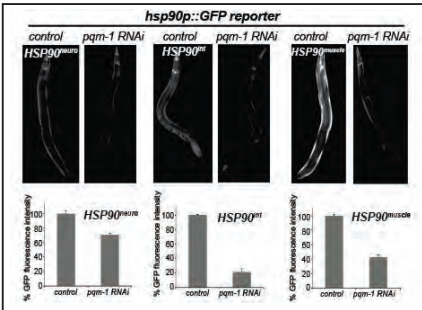


**Figure 2:** RNAi mediated knockdown of *pqm-1* reduces TCS. *pqm-1* RNAi in tissue-specific HSP90 overexpression strains reduces transcellular *hsp90p::GFP* reporter expression. Fluorescence intensity is measured by ImageJ.

responses (Figure 3A). Furthermore, to test the requirement of PQM-1 for the maintenance of proteostasis we took advantage of *C. elegans* expressing Q35::YFP in the bodywall muscle. These strains are used as models for polyQ diseases (e.g. Huntington's Disease). Importantly, aggregation of Q35 is dependent on the efficiency of the proteostasis network, thus these strains also provide a measure for the efficiency of the proteostasis network. Interestingly, the absence of PQM-1 accelerates Q35 aggregation by 1.5-fold, suggesting that PQM-1 is required for the maintenance of proteostasis (Figure 3B). Current efforts are aimed at elucidating how PQM-1 "signals" TCS from one tissue to another to modulate organismal proteostasis.

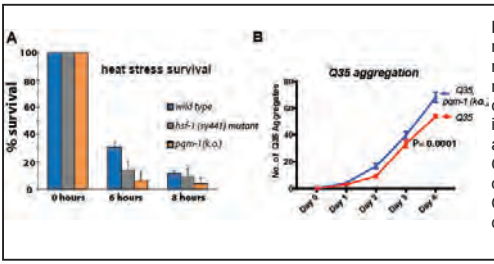


**Figure 3:** PQM-1 is required for the maintenance of proteostasis. **(A)** PQM-1 is required for heat stress survival. A null mutant of *pqm-1* is sensitive to heat stress, comparable to a *hsf-1* mutant that cannot induce the heat shock response. **(B)** Q35 aggregation kinetics in *C.elegans* expressing Q35::YFP in the bodywall muscle. Depletion of *pqm-1* leads to increased accumulation of Q35 aggregates when compared to Q35 control animals. P=0.0001.

**Publications**

O'Brien D. & van Oosten-Hawle P. (2016). Regulation of cell nonautonomous proteostasis in metazoans. *Essays Biochem.* **60**:133-142.

**Funding**

We are grateful for support from the Wellcome Trust, the NC3Rs, and a BBSRC and MRC doctoral studentship.

**Collaborators**

*University of Leeds:* D. Westhead.

## Proteins under the computational microscope: folding, disorder, mechanics, dynamics and self-assembly

Emanuele Paci

Our research focuses on the development and application of novel computational tools to investigate structure and functional dynamics of biomolecules. One of our aims is fully exploit the wealth of structural data obtained with the advanced experimental probes available at Astbury. Most of our research involves experiments performed in collaboration with colleagues from the Astbury Centre and further afield.

One topic where models and simulations provided information that experiments cannot provide and suggestions for more insightful experiments relates to the structural propensity of polypeptides with specific sequence patterns. These range from the simplest repeat, a homopolypeptide, i.e., repeats of the same aminoacid, or repeats short patterns of amino acids. While polymer theory suggests that most of these sequences are unstructured we found evidence of the emergence of structural preferences and unique, sequence and length dependent, dynamical properties. In collaboration with Michelle Peckham at Astbury and Ben Schuler in Zurich we are exploring the properties of polyampholyte repeat sequences that are strongly helical using FRET and simulation.

Characterization of disordered states is one of the current focuses of our group. In this context, in collaboration with Jane Clarke (Cambridge) we explored the role of an intrinsically disordered domain in the folding of SasG, a protein that forms extended fibrils in the surface of *Staphylococcus aureus* and promotes host adherence and biofilm formation (Gruszka 2015 and 2016). Much of our work involves molecular simulation of the dynamics and interactions within and between protein systems. Data generated from simulation are used to interpret and direct experimental measurements such as hydrogen-deuterium exchange probed by mass spectroscopy (in collaboration with Roman Tuma), the response to mechanical of proteins that evolutionary adapted to function in extreme environments (Tyck 2016).

Another challenge undertaken in our group (in collaboration with Bruce Turnbull) is rational design of capsids (for various practical purposes and to assess our understanding of the forces involved in capsid formation and stability). We developed an original approach to estimate the stability and effect of mutations on capsids of known structure (a preliminary step to the design of novel capsids) that has been shown to be accurate in an application to lumazine synthase, a non-viral protein that form capsids in several organisms (Hickman 2015).

In collaboration with Stephen Muench (Astbury) we used simulation to characterize the flexibility of the peripheral stalk of prokaryotic rotary A-ATPases. Structures have been reported for the peripheral stalk, thought to represent conformational states of the stator during different stages of rotary catalysis. We showed instead that those structures are conformers

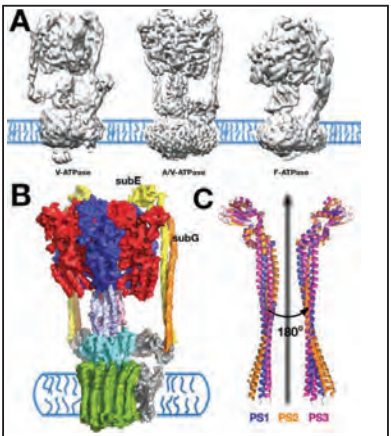


**Figure 1:** structural organization of the prokaryotic A-ATPase. **(A)** electron-microscopy 3D maps of ion-pumping rotary ATPases: V-ATPase (left), A/V- ATPase (middle) and F-ATPase (right). **(B)** two copies of the peripheral stator EG complex (colored in yellow and orange) connect the catalytic subunits A/B (subunits colored in blue and red) with the membrane-bound subunit I (colored in grey). **(C)** superposition of the three peripheral stator EG conformers PS1, PS2 and PS3.

explored through thermal fluctuations, but not stable states. The coiled coil tail domain has a high persistence length (i.e., it is surprisingly rigid), but retains the ability to adapt to different conformational states through the presence of two hinge regions and accommodate structural changes in the catalytic domain whilst resisting the large torque generated by catalytic cycling. These results are important to understand the role the stators play in the rotary-ATPase mechanism.

In our group we also develop and implement methods to determine free energy changes along pathways connecting different conformational states of proteins. One particular topic on which we have been working for the past 20 years is that of interpreting single molecule force spectroscopy experiments. We are currently collaborating with David Brockwell to interpret measurements of the response to force of the transmembrane machinery that transports vitamin $B_{12}$ and the structural propensity of disordered regions of the same machinery from simulation and small angle X-ray scattering data.

**Publications**

Tych K.M., Batchelor M., Hoffmann T., Wilson M.C., Hughes M.L., Paci E., Brockwell D.J. & Dougan L. (2016) Differential effects of hydrophobic core packing residues for thermodynamic and mechanical stability of a hyperthermophilic protein. *Langmuir* **32**:7392-7402.

Tych K.M., Batchelor M., Hoffmann T., Wilson M.C., Paci E., Brockwell D.J. & Dougan L. (2016) Tuning protein mechanics through an ionic cluster graft from an extremophilic protein. *Soft Matter* **12**:2688-2699.

Papachristos K., Muench S.P. & Paci E. (2016) Characterization of the flexibility of the peripheral stalk of prokaryotic rotary A-ATPases by atomistic simulations. *Proteins* **84**:1203-1212.

O'Connor M., Paci E., McIntosh-Smith S. & Glowacki D.R. (2016) Adaptive free energy sampling in multidimensional collective variable space using boxed molecular dynamics. *Faraday Discuss.* **195**:395-419.

Gruszka D.T., Mendonca C., Paci E., Whelan F., Hawkhead J., Potts J.R. & Clarke J. (2016) Disorder drives cooperative folding in a multidomain protein. *Proc. Natl. Acad. Sci. USA.* **113**:11841-11846.

**Collaborators**

*University of Leeds:* B. Turnbull, D. Brockwell, L. Dougan, R. Tuma, S. Muench, M. Peckham.
*External:* J. Clarke (Cambridge), A. Plückthun (Zurich), D. Glowacki (Bristol).

## How myosin 10 travels to filopodia tips

Ruth Hughes, Marcin Wolny, Matthew Batchelor, Francine Parker, Brendan Rogers, Glen Carrington, Marta Kurzawa, Tom Baboolal and Michelle Peckham

### Introduction

Our research interests focus on the cytoskeleton in both muscle and non-muscle cells. This year, we our research has ranged from investigating the effects of mutations in the Z-disc protein α-actinin in cardiac muscle cells to understanding how myosin 10 traffics to the filopodial tip in non-muscle cells. We continue to developm in super-resolution imaging, to image proteins within primary cilia in mammalian cells (with Colin Johnson, in the faculty of Medicine and Health), recently funded from a joint BBSRC-SFI grant. A collaboration with the company Orla Technologies, has led to the development of novel surfaces that better promote muscle differentiation in culture.

Myosin 10 (Myo10) is part of the myosin super-family, which consists of 38 genes, arranged into 12 classes. Myo10 is essential for the formation of filopodia; thin actin rich projections formed at the cell edge, which can act as pathfinders in migrating cells. Myo10 is important for both breast and prostate cancer metastasis. Our question was, how does this myosin find its way to the tip of filopodia? To answer this question, we performed live cell total internal reflection microscopy (TIRFM) to image fluorescently tagged Myo10, and determine its dynamics (in collaboration with Dr Justin Molloy and his group at the Crick).

### Results

Our imaging showed how eGFP-Myo10 (Fig. 1a) moves to and accumulates at the tip of filopodia (Fig. 1 b, c). Single molecules corresponding to eGFP-Myo10 were observed (Fig.

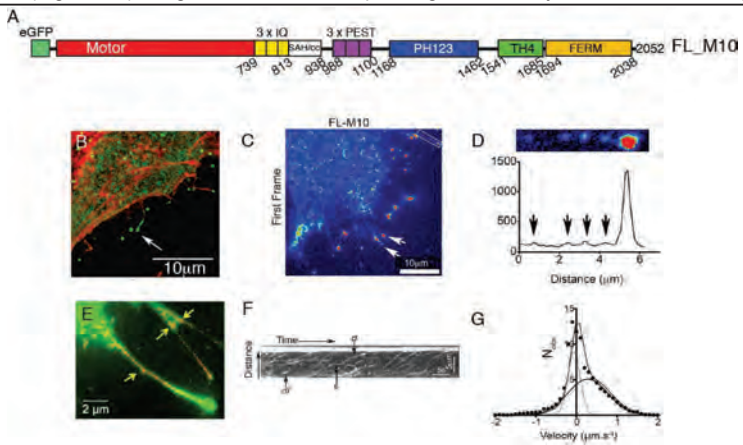


**Figure 1:** eGFP-Myosin 10 and its behaviour in live cells. **(A)** eGFP-Myo10 construct **(B)** eGFP-Myo10 localises to the tips of filopodia (arrow) (confocal image). **(C)** the first frame of a TIRFM image. Arrows show Myo10 at filopodial tips. **(D)** the boxed filopodium in C is shown shows fluorescent spots within the filopodium that correspond to single molecules of eGFP-myo10 (arrowed below). **(E)** All the fluorescent object localisations obtained during a video recording, used to generate a super-resolution image of the paths taken by eGFP-Myo10 within a live cell. Individual spot localisations (red) are superimposed over the average fluorescence data (green). **(F)** a kymograph of eGFP-Myo10 motility within a filopodium. The tracks show a mixture of directed (d), stalled (s) and diffusive (df) motion. **(G)** Instantaneous velocities of eGFP-Myo10 within a filopodium, showing two distributions: one with an average instantaneous velocity close to zero (stalled and diffusive behaviours) and the other with an average positive velocity, showing directional (motorized) motion toward the filopodial tip.

1d) and the localisations of these molecules were tracked. A super-resolution image of eGFP-Myo10 was generated by accumulating all of the fluorescent object localisations obtained during a video recording (Fig. 1e). The diameter of the filopodium was estimated from an analysis of the average fluorescence image (shown in green) and the estimate obtained by the individual FL-M10 spot localizations (red). Both approaches show that the filopodial diameter estimated towards the base is similar. However, this estimate starts to diverge within the shaft of the filopodium. Super-resolution data shows that FL-M10 molecules are confined within an average filopodial diameter of 116.5+/-18 nm (full-width at half maximum height) whereas the diffraction limited, average fluorescence image reports 357+/-28 nm (n=39). The super-resolution image additionally shows interesting subfeatures in the super-resolved image. These include a bulge on the side of one filopodium and a connecting bridge between two filopodia on the upper right (yellow arrows). The image also shows short tracks of eGFP-Myo10 as they accumulate in the cell body just before entering the filopodium.

Analysis of the movement of eGFP-Myo10 within the filopodium demonstrates that the myosin exhibits three main types of movement: directed motion (df), diffusive motion (d) and stalled motion (s) as the molecules move to the tip (Fig. 1f). Single particle tracking was used to quantify the motion of individual particles. Plotting the instantaneous velocities showed the complex behaviour of these molecules, in which the distribution required a fit to two Gaussian functions. One type of motion had an average instantaneous velocity close to zero (i.e. stalled and diffusive behaviors), the other had an average positive velocity, indicating directional (motorized) motion toward the filopodial tip. Overall, our work demonstrated that a combination of diffusive and active movements is required to rapidly target myosin 10 to the filopodial tip. Further work is underway to understand how this motility behaviour is regulated.

**Publications**

Peckham M. (2016) How myosin organization of the actin cytoskeleton contributes to the cancer phenotype. *Biochem. Soc. Trans.* **44**:1026-1034.

Parker F., White K., Phillips S. & Peckham M. (2016) Promoting differentiation of cultured myoblasts using biomimetic surfaces that present alpha-laminin-2 peptides. *Cytotechnology* **68**:2159-2169.

Lambacher N.J., Bruel A.L., Van Dam T.J.P., Szymanska K., Slaats G.G., Kuhns S., McManus G.J., Kennedy J.E., Gaff K., Wu K.M.*, et al.* (2016) TMEM107 recruits ciliopathy proteins to subdomains of the ciliary transition zone and causes Joubert syndrome. *Nat. Cell Biol.* **18**:122-131.

Haywood N.J., Wolny M., Rogers B., Trinh C.H., Yu S.P., Edwards T.A. & Peckham M. (2016) Hypertrophic cardiomyopathy mutations in the calponin-homology domain of ACTN2 affect actin binding and cardiomyocyte Z-disc incorporation. *Biochem. J.* **473**:2485-2493.

Baboolal T.G., Mashanov G.I., Nenasheva T.A., Peckham M. & Molloy J.E. (2016) A combination of diffusion and active translocation localizes myosin 10 to the filopodial tip. *J. Biol. Chem.* **291**:22373-22385.

**Funding**

Our work was funded by BBSRC, MRC and the British Heart Foundation.

**Collaborators**

*External:* G. Mashanov and J. Molloy (The Crick Institute, London).

## Insights into the folding mechanisms of periplasmic chaperones

Bob Schiffrin, Julia Humes, Anton Calabrese, Paul Devine, Sarah Harris, Alison Ashcroft, David Brockwell and Sheena Radford

### Introduction

Chaperones are a large, diverse class of proteins essential for maintaining proteostasis. Most proteins in the cell require chaperones for correct folding, and most chaperones interact with an array of clients. During times of cellular stress chaperones are important in assisting protein folding and preventing aberrant interactions which could lead to aggregation. By contrast with the well-studied chaperone systems which require ATP and other co-chaperones to promote folding (such as the chaperonins and Hsp70s) the mechanisms by which ATP-independent chaperones function remain unclear, despite their fundamental biological importance. Here we have studied two ATP-independent chaperones found in the periplasm of gram-negative bacteria: Skp and Spy. Skp is a 16 kDa homotrimer, which selectively binds β-barrel outer membrane proteins (OMPs) within a hydrophobic cavity, facilitating their transport across the periplasm before folding into the outer membrane (OM). Spy is 16 kDa homodimer with a cradle-like structure, which is dramatically upregulated to concentrations of ~2 mM under stress conditions. Key questions include: (1) how do substrates bind chaperones? (2) what are the conformations of chaperones and substrates during binding? and (3) and how are substrates released? Our work aims to gain insight into the mechanisms of ATP-independent chaperone action using a broad range of *in vitro* biochemical and biophysical techniques, as well as computer simulation and modelling.

### Results

Skp interacts with a >30 OMPs *in vivo* including many OMPs which appear to be too large to be accomodated within the Skp hydrophobic cavity, yet all models suggested a 1:1 Skp:OMP stoichiometry. To investigate how Skp is able to accommodate its larger substrates we used kinetic folding assays, native mass spectrometry and molecular dynamics (MD) simulations to examine the interactions of Skp with a range of OMPs of different size. Kinetic assays showed that greater Skp:OMP molar ratios are required to prevent the folding of 16-stranded OMPs compared with those containing 8 β-strands in their native state. Consistent with these results Electrospray Ionisation Mass Spectrometry (ESI-MS) combined with Ion Mobility Spectrometry (IMS) revealed that Skp forms multivalent 2:1 Skp:OMP complexes with larger OMPs, and that binding of OMPs of increasing size requires dynamic expansion of the Skp hydrophobic cavity. We furher used modelling and MD simulations to provide the first glimpses into possible structures of these multivalent complexes. (Figure 1).

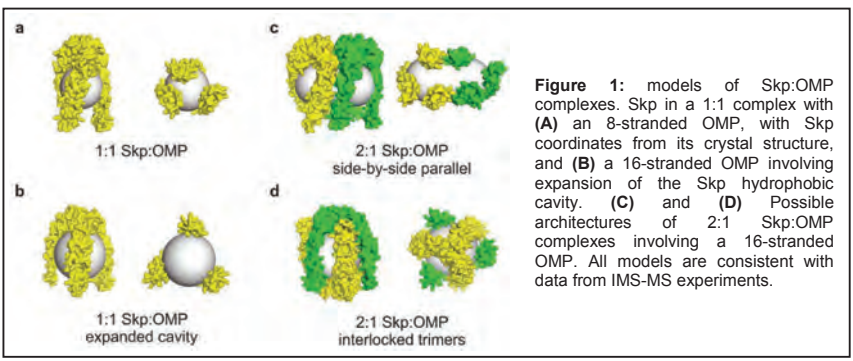


**Figure 1:** models of Skp:OMP complexes. Skp in a 1:1 complex with **(A)** an 8-stranded OMP, with Skp coordinates from its crystal structure, and **(B)** a 16-stranded OMP involving expansion of the Skp hydrophobic cavity. **(C)** and **(D)** Possible architectures of 2:1 Skp:OMP complexes involving a 16-stranded OMP. All models are consistent with data from IMS-MS experiments.

To study the Spy chaperone the small, four-helix bundle protein Im7 was chosen as the client protein. ITC experiments revealed that Spy is able to bind native folded Im7, in addition to mutants which are either partially or fully unfolded. We used stopped-flow fluorescence kinetic experiments in which folded or unfolded wild-type Im7 (in 8 M urea), or destabilised Im7 mutants, were rapidly diluted in the presence of increasing concentrations of Spy. The data showed that Spy rapid associates with client proteins to prevent aggregation. Remarkably, globally fitting of all fluorescence data to different kinetic models (Figure 2) revealed that Im7 is able to fold and unfold while in complex with Spy, providing the first evidence that substrates can fold while remaining bound to a chaperone.

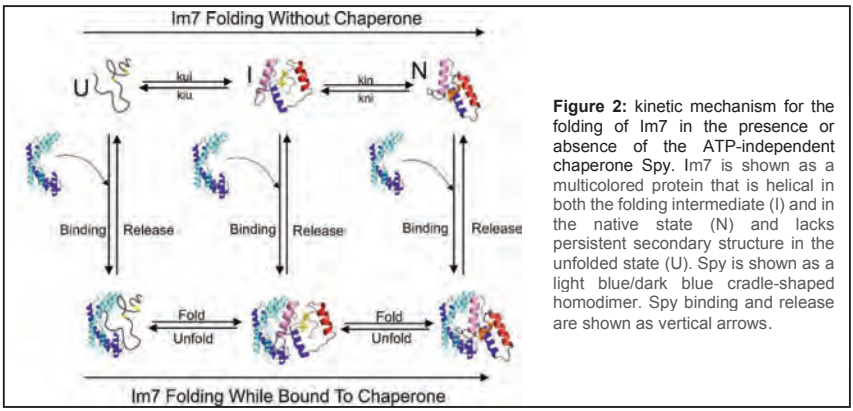


**Figure 2:** kinetic mechanism for the folding of Im7 in the presence or absence of the ATP-independent chaperone Spy. Im7 is shown as a multicolored protein that is helical in both the folding intermediate (I) and in the native state (N) and lacks persistent secondary structure in the unfolded state (U). Spy is shown as a light blue/dark blue cradle-shaped homodimer. Spy binding and release are shown as vertical arrows.

We are now using additional experimental techniques to map client-chaperone interactions in more detail, as well as expanding the range of chaperones and client proteins studied. Our aim is to gain further insight into the molecular mechanisms of periplasmic folding factors, including the chaperone-mediated delivery of OMP substrates to the β-barrel Assembly Machinery (BAM) for folding in the OM.

**Publications**

Schiffrin B., Calabrese A.N., Devine P.W.A., Harris S.A., Ashcroft A.E., Brockwell D.J. & Radford S.E. (2016) Skp is a multivalent chaperone of outer-membrane proteins. *Nat. Struct. Mol. Biol.* **23**:786-793.

Stull F., Koldewey P., Humes J.R., Radford S.E. & Bardwell J.C.A. (2016) Substrate protein folds while it is bound to the ATP-independent chaperone Spy. *Nat. Struct. Mol. Biol.* **23**:53-58.

**Funding**

This work was funded by the BBSRC and the NIH.

**Collaborators**

*External:* J. Bardwell (NIH, USA).

## The molecular details of amyloid fibril-glycosaminoglycan binding

Katie Stewart and Sheena Radford

### Introduction

Amyloid plaques contain an assortment of molecules that co-localize generically with amyloid fibrils, including metal ions, nucleic acids, and glycosaminoglycans (GAGs), linear negatively charged carbohydrates. Previous work from our laboratory indicated that the GAG heparin interacts differently with Aβ40 fibrils with different structures, binding strongly to a three-fold symmetric morphology ($K_d$= 34 μM ± 12 μM), and arguing that structure, in addition to sequence, plays a role in heparin:fibril binding. Using solid-state NMR (SSNMR) and an *in vitro* binding assay, we have recently mapped the molecular details of binding from the perspective of both the Aβ40 fibril and the GAG. Our results reveal a tight and specific interaction, with the heparin chain fully constrained in contact with the fibril. Binding involves a cluster of positive charges on the fibril aligning with specific negatively charged sulfates on low molecular weight heparin (LMWH). The tight coordination observed between 3Q amyloid fibrils and LMWH illuminates how differences in fibril or GAG polymorphs may contribute to the diversity in manifestation and progression of Alzheimer's disease.

### Detection of octasaccharide binding to Aβ40 3Q fibrils along the fibril axis.

Aβ40 fibrils with a 3Q morphology were prepared by seeded elongation and their morphology was verified by SSNMR. To map the LMWH binding site, a $^{13}$C-labelled octasaccharide construct (a shorter proxy of LMWH with similar binding to 3Q fibrils) was added to $^{15}$N-labelled 3Q fibrils (Figure 1A), allowing interaction crosspeaks to be mapped by SSNMR upon fibril:octasaccharide binding. The spectra indicated that the GAG was fully constrained in the presence of 3Q fibrils, suggesting that the LMWH and 3Q fibril share multiple contacts along the fibril axis (Figure 1A and 1B). Chemical shift differences in the presence and absence of the octasaccharide suggested in particular that one or more histidine residues on the 3Q fibril are involved in binding.

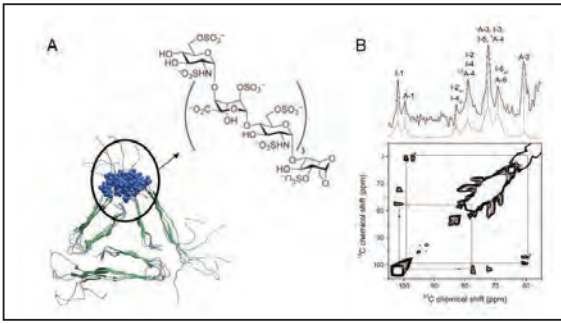


**Figure 1:** heparin octasaccharide-binds to Aβ40 3Q fibrils. **(A)** Proposed binding between 3Q fibrils (green, from PDB file 2LMQ) and LMWH (blue, with one binding site shown), and a detailed view of the $^{13}$C-labelled octasacchride shown above. **(B)** $^{13}$C CP-MAS spectrum of the octasaccharide bound to 3Q fibrils at 4 °C; actual (black) and simulated (red, upper) and $^{13}$C-$^{13}$C spectrum with DARR mixing time of 20 ms (lower).

### The role of amino acid sidechains on fibril:heparin binding.

To investigate the role of positively charged residues on the 3Q fibril as heparin binding sites, single substitution variants of Aβ40 were developed throughout the protein. Binding of 3Q-seeded variants was measured using an *in vitro* assay in which the LMWH bound to variant Aβ40 fibrils was pelleted by centrifugation and the saccharide content in the supernatant was quantified by enzymatic digestion with heparinase II followed by UV spectroscopy. The largest ΔΔG° of binding occurred in residues located at the N-terminus and central loop of Aβ40. In the 3Q fibril structure, these regions are spatially adjacent, forming a cluster of positively charged residues which appear vital for LMWH binding (Figure 2A).

**The role of heparin substituents on fibril:heparin binding.**
We assessed the role of the heparin molecule in binding amyloid fibrils by removing sulfate groups from the heparin chain systematically and testing binding to WT 3Q fibrils by the *in vitro* assay. The results indicated that removal of the 2-O-sulfate did not reduce binding, but removal of the 6-O-sulfate eliminated heparin binding (Figure 2B). The NS sulfate also reduced binding, but the effects varied by the substitution, indicating that the spatial arrangement of negative charges on heparin is important. These results were further confimed by seeded aggregation kinetics (using thioflavin T fluoresence), in which the 3Q-seeded Aβ40 aggregation rate changed in the presence of LMWH but not in the presence of heparin without the NS and 6-O sulfates versus Aβ40 seeded without heparin.

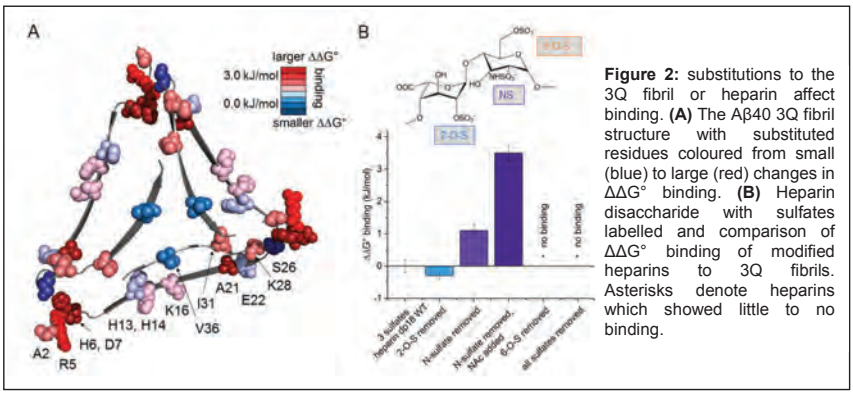


**Figure 2:** substitutions to the 3Q fibril or heparin affect binding. **(A)** The Aβ40 3Q fibril structure with substituted residues coloured from small (blue) to large (red) changes in ΔΔG° binding. **(B)** Heparin disaccharide with sulfates labelled and comparison of ΔΔG° binding of modified heparins to 3Q fibrils. Asterisks denote heparins which showed little to no binding.

**Tight and specific coordination are key to fibril:heparin interaction.**
Our results suggest that the interaction between 3Q fibrils of Aβ40 and heparin are driven by complementary charges packed into specific arrangements and are not simply the result of electrostatic patterning, as is the case in other accessory molecules such as nucleic acids. Instead, the tight and specific binding we observe is the result of a precise and compatible alignment of charges. These results suggest that the prevalence of plaque-associated GAGs may be dictated by a patient's fibril morphology(ies), and may play a role in the progression and severity of Alzheimer's disease.

**Publications**
Stewart K.L., Hughes E., Yates E.A., Akien G.R., Huang T.Y., Lima M.A., Rudd T.R., Guerrini M., Hung S.C., Radford S.E., *et al.* (2016) Atomic details of the interactions of glycosaminoglycans with amyloid-beta fibrils. *J. Am. Chem. Soc.* **138**:8328-8331.

**Funding**
This work was funded by the BBSRC.

**Collaborators**
*External:* D. Middleton (Lancaster University), E. Yates (University of Liverpool), S.-C. Hung (Genomics Research Center, Academia Sinica, Taiwan).

## Lateral opening in the intact β-barrel assembly machinery captured by cryo-EM

Anna Higgins, Matthew Iadanza, Bob Schiffrin, Antonio Calabrese, Alison Ashcroft, David Brockwell, Sheena Radford and Neil Ranson

### Introduction

Outer membrane proteins (OMPs) mediate the survival and pathogenicity of Gram negative bacteria. The biogenesis of these proteins is complex, however, as they are synthesised in the cytoplasm, are transported by chaperones across the periplasm, and must then be inserted and folded correctly into the bacterial outer membrane in the absence of ATP. The β-barrel assembly machinery (BAM) complex of *E.coli* is a ~203 kDa assembly of five proteins (BamA-E) that enables the membrane insertion and folding of substrate OMPs on a physiological timescale. Despite the availability of crystal structures for each of the five BAM subunits, various subcomplexes, OMP substrates, and most recently the full *E.coli* BAM complex, the mechanism of this vital protein assembly is unknown. An understanding of how BAM-mediated OMP folding and insertion occurs will provide insight into OMP biogenesis in *E. coli*, and potentially of homologous proteins in the outer membranes of mitochondria and chloroplasts. Also, because BAM is surface-located, essential, and conserved, it is an attractive potential target for the development of novel antibacterials. Here we have used a variety of structural and biochemical tools to probe the nature of BAM-assisted OMP folding.

### Results

The β-barrel of BamA is known to exist in two conformations: in the first it is sealed on its extracellular face and open to the periplasm, and in the second there is a separation of the β1 and β16 β-strands of the β-barrel, creating a structure “lateral open” to the outer membrane and extracellular face. Such conformational changes are significant for several reasons. Firstly as BamA is hypothesised to assist substrate folding through its lateral opening, such flexibility may be critical for the BamA functional cycle. Secondly, thus far lateral open conformations have only been observed in BAM crystal structures which lack the 42 kDa, β-propeller protein BamB, raising the possibility that changes in BamA may represent a gating reaction driven by BamB binding.

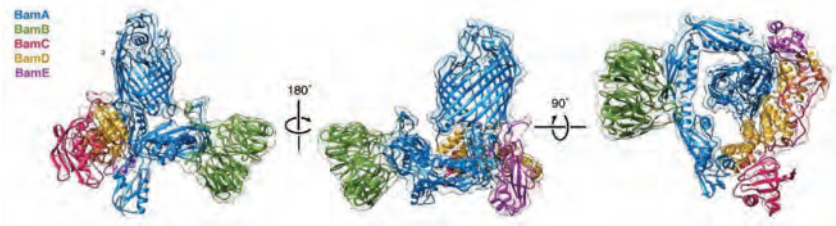


**Figure 1:** three views of a 4.9Å cryo-EM map of the BAM complex with a fitted psuedo-atomic model, showing the complex in the laterally open conformation in the presence of BamB.

Utilising the BAM complex recombinantly expressed and purified from *E.coli* outer membranes in DDM detergent micelles, we were able to elucidate the first cryo-electron microscopy structure of the full complex, at a resolution of 4.9 Å[1] (Fig. 1). The structure reveals distinct conformational changes relative to existing crystal structures and, for the first time, reveals interactions between BAM subunits and the detergent micelle, suggesting modes of communication between BAM and the lipid bilayer. Additionally, the structure reveals the intact BAM complex in which BamA is in a laterally-open conformation, with separation between the first (β1) and last (β16) strands of the barrel, in the presence of BamB-E. The suggestion that BamA lateral opening is important for activity in substrate folding has been supported by *in vivo* data showing that disulfide cross-linking of the strands is lethal in *E.coli*. To examine

whether lateral gating in BamA is required for BAM-mediated OMP folding *in vitro*, we created the same BamA mutants designed to cross-link β1-β16 and examined the ability of BAM containing mutant BamA to fold the substrate OmpT (Fig. 2a).

OmpT folding was assayed using a self-quenching fluorogenic reporter peptide which is cleaved by the correctly folded/membrane inserted endoprotease OmpT. In *E.coli* polar lipid liposomes correct folding of OmpT is known to require the presence of active BAM and the OMP-chaperone, SurA. While proteoliposomes reconstituted with the wild-type BAM, or containing a Cys-free BamA mutant show high levels of activity in folding OmpT, BAM proteoliposomes that incorporate disulfide cross-linked BamA show significantly lower activity (Fig. 2b,c), indicating that the disulfide cross-link across the β-barrel impairs, but does not prevent, BAM-mediated folding of OmpT *in vitro*. Consistent with this notion, addition of reducing agent rescues BAM activity to near wild-type levels.

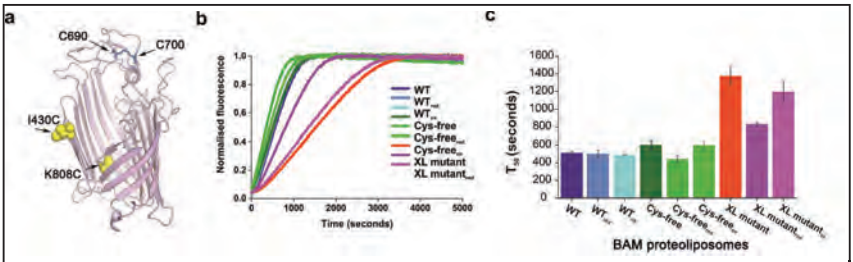


**Figure 2:** importance of BamA lateral gating in BAM complex function. **(A)** The position of the natural cysteines of BamA (replaced with Ser) are indicated with arrows, and those that were introduced to form a disulfide cross-link are indicated by yellow spheres. **(B)** Example traces of fluorescence due to OmpT folding comparing BAM proteoliposomes containing disulfide mutant (purple) BamA, wild-type (blue) and Cys-free (green) BamA in reduced and oxidised conditions. **(C)** Bar chart showing average half-time for each reaction.

Our functional assays provide the first *in vitro* evidence of the importance of BamA lateral gating in BAM function, demonstrating that lateral gating of BamA diminishes, but does not eradicate, the ability of BAM to assist OmpT folding. Additionally the cryo-EM structure shows that BamA lateral opening occurs independently of BamB binding. Current work is focusing on using other membrane mimetics for cryo-EM structure and other functional assays to determine the molecular mechanism(s) of BAM function.

**Publications**

Iadanza M.G., Higgins A.J., Schiffrin B., Calabrese A.N., Brockwell D.J., Ashcroft A.E., Radford S.E. & Ranson N.A. (2016) Lateral opening in the intact β-barrel assembly machinery captured by cryo-EM. *Nat. Commun.* **7**:12865.

**Funding**

This work was funded by The Wellcome Trust and the BBSRC.

## Coordinate regulation of antimycin and candicidin biosynthesis

Thomas McLean and Ryan Seipke

### Introduction

*Streptomyces* species produce an incredible array of high-value specialty chemicals and medicinal therapeutics. A single species typically harbours ~30 biosynthetic pathways, but only a few them are expressed in the laboratory; thus, poor understanding of how natural-product biosynthesis is regulated is a major bottleneck in drug discovery. Antimycins are potent antifungal compounds made by *Streptomyces* bacteria that are also selective inhibitors of the Bcl-2/Bcl-$x_L$-family of anti-apoptotic proteins which are often over-produced in drug-resistant cancers. Antimycins are produced by a hybrid non-ribosomal peptide synthetase / polyketide synthase biosynthetic pathway which we identified and characterised in *Streptomyces albus*. The biosynthetic gene cluster consists of 15 genes organised into three operons: *antBA*, *antCDE*, *antFG* and *antHIJKLMNO.* The gene cluster harbours a single cluster-situated regulator, an orphan alternative RNA polymerase sigma factor encoded by *antA* ($\sigma^{AntA}$). $\sigma^{AntA}$ regulates the expression of *antFG* and *antHIJKLMNO,* which direct the biosynthesis and activation of the 3-formamidosalicylate precursor, but not *antBA* or *antCDE*. Here we show that FscRI co-ordinately regulates production of both candicidin and antimycin.

### Results

A series of bioinformatics analyses suggested that FscRI may regulate *antBA* and *antCDE*. To test this hypothesis, we deleted the *fscRI* gene in *Streptomyces albus* using CRISPR/Cas9 genome editing and tested the resulting mutant (Δ*fscRI*) for the production of antimycins. As predicted, the Δ*fscRI* strain could no longer produce antimycins, a phenotype which we were able to rescue by ectopically expressing fscRI from a constitutive promoter. We then performed chromatin immunoprecipitation sequencing using a 3xFLAG-tagged variant of FscRI. The results revealed that 3xFLAG-FscRI binds to the *antBA* and *antCDE* promoter regions *in vivo*. Our study provides direct *in vivo* evidence of the cross-regulation of disparate biosynthetic gene clusters specifying unrelated natural products and expands the paradigmatic understanding of the regulation of secondary metabolism.

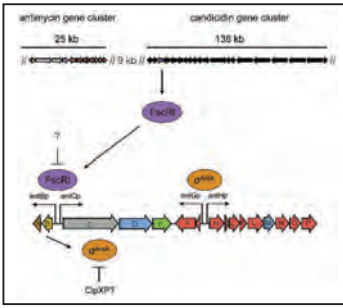


**Figure 1:** model for the regulation of antimycin biosynthesis: **(top)** the relative locations of the antimycin and candicidin gene clusters in the *S. albus* chromosome. **(bottom)** FscRI activates transcription of *antBA* and *antCDE*, which results in production of the core AntC/AntD NRPS/PKS megasynthase and production of the discrete acyltransferase AntB and AntA, which in turn activates transcription of the ketoreductase *antM* and nine genes (*antFGHIJKLNO*) required for the biosynthesis and activation of the 3-formamidosalicylate precursor utilised by AntC. AntA does not possess a cognate anti-sigma factor and instead appears to be inactivated by the ClpXP protease.

### Publications

McLean T.C., Hoskisson P.A. & Seipke R.F. (2016) Coordinate regulation of antimycin and candicidin biosynthesis. *mSphere* **1**:e00305.

### Funding

This work was funded by the BBSRC.

### Collaborators

*External:* P. Hoskisson (University of Strathclyde).

## Study of sensory neurons of *C.elegans* using a microfluidic device

Jinyang Chung and Jung-uk Shim

### Introduction

*Caenorhabditis elegans* (*C.elegans*) is a roundworm in the phylum of nematode. It has a simple but highly developed neuron system. Especially, 12 pairs of anatomically symmetrical sensory neurons are located left and right side in the head. Among them, ASH neuron is known as a nociceptor to sense the osmotic, chemical and mechanical stimuli, which may likely damage the organism. And, ASE neuron is a functionally asymmetric chemosensory neurons e.g. sensing NaCl; ASEL responds to the increase of NaCl concentration and ASER to the decrease of it. However, it is challenging to investigate both neurons at once on a same focal plane with a typical microscope slide because the worm swam or/and crawled with its side orientated out-of-plane. The aim of this study is to develop an approach, which would enable us to immobilize C.elegans, control microenvironment and investigate its sensory neurons in dorso-ventral aspect. Here, we report that a microfluidic device have been developed to trap the worm, treat with the stimulus and image them from the side-view (dorso-ventral view). It has enabled us to observe a pair of the neurons in the same focal plane. A worm was genetically modified to express calcium indicator protein (GCaMP) in its ASH/ASE neurons, immobilized in the device and the stimulus (NaCl) was treated to the amphid of the worm.

### Results

#### Development of a microfluidic device

A microfluidic device has been developed by polishing the side of the channel in order to observe a pair of neurons in the same focal plane. The stimulus channel is asymmetrically placed in the device to secure the working distance of the objective lens. The entire device was built with PDMS; moulded PDMS block was covalently bound on other PDMS plate via the oxygen plasma treatment and the device was cut along the trap channel. The thickness of the PDMS from the surface of the side to the channel was approximately 2 mm, which was within the working distance of the microscope lens.

#### Response of ASH neurons to the stimulus through the side-view

The ASH-worm was injected and immobilized in the trap in the device by application of the external pressure. The device enables us to incubate the immobilized worm for more than 30 minutes. The amphid of the worm exposed to buffer/stimulus through the trap-orifice in the flowing channel. The stimulus (500 mM NaCl) is treated to the worm using the flow control system. Cell bodies of the neuron and dendrites elongated to the amphid are fluorescently visible and the intensity increases when the amphid touched the stimulus stream, which indicates Ca ion intake and the depolarization of the neuron.

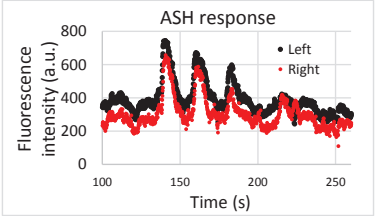


**Figure 1:** the fluorescence of GCaMP expressed on the ASH neuron is measured with the application of the stimulus (500 mM NaCl). Three repeated pulses (10 seconds on and 10 seconds off) of stimulus was applied.

### Collaborators

*University of Leeds:* C. Brittin, N. Cohen.

## Simvastatin and fluvastatin interact with human gap junction gamma-3 protein

Paul Taylor

### Introduction

Finding pleiomorphic targets for drugs allows new indications or warnings for treatment to be identified. As test of concept, we applied a new chemical genomics approach to uncover additional targets for the widely prescribed lipid-lowering pro-drug simvastatin.

### Results

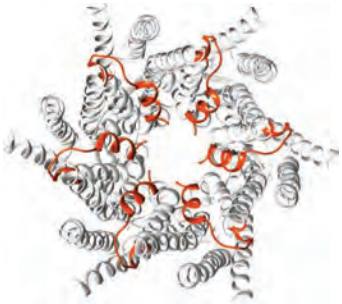

**Figure 1:** discovered *N*-terminal residues 1–25 (orange).

We used mRNA extracted from internal mammary artery from patients undergoing coronary artery surgery to prepare a viral cardiovascular protein library, using T7 bacteriophage. We then studied interactions of clones of the bacteriophage, each expressing a different cardiovascular polypeptide, with surface-bound simvastatin in 96-well plates. To maximise likelihood of identifying meaningful interactions between simvastatin and vascular peptides, we used a validated photo-immobilisation method to apply a series of different chemical linkers to bind simvastatin so as to present multiple orientations of its constituent components to potential targets. Three rounds of biopanning identified consistent interaction with the clone expressing part of the gene *GJC3*, which maps to *Homo sapiens* chromosome 7, and codes for gap junction gamma-3 protein, also known as connexin 30.2. Further analysis indicated the binding site to be for the *N*-terminal domain putatively 'regulating' connexin hemi-channel and gap junction pores. Using immunohistochemistry we found connexin 30.2 to be present in samples of artery similar to those used to prepare the bacteriophage library. Surface plasmon resonance revealed that a 25 amino acid synthetic peptide representing the uncovered *N*-terminus did not interact with simvastatin lactone, but did bind to the hydrolysed, HMG CoA inhibitor, simvastatin acid. This interaction was also seen for fluvastatin. The hemichannel blockers carbenoxolone and flufenamic acid also interacted strongly with the same peptide providing novel insight into their potential mechanism of inhibition. These findings raise key questions about the functional significance of *GJC3* transcripts in the vasculature and other tissues, and this connexin's role in therapeutic and adverse effects of statins in a range of disease states.

### Publications

Marsh A., Casey-Green K., Probert F., Withall D., Mitchell D.A., Dilly S.J., James S., Dimitri W., Ladwa S.R., Taylor P.C., et al. (2016) Simvastatin sodium salt and fluvastatin interact with human gap junction gamma-3 protein. *PLoS One* **11**: e0148266.

### Funding

This work was funded by EPSRC, Tangent Reprofiling Ltd. & Advantage West Midlands.

### Collaborators

*External:* A. Marsh, K. Casey-Green, F. Probert, D. Withall, D.A. Mitchell, S.J. Dilly, S. James, W. Dimitri, S.R. Ladwa, D.R.J. Singer (University of Warwick).

## Positive allosteric modulation of TRPV1 using Affimer reagents

Rob Bedford, Mike McPherson and Darren Tomlinson

### Introduction

TRPV1 is a major target for the management of chronic pain and specific modulators are highly sought for their analgesic potential. Despite promising results using TRPV1 inhibitors for the management of chronic pain, a number of severe side effects resulted in their withdrawal from clinical trials. Conversely, TRPV1 activation has been explored as an alternative mechanism of pain management, yet a number of side effects still occur owing to targeting of non-pathological receptors. A novel approach targeting only activated receptors selectively desensitises TRPV1 at sites of chronic pain only; this is termed positive allosteric modulation. Our work demonstrates the selection of Affimer reagents able to positively modulate TRPV1 by binding of the outer pore domain.

### Results

Affimers are a 91 amino acid scaffold with two randomised loop regions for molecular recognition that are selected using phage display. Initially, a peptide sequence taken from the TRPV1 outer pore domain was screened using phage display. Phage ELISA subsequently confirmed Affimer binding. TRPV1 specific clones were sequenced and, interestingly, results revealed homology of Affimer loops with the TRPV1-interacting loop of DkTx, a toxin that activates the receptor by binding the peptide region screened. Affimers were subsequently expressed and their ability to bind to TRPV1 in mammalian cells assessed by affinity fluorescence. A number of the Affimers showed specific membrane staining (Figure 1).

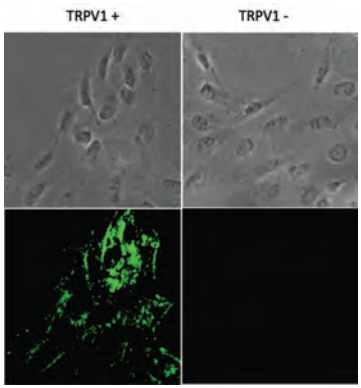


**Figure 1:** immune-cytochemical staining of TRPV1 using Affimers. TRPV1 receptor was overexpressed on a mammalian cell line and incubated with Affimer reagents. Results revealed membrane staining of cells over-expressing TRPV1 compared to a negative control cell line suggesting Affimers were able to identify full-length TRPV1.

Next we determined the ability of Affimers to modulate TRPV1. Despite homology to the toxin that activates TRPV1, the Affimers had no direct effect. However, Affimers demonstrated positive allosteric modulation of TRPV1 when activated by capsaicin (Figure 2). Taken together, these results demonstrate the identification and modulation of a clinically relevant ion channel, TRPV1, using Affimer reagents.

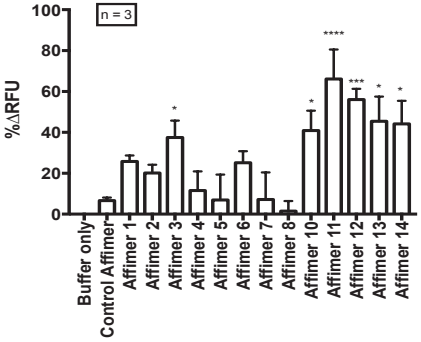


**Figure 2:** positive allosteric modulation of TRPV1 using Affimers. TRPV1 was overexpressed on mammalian cells and incubated with the $Ca^{2+}$ dye, Fluo4-AM. Using a Flexstation multiwall plate reader, cells were stimulated with 0.2M capsaicin and the change in fluorescence measured. Results demonstrated that presence of Affimers caused an increase in capsaicin-induced activation of TRPV1, compared to cells exposed to control Affimer.

Future work will now focus on understanding the interaction between Affimer reagents and TRPV1 at a molecular level. Insights provided by this mechanism of TRPV1 modulation may aid future drug discovery for the treatment of chronic pain.

**Funding**
Neusentis, Pfizer and the University of Leeds funded this work.

**Collaborators**
*University of Leeds:* J. Lippiat.

## Regulation of muscle contraction by titin and myosin binding protein C

Charlotte Scarff, Alba Fuentes Balaguer,
Mehrnaz Montazeri, Larissa Tskhovrebova and John Trinick

### Introduction

Titin is the largest known protein (chain weight ~3.5 MDa) and the third most abundant protein of muscle, after myosin and actin. Individual titin molecules span between the Z- and M-lines and in the A-band are attached to the surface of the myosin filament shaft. Until recently vertebrate striated muscle contraction was thought to be regulated solely by blocking of myosin access to actin in thin filaments by troponin and tropomyosin. Recently, however, there has been mounting evidence that titin is involved in activating myosin. The data indicate that titin acts on myosin binding protein C (mybp-C, also known as C-protein), which in turn acts on force producing myosin cross-bridges, accelerating their cycling rate on actin. Phosphorylation of C-protein also speeds the rate of cross-bridge cycling.

### Results

We expressed whole human C-protein (150 MDa) in insect cells and our collaborator, Donald Winkelmann, supplied expressed human heavy meromyosin (HMM), which is the N-terminal half of myosin that forms cross-bridges with actin. We have carried out electron microscopy on the C-protein and on the complex it forms with HMM. Negatively stained images of C-protein alone show the individual immunoglobulin (C2) and fibronectin (type 3) domains from which the molecule is constructed. The images show a V-shaped molecule about 40 nm long and 3 nm wide. There is often a kink in one of the arms, which probably is the N-terminal end of the molecule. We are also using electron microscopy to image the C-protein/HMM complex, using both negative staining and cryo-EM of frozen hydrated specimens. A preliminary 3D model of the complex has been produced from the stain data.

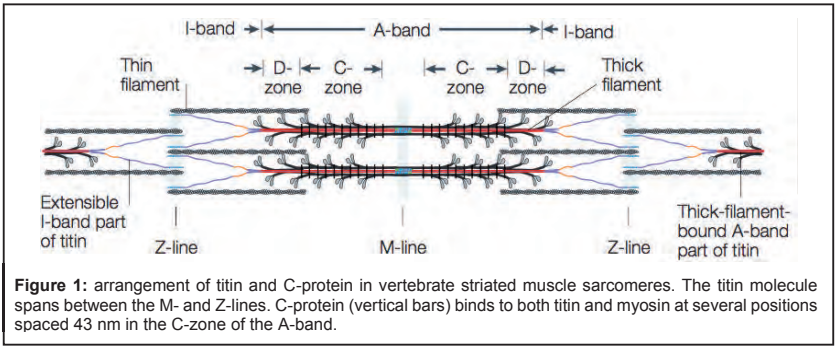


**Figure 1:** arrangement of titin and C-protein in vertebrate striated muscle sarcomeres. The titin molecule spans between the M- and Z-lines. C-protein (vertical bars) binds to both titin and myosin at several positions spaced 43 nm in the C-zone of the A-band.

### Funding

Funded by the British Heart Foundation and the Leverhulme Trust.

### Collaborators

*External:* D. Winkelmann (Rutgers University).

## Co-operative mechanism of protein translocation through Sec machinery

Peter Oatley, Tomas Fessl, Stephen Baldwin, Sheena Radford and Roman Tuma

### Introduction

Protein transport across the bacterial inner membrane occurs primarily via the Sec translocon. The translocon core, SecY, comprises 10 trans-membrane helices (TMs) in a 'clamshell' arrangement forming a central channel through the membrane. A lateral gate (LG) is located between TMs 2, 3 and 7 (Fig. 1A) and provides an exit pathway for the signal sequence and for membrane protein insertion into the membrane. In bacteria, secretion is generally post-translational and substrates are recognised by the cytosolic ATPase SecA which subsequently associates with SecYEG. The ATPase acts as a molecular motor and drives the substrate through the protein-channel using energy from ATP binding and hydrolysis together with proton motive force. Within SecA, two RecA-like nucleotide binding domains (NBD1 and NBD2) form the nucleotide-binding site (NBS), connected to a 'two-helix finger' (2HF), and a pre-protein cross-linking domain (PPXD, Fig. 1A). Upon SecA binding to SecYEG, the 2HF penetrates into the protein channel of SecY and the PPXD forms a 'clamp' for the secretory substrate. Several structures of Sec-translocons have been determined in the presence of various substrates, in both open and closed conformations. However, the mechanism through which ATP hydrolysis is coupled to directional movement of substrate is unclear. Here, we combine all-atom molecular dynamics (MD) simulations with single molecule FRET and biochemical assays in order to address allosteric mechanism of coupling between ATP hydrolysis at SecA and protein translocation through SecY.

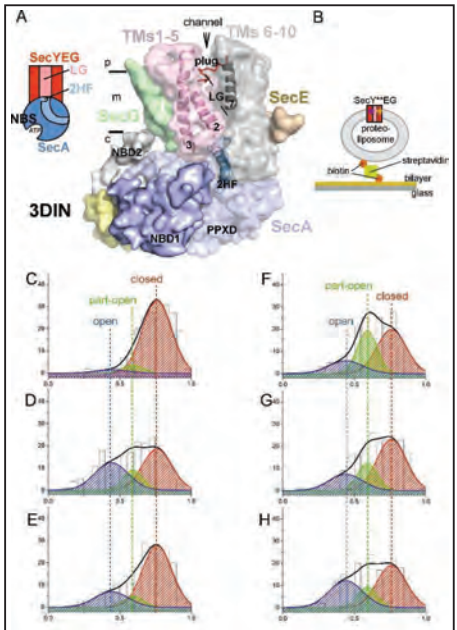


**Figure 1: (A)** structure of SecYEG:SecA complex and schematic depiction of the translocon (left). **(B)** Schematics of proteoliposome immobilisation for single molecule imaging. **(C-H)** FRET efficiency histograms for different states: **(C)** SecYEG only, **(D)** SecYEG:SecA:AMP-PNP, **(E)** SecYEG:SecA:ADP, **(F)** SecYEG:SecA:ATP, **(G)** SecYEG:SecA:ATP:pOA, **(H)** SecYEG:SecA:ATP:pOA with excess of SecA.

### Results

MD simulation were initiated from a transition state structure (SecA:ADP:$AlF_x$) but with SecA nucleotide binding pocket occupied with either ADP or ATP (AMP-PNP). The ADP-bound structure converged into state with LG closed while ATP binding biased the SecY LG towards an open state. Overall, nucleotide exchange at SecA elicited nanometer motions within the distal LG of SecY. In order to monitor these motions we have positioned an Alexa Fluor FRET pair (AF488 and AF594) across the LG and reconstituted SecYEG into unilamellar lipid vesicles which were then immobilised on a glass slide cover slip for imaging with total internal reflection microscopy (Fig. 1B). Single molecule fluorescence traces were collected for different states, converted into FRET efficiencies and collated into histograms (Fig. 1 C-H). In

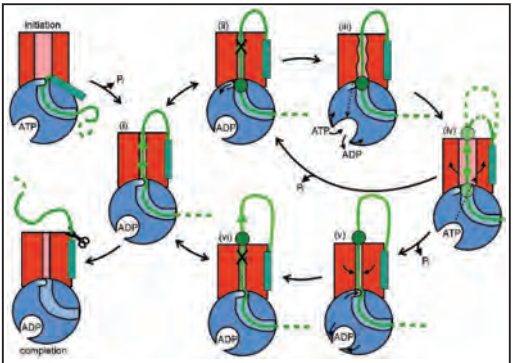


**Figure 2:** a Brownian motor model for translocation of unfolded polypeptide chain through Sec translocon. After initiation SecA stays in the ADP state (i), forcing LG to the closed conformation through which only small side chains can diffuse. Upon encountering a charged or a bulky side chain (ii) 2HF triggers nucleotide exchange at SecA for ATP (iii) which in turn opens LG to allow diffusion of the bulky residues (iv). Upon ATP hydrolysis LG closes (v) blocking the re-entry of the bulky side chain from the periplasmic side (vi). After multiple cycles the translocation process completes by a cleavage of the signal peptide.

the apo-SecYEG state LG remained closed as manifested by high FRET efficiency (closely spaced dyes). However, upon addition of SecA and AMP-PNP LG populated open conformation while in the presence of ADP it was mostly closed. This reproduced the results from MD simulations and confirmed existence of long-range allosteric control of LG opening by nucleotide state of SecA. Furthermore, in the presence of ATP additional, partly open state was detected (Fig. 1F) while during translocation of pro-OmpA substrate LG co-existed in all three states, indicating nucleotide-dependent changes in the channel aperture during translocation. Crosslinking of the LG in the closed state promoted ADP binding while crosslinking of a short oligopeptide containing bulky side chains (a translocating chain mimetic) to 2HF promoted ADP release, which constitutes the rate limiting step. This indicates that the LG state and the two-helix finger environment are both communicated back to the SecA ATPase site. Hence, there exists a two-way communication between the SecY-channel and the nucleotide binding site of SecA: ATP binding causes opening of the channel, while bulky substrates at the channel entrance regulate nucleotide exchange. The data suggest a novel mechanism for biological motors that transport proteins and nucleic acids, whereby ATP turnover provides force by biasing the direction of substrate diffusion (Fig. 2).

**Publications**

Allen W.J., Corey R.A., Oatley P., Sessions R.B., Baldwin S.A., Radford S.E., Tuma R. & Collinson I. (2016) Two-way communication between SecY and SecA suggests a Brownian ratchet mechanism for protein translocation. *eLife* **5:** e15598.

**Funding** This work was funded by the BBSRC.

**Collaborators**

*External:* W. Allen, R. Corey, R. Sessions and I. Collinson (University of Bristol).

## The role of structured RNA in early virus replication events

Andrew Tuplin

### Overview

A phylogenetically conserved RNA structure within the NS5B coding region of hepatitis C virus functions as a cis-replicating element (CRE). Integrity of this CRE, designated SL9266, is critical for genome replication. SL9266 forms the core of an extended pseudoknot, designated SL9266/PK, involving long distance RNA-RNA interactions between unpaired loops of SL9266 and distal regions of the genome. Previous studies demonstrated that SL9266/PK is dynamic, with 'open' and 'closed' conformations predicted to have distinct functions during virus replication. Using a combination of site-directed mutagenesis and locked nucleic acids (LNA) complementary to defined domains of SL9266 and its interacting regions, we have explored the influence of this structure on genome translation and replication. We demonstrate that LNAs which block formation of the closed conformation inhibit genome translation. Inhibition was at least partly independent of the initiation mechanism, whether driven by homologous or heterologous internal ribosome entry sites or from a capped message. Provision of SL9266/PK in trans relieved translational inhibition, and mutational analysis implied a mechanism in which the closed conformation recruits a cellular factor that would otherwise suppresses translation. We propose that SL9266/PK functions as a temporal switch, modulating the mutually incompatible processes of translation and replication (Figure 1).

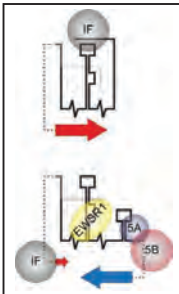


**Figure 1:** A cartoon interpretation of SL9266/PK conformational rearrangement as part of a translation/replication switch; illustrating the mechanism and role of negative feedback interactions in the proposed model. The upper cartoon illustrates up-regulation of HCV IRES initiated translation (large red arrow) due to the SL9266/PK closed conformation sequestering a cellular IRES inhibition factor (IF). The lower cartoon illustrates the open conformation, initiated by virally encoded non-structural proteins (5A and 5B) binding the 3'NCR and blocking 'kissing loop' formation. The open structure favours interaction between cellular protein EWSR1 and SL9266, up-regulating RNA replication (large blue arrow). As demonstrated in the current study the resulting open conformation actively inhibits HCV translation (small red arrow), which we speculate is due to EWRS1 displacing - and thus making available - translation inhibition factor IF.

### Publications

Khasnatinov M.A., Tuplin A., Gritsun D.J., Slovak M., Kazimirova M., Lickova M., Havlikova S., Klempa B., Labuda M., Gould E.A., *et al.* (2016) Tick-borne encephalitis virus structural proteins are the primary viral determinants of non-viraemic transmission between ticks whereas non-structural proteins affect cytotoxicity. *PLoS One* **11**:e0158105.

Stewart H., Bingham R.J., White S.J., Dykeman E.C., Zothner C., Tuplin A.K., Stockley P.G., Twarock R. & Harris M. (2016) Identification of novel RNA secondary structures within the hepatitis C virus genome reveals a cooperative involvement in genome packaging. *Sci. Rep.* **6**:22952.

### Funding

This work was funded by a MRC New Investigator Research Grant.

### Collaborators

*University of Leeds:* M. Harris, A. Zhuravleva, N. Stonehouse and J. Mankouri.
*External:* A. Kohl (MRC Centre for Virus Research, UK); A. Davidson (University of Bristol, UK) and A. Merits (University of Tartu, Estonia).

## Novel antiviral strategies for human herpesviruses

Sophie Schumann, Belinda Baquero-Perez, Charlotte Revill, Richard Foster and Adrian Whitehouse

### Introduction

Human herpesviruses are responsible for a range of acute and chronic diseases, including several cancers. Kaposi's sarcoma-associated herpesvirus (KSHV) is the etiologic agent of Kaposi's sarcoma and two lymphoproliferative disorders; primary effusion lymphoma and multicentric Castleman's disease. Like all herpesviruses, KSHV has two distinct forms of infection; latency and lytic replication. While the majority of KSHV-associated tumorigenic cells harbour latent virus, lytic gene expression occurs to various levels in each KSHV-associated disorder, suggesting that lytic replication inhibition may provide therapeutic intervention. Currently, drugs in clinical use are inhibitors of herpesvirus DNA polymerases and are highly effective against a variety of herpesviruses. Although drug-resistant strains are emerging in immunocompromised patients and varying efficacy has been reported against oncogenic herpesviruses. Consequently, there is an urgent need for the continued development of anti-herpesvirus drugs, particularly targeting oncogenic herpesviruses.

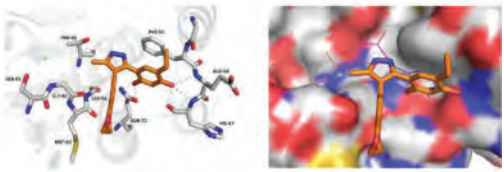

**Figure 1:** predicted binding model of hit compound to the UAP56 ATP binding pocket.

RNA helicases contribute to remodelling of intramolecular RNA-, RNA-protein and protein-protein interactions in an ATP-dependent manner. Both viral and cellular RNA helicases have central roles in virus life cycles and have emerged as therapeutic targets. Numerous studies have evaluated the potential of targeting virally-encoded RNA helicases. However, to circumvent viral resistance, inhibiting cellular RNA helicases has also been explored, supported by efforts targeting eIF4A for the treatment of cancer and DDX3 to inhibit HIV replication, illustrating selective pharmacological targeting of RNA helicases is possible.

The KSHV open reading frame (ORF) 57 protein, which has a functional homologue in each human herpesvirus, is essential for viral lytic replication. It is a multifunctional protein involved in all stages of viral mRNA processing via an interaction with the human transcription/export (hTREX) complex. hTREX is a large multiprotein complex involved in Nxf1-mediated cellular bulk mRNA nuclear export. Notably, ORF57-mediated hTREX recruitment produces a viral ribonucleoprotein particle (vRNP) essential for KSHV lytic replication. ORF57 forms a direct interaction with the cellular export adapter Aly, however, redundancy in the cellular mRNA export pathway also allows ORF57 to facilitate vRNP formation via an interaction with UIF. As such, disrupting the ORF57-hTREX interaction requires blocking multiple protein-protein interactions.

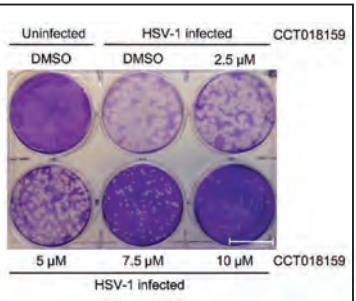


**Figure 2:** inhibition of HSV-1 replication in the presence of increasing amounts of the hit compound.

Alternatively, the cellular RNA-helicase UAP56 functions as an essential hTREX assembly factor, forming an ATP-dependent trimeric complex with Aly and CIP29, as well as recruiting further hTREX components onto mRNAs. Therefore, we examined the potential of inhibiting UAP56 ATPase activity, to prevent KSHV vRNP formation and lytic replication. In silico high-throughput screening identified small molecules capable of binding the UAP56 ATP-binding pocket (Fig.1). Strikingly, results demonstrate that inhibiting UAP56 ATPase activity represents an antiviral target (Fig. 2).

**Publications**

Schumann S., Jackson B.R., Yule I., Whitehead S.K., Foster R. and Whitehouse A. (2016) Targeting the ATP-dependent formation of herpesvirus ribonucleoprotein particle assembly as an antiviral approach. *Nat. Micro*. **2**:16201.

Schumann S., Baquero-Perez B. & Whitehouse A. (2016) Interactions between KSHV ORF57 and the novel human TREX proteins, CHTOP and CIP29. *J. Gen. Virol.* **97**:1904-1910.

Wood J.J., Boyne J.R., Paulus C., Jackson B.R., Nevels M.M., Whitehouse A. & Hughes D.J. (2016) ARID3B: A novel regulator of the Kaposi's sarcoma-associated herpesvirus lytic cycle. *J. Virol.* **90**:9543-9555.

**Funding**

This work was funded in parts by Worldwide Cancer Research, BBSRC and Wellcome Trust.

## Designed inhibitors of protein-protein interactions

George Burslem, Claire Grison, Sarah Hewitt, Katherine Horner, Thomas James, Hannah. Kyle, Jennifer Miles, Chris Pask, Silvia Rodriguez-Marin, Philip Rowell, Alex Breeze, Thomas. Edwards, Adam. Nelson, Stuart Warriner, Andrew Wilson

**Introduction**
This report summarises our group's efforts to develop inhibitors of protein-protein interactions (PPIs) where we emphasize development of constrained peptides, novel proteomimetics based on aromatic oligoamides and surface mimetics based on co-ordination complexes.

**Hydrocarbon constrained peptides – understanding preorganisation and binding affinity** The development of constrained peptides is an active and productive strand of research in the search for ligands to inhibit α-helix mediated PPIs. We performed structural and biophysical studies on Bcl-2 family proteins using constrained variants of the BH3 domains of BID and BIM. Our structural investigations showed that the bound states of constrained and wild type peptides are similar (Figure 1), with no enhancement in inhibitory potency observed on the introduction of peptide constraints. SPR and Van't Hoff analyses gave results consistent with an induced fit binding mechanism and enthalpy-entropy compensation, contradicting the hypothesis that pre-organising a peptide should enhance its target binding affinity.

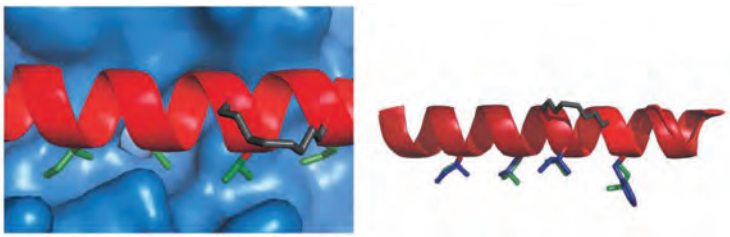

**Figure 1:** crystal structure of constrained peptide/protein interactions (a) enlargement of Mcl-1/BID-MM (b) overlay of BID-MM and Mcl-1/BIM-WT, side chains from BID-MM are shown in green, with BIM-WT side chains in blue.

**Development of topological α-helix mimetics scaffolds** Identification of effective mimics of protein secondary structures that act as inhibitors of PPIs remains a major challenge. We designed and synthesized foldamers based on successive α-, β- and γ-amino acids, α/β/γ-peptides, in which *trans*-2-aminocyclobutanecarboxylic acid (*t*ACBC) promotes a hydrogen-bonded 12,13-helical conformation, hence mimicking the α-helical conformation (Figure 2a). Suitably functionalized α/β/γ-peptides were shown to exhibit enhanced proteolytic stability in comparison to the wild-type α-peptide parent sequence from which they are derived, and act as potent and selective peptide inhibitors of the p53/*h*DM2 interaction.

**HIF-1 α/p300 inhibition with "bionic" proteins** The ability to incorporate non-natural functionality into bio-molecules represents an emergent theme in synthetic biology. Creating such "chimeric" bio-molecules may impart new functionality and orthogonal properties into known bio-macromolecules. Our efforts in this area focussed on the incorporation of oligobenzamide sequences (which topographically mimic an α-helix) into truncated HIF-1α sequences to generate "bionic" proteins (Figure 2b). These novel peptide-oligobenzamide hybrids were show to efficiently bind p300 with affinity comparable to the parent peptide (Figure 2b). Furthermore, the selectivity over a similar α-helix mediated PPI (p53/*h*DM2) was increased compared to that of the non-hybrid oligobenzamide sequence.

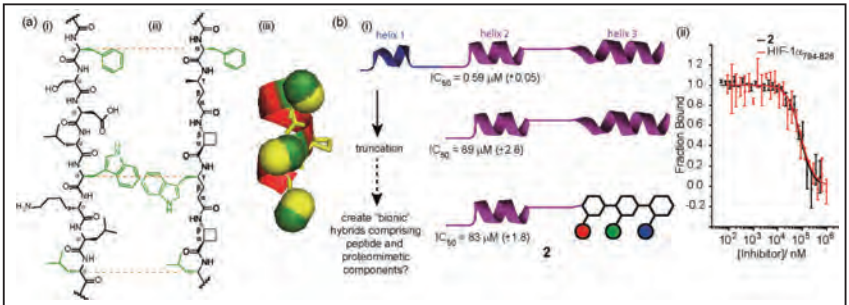


**Figure 2:** design synthesis and testing of **(a)** $\alpha/\beta/\gamma$-peptides as inhibitors of the p53/hDM2 interaction and (i) the native $\alpha$-p53 peptide and (ii) $\alpha/\beta/\gamma$-peptide helix mimetic (iii) Superimposition of the helical segment of p53 highlighting the helical backbone (in red), the hot-spot side chains (in green) and the molecular modelling of the lowest energy $\alpha/\beta/\gamma$-peptide conformer (in yellow) **(b)** "bionic" peptide-oligobenzamide hybrids. (i) peptide-oligobenzamide hybrids inspired by a truncated HIF-1α sequence (ii) Fluorescence anisotropy (FA) competition data for inhibition of p300/FITC-HIF-1α C-TAD for HIF-1$\alpha_{794\text{-}826}$ (orange) and hybrid **2** (black).

**Publications**

Azzarito V., Rowell P., Barnard A., Edwards T.A., Macdonald A., Warriner S.L. & Wilson A.J. (2016) Probing protein surfaces: QSAR analysis with helix mimetics. *ChemBioChem* **17**:768-773.

Liu L.J., He B.Y., Miles J.A., Wang W.H., Mao Z.F., Che W.I., Lu J.J., Chen X.P., Wilson A.J., Ma D.L., *et al.* (2016) Inhibition of the p53/hDM2 protein-protein interaction by cyclometallated iridium(iii) compounds. *Oncotarget* **7**:13965-13975.

Miles, J. A. Yeo, D. J. Rowell, P. Rodriguez-Marin, S. Pask, C. M. Warriner, S. L. Edwards, T. A. & Wilson A. J. (2016) Hydrocarbon constrained peptides – understanding preorganization and binding affinity, *Chem. Sci.*, 7, 3694-3702

Burslem G.M., Kyle H.F., Breeze A.L., Edwards T.A., Nelson A., Warriner S.L. & Wilson A.J. (2016) Towards "bionic" proteins: replacement of continuous sequences from HIF-1$\alpha$ with proteomimetics to create functional p300 binding HIF-1$\alpha$ mimics. *Chem. Commun.* **52**:5421-5424.

Hewitt S.H. & Wilson A.J. (2016) Metal complexes as "protein surface mimetics". *Chem. Commun.* **52**:9745-9756.

Grison C.M., Miles J.A., Robin S., Wilson A.J. & Aitken D.J. (2016) An -helix-mimicking 12,13-helix: Designed $\alpha/\beta/\gamma$-foldamers as selective inhibitors of protein-protein interactions. *Angew. Chem.-Int. Edit.* **55**:11096-11100.

**Funding**

We gratefully acknowledge The University of Leeds, EPSRC, ERC, and The Leverhulme Trust for financial support of this research.

**Collaborators**

*External:* D.-L. Ma (Hong Kong Baptist University), C.-H. Leung (University of Macau), S. Robin and D. Aitken (University of Paris-Saclay).

## Profiling protein lipidation in parasites with chemical tools

Megan Wright

### Introduction

The cell exerts precise and dynamic control over protein function by modifying proteins, a process known as post-translational modification (PTM). One such PTM is lipidation, where lipids are incorporated into proteins. This often directs the protein to the membrane and is crucially important for protein function. Because lipidation is an essential process, there is interest in manipulating the enzymes and pathways that carry out these modifications for therapy. However, globally identifying which proteins are lipidated in the whole cell and studying changes in acylation using biochemical methods is very challenging.

We have exploited recent advances in mass spectrometry-based proteomics and bioorthogonal ligation chemistry to develop chemical biology approaches to profile lipidated proteins in different organisms. In the current project, we applied our approach to analyse lipidation in the Human African Trypanosomiasis parasite, *T. brucei*. T. brucei has a complex lifecycle, involving both an insect and mammalian host. The focus of the project was on *N*-myristoylation: the attachment of the fatty acid myristate to protein N-termini by the enzyme *N*-myristoyltransferase (NMT).

### Results

We synthesised alkyne-modified lipid probes, including myristate analogue YnMyr, which were fed to parasites and metabolically incorporated into lipidated proteins by the cellular machinery (Fig. 1). The alkyne tag is small, inert and therefore tolerated by the biological system, but can subsequently be detected by attachment of fluorophores or affinity labels via click chemistry. Experiments were performed in both bloodstream form (BSF, the host-infective stage) and procyclic form (PCF, insect stage) parasites. We observed markedly different profiles (Fig. 1), largely reflecting differential protein expression in the parasite, as well as incorporation of YnMyr into stage-specific complex glycolipids. Using potent and selective inhibitors of the acyltransferase NMT, reduction in YnMyr incorporation into specific proteins was observed (Fig. 1), indicating that these are *N*-myristoylated and also providing direct evidence that the inhibitors act on-target in cells.

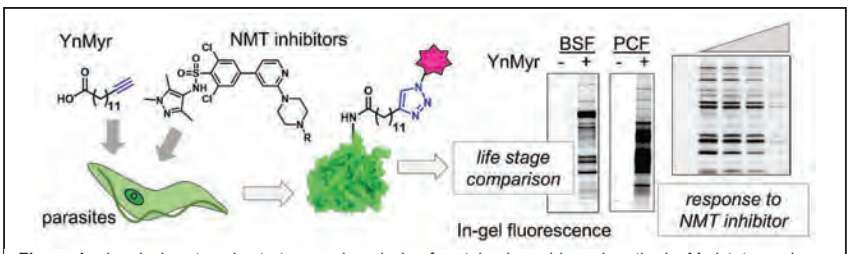


**Figure 1:** chemical proteomic strategy and analysis of proteins by gel-based methods. Myristate analogue YnMyr is metabolically incorporated into proteins. Subsequent labelling via click chemistry enables visualisation of proteins tagged by the probe, e.g. in different life stages (BSF, PCF). Inhibitors of acyltransferase NMT inhibited YnMyr incorporation in a dose-dependent manner (right).

Tagged proteins were labelled with a biotinylated click reagent, enriched on streptavidin beads, subject to tryptic digest and peptides analysed via LC-MS/MS. We used label-free quantification to compare across samples: YnMyr vs Myr control; BSF vs PCF parasites; cells treated with and without NMT inhibitors.

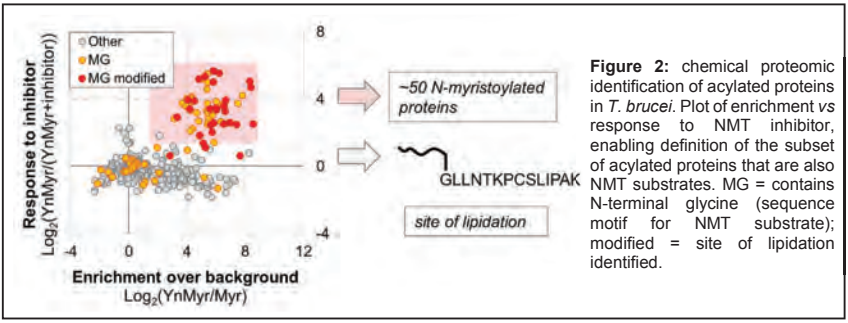


**Figure 2:** chemical proteomic identification of acylated proteins in *T. brucei*. Plot of enrichment *vs* response to NMT inhibitor, enabling definition of the subset of acylated proteins that are also NMT substrates. MG = contains N-terminal glycine (sequence motif for NMT substrate); modified = site of lipidation identified.

We subsequently compared the data from these experiments with other recent published datasets from our labs and others, to yield information on the profile of lipidated proteins across different protozoan parasites. This analysis highlighted the complementarity of different chemical proteomics methods that have been developed to investigate *S*-acylation, and showed that acylation of some proteins is conserved across organisms, but that some acylated proteins are unique to particular species. These datasets provide a wealth of information on global lipidation patterns in parasites, and suggest that these modifications are both widespread and functionally important.

In summary, chemical proteomics methods provide a global and unbiased way to study protein lipidation in diverse organisms. This contributes to the annotation of proteomes, and increases our understanding of protein modification pathways and how they may be targeted for therapy.

**Publications**

Wright M.H., Paape D., Price H.P., Smith D.F. & Tate E.W. (2016) Global profiling and inhibition of protein lipidation in vector and host stages of the sleeping sickness parasite *Trypanosoma brucei*. *ACS Infect. Dis.* **2**:427-441.

**Funding**

We thank the University of Leeds for start-up funding. Experimental work was carried out at Imperial College London and the University of York, and was funded by EPSRC, Wellcome Trust, and BBSRC.

**Collaborators**

*External:* D. Paape, H. P. Price and D. F. Smith (University of York); E. W. Tate (Imperial College London).

## Probing multivalent protein-carbohydrate interactions using compact, polyvalent glycan-quantum dot and Förster resonance energy transfer

Yuan Guo, Chadamas Sakonsinsiri, Emma Pool, Weili Wang, W. Bruce Turnbull and Dejian Zhou

### Introduction

Multivalent protein-carbohydrate interactions are widespread in biology and play a central role in viral/bacterial infection, cell-cell communication and host immune response. They initiate the first contact between pathogens and target cells that ultimately leads to infection. However, monovalent protein-glycan interactions are intrinsically weak, hence pathogens are displayed with arrays of glycans their surfaces, allowing them to bind efficiently to multimeric lectins on target cell surfaces and exploit multivalency to enhance affinity. Understanding the structure mechanism behind such bindings is essential to develop potent multivalent inhibitors. A major challenge here is a lack of structural information for key cell surface multimeric lectins, due to problems in solving such flexible, complex and multimeric protein structure by crystallography. Although other techniques (*e.g.* isothermal titration calorimetry, surface plasmon resonance) are powerful in providing binding affinities, kinetics, and thermodynamics, they cannot reveal key structure information. For example, despite 20 years of extensive research worldwide, the complete structure of two vitally important tetrameric receptors, the dendritic cell receptor DC-SIGN and its closely-related endothelial cell receptor DC-SIGNR, remain unknown. These two receptors bind to virus surface mannose-containing glycans and facilitate the HIV/Ebola virus (EBOV) infection. Hence there is an urgent need for a new method that can provide not only quantitative binding but also structural information to advance this research field.

### Results

To address this challenge, we have developed a novel Förster resonance energy transfer (FRET) based ratiometric method to probe multivalent receptors DC-SIGN/R-glycan

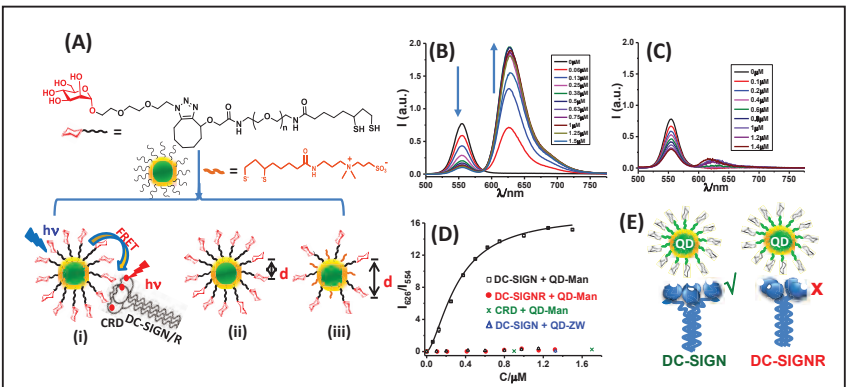


**Figure 1**: **(A)** our approach to compact, polyvalent mannose capped quantum dot (QD-Man) and probe its multivalent binding with tetrameric receptors DC-SIGN/R *via* FRET (i) and tuning inter-mannose distance via the PEG linker length (ii) and diluting with inert DHLA-zwitterion ligand (iii). **(B, C)** directed excitation background corrected fluorescence spectra of QD-Man after binding to different concentration of Atto-594 labelled DC-SIGN (B) or DC-SIGNR (C). **(D)** plot of the apparent FRET ratio I626/I554 as a function of protein concentration: the QD-Man-DC-SIGN binding data were fitted by the Hill's equation. **(E)** our proposed binding models for DC-SIGN and DC-SIGNR binding to QD-Man.

interactions. We have developed a highly-efficient cap-exchange method using deprotonated DHLA-PEG-Man ligand and performing reaction in homogenous solution. This substaintially improved the cap-exchange efficiency and greatly reduced the amount of ligand required for complete cap-exchange over literature methods by 20-200 fold. Compact (<10 nm), polyvalent mannose-QD conjugates (QD-Man, valency >150) were readily prepared. Importantly, the glycan valency can be readily tuned by the linker length and diluting with a spacer ligand (Figure 1A).

The QD-Man was used to probe multivlaent binding with DC-SIGN/R *via* a FRET based ratiometic readout strategy. DC-SIGN was found to bind strongly to QD-Man ($K_d$ ~ 0.3-0.6 μM) which is >5000 fold tighter than monovalent CRD-mannose binding ($K_d$ = 3.5 mM). In contrast, DC-SIGNR binding with QD-Man was rather weak: the resulting FRET signal was indistinguishable from that of monovalent CRD-QD-Man binding or non-specific interaction between DC-SIGN and a DHLA-zwitterion ligand capped control QD (Figure 1D), indicating that DC-SIGNR cannot form strong multivalent binding with QD-Man. The FRET signal arising from DC-SIGN binding was >60 fold stronger than that of DC-SIGNR. This level of discrimination has been unprecedented for the two closely related, almost identical tetrameric receptors. The different DC-SIGN/R binding properties observed by FRET was confirmed by QD-Man's ability to specifically inhibit pseudo-Ebola virus infection of only DC-SIGN-, but not DC-SIGNR-, expressing cells. A structural model to account for such different QD-binding has been proposed: the CRDs in DC-SIGN face the same direction, hence readily bind to QD-Man multivalently; whereas those in DC-SIGNR point to different directions, making them unable to bind multivalently to QD-Man (Figure 1E). The different CRD orientation revealed herein may also account for their different virus binding and transfection properties.

**Publications**

Guo Y., Sakonsinsiri C., Nehlmeier I., Fascione M.A., Zhang H.Y., Wang W.L., Pohlmann S., Turnbull W.B. & Zhou D.J. (2016) Compact, polyvalent mannose quantum dots as sensitive, ratiometric fret probes for multivalent protein-ligand interactions. *Angew. Chem.-Int. Edit.* **55**:4738-4742.

Kong Y.F., Chen J., Fang H.W., Heath G., Wo Y., Wang W.L., Li Y.X., Guo Y., Evans S.D., Chen S.Y.*, et al.* (2016) Highly fluorescent ribonuclease-a-encapsulated lead sulfide quantum dots for ultrasensitive fluorescence *in vivo* imaging in the second near-infrared window. *Chem. Mat.* **28**:3041-3050.

Zhang W., Wang F., Wang Y., Wang J., Yu Y., Guo S., Chen R. & Zhou, D. (2016) pH and near-infrared light dual-stimuli responsive drug delivery using DNA-conjugated gold nanorods for effective treatment of multidrug resistant cancer cells. *J. Controlled Release* **232**: 9-19.

Wang J.N., Wang F.H., Li F.Z., Zhang W.J., Shen Y.Y., Zhou D.J. & Guo S.R. (2016) A multifunctional poly(curcumin) nanomedicine for dual-modal targeted delivery, intracellular responsive release, dual-drug treatment and imaging of multidrug resistant cancer cells. *J. Mat. Chem. B* **4**:2954-2962.

**Funding**

This work was supported by the Wellcome Trust (Grant No: 097354/Z/11/Z) and the University of Leeds.

**Collaborators**

*External:* S. Pöhlmann (German Primate Centre, Germany).

## ASTBURY SEMINARS 2016

**14th January**
*Deciphering molecular virus - host interactions by an integrated structural cell biology approach*
Prof Kay Grunewald, University of Oxford

**4th February**
*Solving the structures of protein-drug interactions using an optical analogue of 2D NMR: current progress and future prospects*
Prof David Klug, Imperial College London

**3rd March**
*Structural insights on small-molecule stabilization of 14-3-3 protein-protein interactions*
Dr Christian Ottmann, Eindhoven University of Technology

**7th April**
*Developing better in vitro models of the E. coli outer membrane - with the help of neutrons*
Prof Jeremy Lakey, University of Newcastle

**28th April**
**Cheney Fellowship Lecture**
*Chemical biological modulation of Ras signalling*
Prof Herbert Waldmann, Max Planck

**5th May**
*Protein folding homeostasis in the endoplasmic reticulum*
Prof David Ron, University of Cambridge

**2nd June**
*The bacterial flagellar motor: remodelling a nanomachine as you swim*
Prof Judy Armitage, University of Oxford

**24th June**
**Astbury Annual Lecture 2016**
*The use of recent advances in electron microscopy to study ribosome structure*
Prof Venki Ramakrishnan FRS, MRC Laboratory of Molecular Biology

**10th November**
*Targeting epigenetic reader domains using chemical biology and medicinal chemistry*
Dr Stuart Conway, University of Oxford

**1st December**
*Heat Shock Proteins - the brains of protein quality control*
Prof Harm Kampinga, University of Groningen

## Publications by Astbury Centre Members 2016


Abou-Saleh R.H., Peyman S.A., Johnson B.R.G., Marston G., Ingram N., Bushby R., Coletta P.L., Markham A.F. & Evans S.D. (2016) The influence of intercalating perfluorohexane into lipid shells on nano and microbubble stability. *Soft Matter* **12**:7223-7230.

Ainsworth E.V., Lockwood C.W.J., White G.F., Hwang E.T., Sakai T., Gross M.A., Richardson D.J., Clarke T.A., Jeuken L.J.C., Reisner E.*, et al.* (2016) Photoreduction of *Shewanella oneidensis* extracellular cytochromes by organic chromophores and dye-sensitized $TiO_2$. *ChemBioChem* **17**:2324-2333.

Allen W.J., Corey R.A., Oatley P., Sessions R.B., Baldwin S.A., Radford S.E., Tuma R. & Collinson I. (2016) Two-way communication between SecY and SecA suggests a Brownian ratchet mechanism for protein translocation. *eLife* **5:** e15598.

Azzarito V., Rowell P., Barnard A., Edwards T.A., Macdonald A., Warriner S.L. & Wilson A.J. (2016) Probing protein surfaces: QSAR analysis with helix mimetics. *ChemBioChem* **17**:768-773.

Baboolal T.G., Mashanov G.I., Nenasheva T.A., Peckham M. & Molloy J.E. (2016) A combination of diffusion and active translocation localizes myosin 10 to the filopodial tip. *J. Biol. Chem.* **291**:22373-22385.

Bachmann G., Richards M.W., Winter A., Beuron F., Morris E. & Bayliss R. (2016) A closed conformation of the *Caenorhabditis elegans* separase-securin complex. *Open Biol* **6**:160032.

Baker A., Hogg T.L. & Warriner S.L. (2016) Peroxisome protein import: A complex journey. *Biochem. Soc. Trans.* **44**:783-789.

Bano F., Banerji S., Howarth M., Jackson D.G. & Richter R.P. (2016) A single molecule assay to probe monovalent and multivalent bonds between hyaluronan and its key leukocyte receptor CD44 under force. *Sci. Rep.* **6**: 34176.

Banushkina P.V. & Krivov S.V. (2016) Optimal reaction coordinates. *Wiley Interdiscip. Rev.-Comput. Mol. Sci.* **6**:748-763.

Bawazer L.A., Mcnally C.S., Empson C.J., Marchant W.J., Comyn T.P., Niu X.Z., Cho S., Mcpherson M.J., Binks B.P., Demello A.*, et al.* (2016) Combinatorial microfluidic droplet engineering for biomimetic material synthesis. *Sci. Adv.* **2**: e1600567.

Bayliss R., Choi J., Fennell D.A., Fry A.M. & Richards M.W. (2016) Molecular mechanisms that underpin EML4-ALK driven cancers and their response to targeted drugs. *Cell. Mol. Life Sci.* **73**:1209-1224.

Belousova N., Mikheeva G., Xiong C.Y., Stagg L.J., Gagea M., Fox P.S., Bassett R.L., Ladbury J.E., Braun M.B., Stehle T.*, et al.* (2016) Native and engineered tropism of vectors derived from a rare species D adenovirus serotype 43. *Oncotarget* **7**:53414-53429.

Bhogal M.S., Lanyon-Hogg T., Johnston K.A., Warriner S.L. & Baker A. (2016) Covalent label transfer between peroxisomal importomer components reveals export-driven import interactions. *J. Biol. Chem.* **291**:2460-2468.

Boissinot M., King H., Adams M., Higgins J., Steele L.P., Wurdak H., Bond J., Tomlinson D.C., Lawler S.E. & Short S.C. (2016) Ectopic expression of microRNA-1300 in adult and paediatric glioma cells induces cytokinesis failure and apoptosis via ECT2. *Neuro-Oncology* **18**:18-18.

Borodavka A., Singaram S.W., Stockley P.G., Gelbart W.M., Ben-Shaul A. & Tuma R. (2016) Sizes of long RNA molecules are determined by the branching patterns of their secondary structures. *Biophys. J.* **111**:2077-2085.

Bowen A.M., Jones M.W., Lovett J.E., Gaule T.G., Mcpherson M.J., Dilworth J.R., Timmel C.R. & Harmer J.R. (2016) Exploiting orientation-selective deer: Determining molecular structure in systems containing Cu(ii) centres. *Phys. Chem. Chem. Phys.* **18**:5981-5994.

Brem J., Cain R., Cahill S., Mcdonough M.A., Clifton I.J., Jimenez-Castellanos J.C., Avison M.B., Spencer J., Fishwick C.W.G. & Schofield C.J. (2016) Structural basis of metallo-beta-lactamase, serine-beta-lactamase and penicillin-binding protein inhibition by cyclic boronates. *Nat. Commun.* **7**:12406.

Burgess S.G., Concilio M.G., Bayliss R. & Fielding A.J. (2016) Detection of ligand-induced conformational changes in the activation loop of Aurora-A kinase by PELDOR spectroscopy. *ChemistryOpen* **5**:531-534.

Burgess S.G., Oleksy A., Cavazza T., Richards M.W., Vernos I., Matthews D. & Bayliss R. (2016) Allosteric inhibition of Aurora-A kinase by a synthetic vNAR domain. *Open Biol* **6**:160089.

Burslem G.M., Kyle H.F., Breeze A.L., Edwards T.A., Nelson A., Warriner S.L. & Wilson A.J. (2016) Towards "bionic" proteins: replacement of continuous sequences from HIF-1a with proteomimetics to create functional p300 binding HIF-1a mimics. *Chem. Commun.* **52**:5421-5424.

Burslem G.M., Kyle H.F., Prabhakaran P., Breeze A.L., Edwards T.A., Warriner S.L., Nelson A. & Wilson A.J. (2016) Synthesis of highly functionalized oligobenzamide proteomimetic foldamers by late stage introduction of sensitive groups. *Org. Biomol. Chem.* **14**:3782-3786.

Campbell J.C., Kim J.J., Li K.Y., Huang G.Y., Reger A.S., Matsuda S., Sankaran B., Link T.M., Yuasa K., Ladbury J.E*., et al.* (2016) Structural basis of cyclic nucleotide selectivity in cGMP-dependent protein kinase ii. *J. Biol. Chem.* **291**:5623-5633.

Care M.A., Stephenson S.J., Barnes N.A., Fan I., Zougman A., El-Sherbiny Y.M., Vital E.M., Westhead D.R., Tooze R.M. & Doody G.M. (2016) Network analysis identifies proinflammatory plasma cell polarization for secretion of isg15 in human autoimmunity. *J. Immunol.* **197**:1447-1459.

Caseley E.A., Muench S.P., Fishwick C.W. & Jiang L.H. (2016) Structure-based identification and characterisation of structurally novel human P2X7 receptor antagonists. *Biochem. Pharmacol.* **116**:130-139.

Ceasar S.A., Baker A., Muench S.P., Ignacimuthu S. & Baldwin S.A. (2016) The conservation of phosphate-binding residues among PHT1 transporters suggests that distinct transport affinities are unlikely to result from differences in the phosphate-binding site. *Biochem. Soc. Trans.* **44**:1541-1548.

Chen J., Kong Y.F., Wang W., Fang H.W., Wo Y., Zhou D.J., Wu Z.Y., Li Y.X. & Chen S.Y. (2016) Direct water-phase synthesis of lead sulfide quantum dots encapsulated by beta-lactoglobulin for *in vivo* second near infrared window imaging with reduced toxicity. *Chem.*

*Commun.* **52**:4025-4028.

Chen J., Kong Y.F., Wo Y., Fang H.W., Li Y.X., Zhang T., Dong Y., Ge Y.S., Wu Z.Y., Zhou D.J., *et al.* (2016) Facile synthesis of b-lactoglobulin capped $Ag_2S$ quantum dots for *in vivo* imaging in the second near-infrared biological window. *J. Mat. Chem. B* **4**:6271-6278.

Chenchiliyan M., Timpmann K., Jalviste E., Adams P.G., Hunter C.N. & Freiberg A. (2016) Dimerization of core complexes as an efficient strategy for energy trapping in *Rhodobacter sphaeroides*. *Biochim. Biophys. Acta-Bioenerg.* **1857**:634-642.

Christenson H.K. & Thomson N.H. (2016) The nature of the air-cleaved mica surface. *Surf. Sci. Rep.* **71**:367-390.

Colomer I., Empson C.J., Craven P., Owen Z., Doveston R.G., Churcher I., Marsden S.P. & Nelson A. (2016) A divergent synthetic approach to diverse molecular scaffolds: Assessment of lead-likeness using LLAMA, an open-access computational tool. *Chem. Commun.* **52**:7209-7212.

Concilio M.G., Fielding A.J., Bayliss R. & Burgess S.G. (2016) Density functional theory studies of MTSL nitroxide side chain conformations attached to an activation loop. *Theor. Chem. Acc.* **135**:97.

Costa L., Li-Destri G., Thomson N.H., Konovalov O. & Pontoni D. (2016) Real space imaging of nanoparticle assembly at liquid-liquid interfaces with nanoscale resolution. *Nano Lett.* **16**:5463-5468.

Cross L.L., Ebeed H.T. & Baker A. (2016) Peroxisome biogenesis, protein targeting mechanisms and PEX gene functions in plants. *Biochim. Biophys. Acta-Mol. Cell Res.* **1863**:850-862.

Di Martino E., Tomlinson D.C., Williams S.V. & Knowles M.A. (2016) A place for precision medicine in bladder cancer: Targeting the FGFRs. *Future Oncol.* **12**:2243-2263.

Dobson C.L., Devine P.W.A., Phillips J.J., Higazi D.R., Lloyd C., Popovic B., Arnold J., Buchanan A., Lewis A., Goodman J., *et al.* (2016) Engineering the surface properties of a human monoclonal antibody prevents self-association and rapid clearance *in vivo*. *Sci. Rep.* **6:**38644.

Domingues M.M., Macrae F.L., Duval C., Mcpherson H.R., Bridge K.I., Ajjan R.A., Ridger V.C., Connell S.D., Philippou H. & Ariens R.a.S. (2016) Thrombin and fibrinogen gamma ' impact clot structure by marked effects on intrafibrillar structure and protofibril packing. *Blood* **127**:487-495.

Dondas H.A., Hempshall A., Narramore S., Kilner C., Fishwick C.W.G. & Grigg R. (2016) Gamma-carboline AC190 analogues via palladium catalysed allene insertion stereo and regioselective 3-and 5-component cascades. *Tetrahedron* **72**:1316-1329.

Fascione M.A., Brabham R. & Turnbull W.B. (2016) Mechanistic investigations into the application of sulfoxides in carbohydrate synthesis. *Chem.-Eur. J.* **22**:3916-3928.

Fearnley G.W., Smith G.A., Abdul-Zani I., Yuldasheva N., Mughal N.A., Homer-Vanniasinkam S., Kearney M.T., Zachary I.C., Tomlinson D.C., Harrison M.A., *et al.* (2016) VEGF-A isoforms program differential VEGFR2 signal transduction, trafficking and proteolysis. *Biol. Open* **5**:571-583.

Firth J.D., Craven P.G.E., Lilburn M., Pahl A., Marsden S.P. & Nelson A. (2016) A biosynthesis-inspired approach to over twenty diverse natural product-like scaffolds. *Chem. Commun.* **52**:9837-9840.

Foley D.J., Nelson A. & Marsden S.P. (2016) Evaluating new chemistry to drive molecular discovery: Fit for purpose? *Angew. Chem.-Int. Edit.* **55**:13650-13657.

Foster R.J., Damion R.A., Baboolal T.G., Smye S.W. & Ries M.E. (2016) A nuclear magnetic resonance study of water in aggrecan solutions. *R. Soc. Open Sci.* **3**:150705.

Fowler J.M., Thorp-Greenwood F.L., Warriner S.L., Willans C.E. & Hardie M.J. (2016) M12l8 metallo-supramolecular cube with cyclotriguaiacylene-type ligand: Spontaneous resolution of cube and its constituent host ligand. *Chem. Commun.* **52**:8699-8702.

Fry A.M., O'Regan L., Montgomery J., Adib R. & Bayliss R. (2016) EML proteins in microtubule regulation and human disease. *Biochem. Soc. Trans.* **44**:1281-1288.

Galloway J.M., Bird S.M., Talbot J.E., Shepley P.M., Bradley R.C., El-Zubir O., Allwood D.A., Leggett G.J., Miles J.J., Staniland S.S.*, et al.* (2016) Nano- and micro-patterning biotemplated magnetic copt arrays. *Nanoscale* **8**:11738-11747.

Garcia-Dorival I., Wu W.N., Armstrong S.D., Barr J.N., Carroll M.W., Hewson R. & Hiscox J.A. (2016) Elucidation of the cellular interactome of Ebola virus nucleoprotein and identification of therapeutic targets. *J. Proteome Res.* **15**:4290-4303.

Gerits E., Blommaert E., Lippell A., O'Neill A.J., Weytjens B., De Maeyer D., Fierro A.C., Marchal K., Marchand A., Chaltin P.*, et al.* (2016) Elucidation of the mode of action of a new antibacterial compound active against *Staphylococcus aureus* and *Pseudomonas aeruginosa*. *PLoS One* **11**:e0155139.

Goldman A., Boije af Gennis G., Xhaard H., Meri S. & Yli-Kauhaluoma J. (2016) Pyrofosfaatti lääketieteessä. *Duodecim* **132**:1111–1117 (In Finnish).

Goode D.K., Obier N., Vijayabaskar M.S., Lie-a-Ling M., Lilly A.J., Hannah R., Lichtinger M., Batta K., Florkowska M., Patel R.*, et al.* (2016) Dynamic gene regulatory networks drive hematopoietic specification and differentiation. *Dev. Cell* **36**:572-587.

Grigg R., Elboray E.E., Akkarasamiyo S., Chuanopparat N., Dondas H.A., Abbas-Temirek H.H., Fishwick C.W.G., Aly M.F., Kongkathip B. & Kongkathip N. (2016) A facile palladium catalysed 3-component cascade route to functionalised isoquinolinones and isoquinolines. *Chem. Commun.* **52**:164-166.

Grison C.M., Miles J.A., Robin S., Wilson A.J. & Aitken D.J. (2016) An -helix-mimicking 12,13-helix: Designed a/b/g-foldamers as selective inhibitors of protein-protein interactions. *Angew. Chem.-Int. Edit.* **55**:11096-11100.

Gruszka D.T., Mendonca C., Paci E., Whelan F., Hawkhead J., Potts J.R. & Clarke J. (2016) Disorder drives cooperative folding in a multidomain protein. *Proc. Natl. Acad. Sci. USA.* **113**:11841-11846.

Gunn A.P., Wong B.X., Johanssen T., Griffith J.C., Masters C.L., Bush A.I., Barnham K.J., Duce J.A. & Cherny R.A. (2016) Amyloid- peptide A3PE-42 induces lipid peroxidation, membrane permeabilization, and calcium influx in neurons. *J. Biol. Chem.* **291**:6134-6145.

Guo Y., Sakonsinsiri C., Nehlmeier I., Fascione M.A., Zhang H.Y., Wang W.L., Pohlmann S.,

Turnbull W.B. & Zhou D.J. (2016) Compact, polyvalent mannose quantum dots as sensitive, ratiometric fret probes for multivalent protein-ligand interactions. *Angew. Chem.-Int. Edit.* **55**:4738-4742.

Gupta A., Monteferrante C., Rasina D., Leitis G., Randall C.P., Tomlinson J.H., Jirgensons A., Goessens W.H.F., Hays J.P. & O'Neill A.J. (2016) A polymorphism in leuS confers reduced susceptibility to GSK2251052 in a clinical isolate of *Staphylococcus aureus*. *Antimicrob. Agents Chemother.* **60**:3219-3221.

Harrison P.L., Heath G.R., Johnson B.R.G., Abdel-Rahman M.A., Strong P.N., Evans S.D. & Miller K. (2016) Phospholipid dependent mechanism of smp24, an alpha-helical antimicrobial peptide from scorpion venom. *Biochim. Biophys. Acta-Biomembr.* **1858**:2737-2744.

Harvie A.J., Booth M., Chantry R.L., Hondow N., Kepaptsoglou D.M., Ramasse Q.M., Evans S.D. & Critchley K. (2016) Observation of compositional domains within individual copper indium sulfide quantum dots. *Nanoscale* **8**:16157-16161.

Hauser J.R., Beard H.A., Bayana M.E., Jolley K.E., Warriner S.L. & Bon R.S. (2016) Economical and scalable synthesis of 6-amino-2-cyanobenzothiazole. *Beilstein J. Org. Chem.* **12**:2019-2025.

Hayes J., Thygesen H., Gregory W., Westhead D.R., French P.J., Van Den Bent M.J., Lawler S.E. & Short S.C. (2016) A validated microRNA profile with predictive potential in glioblastoma patients treated with bevacizumab. *Mol. Oncol.* **10**:1296-1304.

Haywood N.J., Wolny M., Rogers B., Trinh C.H., Yu S.P., Edwards T.A. & Peckham M. (2016) Hypertrophic cardiomyopathy mutations in the calponin-homology domain of ACTN2 affect actin binding and cardiomyocyte Z-disc incorporation. *Biochem. J.* **473**:2485-2493.

Heath G.R., Li M., Polignano I.L., Richens J.L., Catucci G., O'Shea P., Sadeghi S.J., Gilardi G., Butt J.N. & Jeuken L.J.C. (2016) Layer-by-layer assembly of supported lipid bilayer poly-L-lysine multilayers. *Biomacromolecules* **17**:324-335.

Herod M.R., Ferrer-Orta C., Loundras E.A., Ward J.C., Verdaguer N., Rowlands D.J. & Stonehouse N.J. (2016) Both *cis* and *trans* activities of Foot-and-Mouth disease virus 3D polymerase are essential for viral RNA replication. *J. Virol.* **90**:6864-6883.

Hewitt S.H. & Wilson A.J. (2016) Metal complexes as "protein surface mimetics". *Chem. Commun.* **52**:9745-9756.

Horne J.E. & Radford S.E. (2016) A growing toolbox of techniques for studying b-barrel outer membrane protein folding and biogenesis. *Biochem. Soc. Trans.* **44**:802-809.

Hover S., King B., Hall B., Loundras E.A., Taqi H., Daly J., Dallas M., Peers C., Schnettler E., Mckimmie C., *et al.* (2016) Modulation of potassium channels inhibits bunyavirus infection. *J. Biol. Chem.* **291**:3411-3422.

Howard J.K., Muller M., Berry A. & Nelson A. (2016) An enantio- and diastereoselective chemoenzymatic synthesis of a-fluoro b-hydroxy carboxylic esters. *Angew. Chem.-Int. Edit.* **55**:6766-6769.

Hughes M.L. & Dougan L. (2016) The physics of pulling polyproteins: A review of single molecule force spectroscopy using the AFM to study protein unfolding. *Rep. Prog. Phys.* **79**:076601.

Hurdiss D.L., Morgan E.L., Thompson R.F., Prescott E.L., Panou M.M., Macdonald A. & Ranson N.A. (2016) New structural insights into the genome and minor capsid proteins of BK polyomavirus using cryo-electron microscopy. *Structure* **24**:528-536.

Hussain R., Harding S.E., Hughes C.S., Ma P., Patching S.G., Edara S., Siligardi G., Henderson P.J.F. & Phillips-Jones M.K. (2016) Purification of bacterial membrane sensor kinases and biophysical methods for determination of their ligand and inhibitor interactions. *Biochem. Soc. Trans.* **44**:810-823.

Huynh N.T., Hesketh E.L., Saxena P., Meshcheriakova Y., Ku Y.C., Hoang L.T., Johnson J.E., Ranson N.A., Lomonossoff G.P. & Reddy V.S. (2016) Crystal structure and proteomics analysis of empty virus-like particles of cowpea mosaic virus. *Structure* **24**:567-575.

Iadanza M.G., Higgins A.J., Schiffrin B., Calabrese A.N., Brockwell D.J., Ashcroft A.E., Radford S.E. & Ranson N.A. (2016) Lateral opening in the intact b-barrel assembly machinery captured by cryo-EM. *Nat. Commun.* **7**:12865.

Iadanza M.G., Jackson M.P., Radford S.E. & Ranson N.A. (2016) Mpul-multi: Software for calculation of amyloid fibril mass per unit length from TB-TEM images. *Sci. Rep.* **6**:21078.

Ivani I., Dans P.D., Noy A., Perez A., Faustino I., Hospital A., Walther J., Andrio P., Goni R., Balaceanu A.*, et al.* (2016) Parmbsc1: A refined force field for DNA simulations. *Nat. Methods* **13**:55-58.

Jackson M.P. & Hewitt E.W. (2016) Cellular proteostasis: degradation of misfolded proteins by lysosomes. *Essays Biochem*. **60**:173-180.

Ji Y.R., Postis V.L.G., Wang Y.Y., Bartlam M. & Goldman A. (2016) Transport mechanism of a glutamate transporter homologue Glt(Ph). *Biochem. Soc. Trans.* **44**:898-904.

Kallus C., Huser J., Jones P.S. & Nelson A.: *The European lead factory*. Edited by Czechtizky W, Hamley P; 2016.

Karamanos T.K., Pashley C.L., Kalverda A.P., Thompson G.S., Mayzel M., Orekhov V.Y. & Radford S.E. (2016) A population shift between sparsely populated folding intermediates determines amyloidogenicity. *J. Am. Chem. Soc.* **138**:6271-6280.

Khan S., Li M.Q., Muench S.P., Jeuken L.J.C. & Beales P.A. (2016) Durable proteo-hybrid vesicles for the extended functional lifetime of membrane proteins in bionanotechnology. *Chem. Commun.* **52**:11020-11023.

Khasnatinov M.A., Tuplin A., Gritsun D.J., Slovak M., Kazimirova M., Lickova M., Havlikova S., Klempa B., Labuda M., Gould E.A.*, et al.* (2016) Tick-borne encephalitis virus structural proteins are the primary viral determinants of non-viraemic transmission between ticks whereas non-structural proteins affect cytotoxicity. *PLoS One* **11**:e0158105.

Kim J.Y., Kinoshita M., Kume S., Hanke G.T., Sugiki T., Ladbury J.E., Kojima C., Ikegami T., Kurisu G., Goto Y.*, et al.* (2016) Non-covalent forces tune the electron transfer complex between ferredoxin and sulfite reductase to optimize enzymatic activity. *Biochem. J.* **473**:3837-3854.

Kong Y.F., Chen J., Fang H.W., Heath G., Wo Y., Wang W.L., Li Y.X., Guo Y., Evans S.D., Chen S.Y.*, et al.* (2016) Highly fluorescent ribonuclease-a-encapsulated lead sulfide quantum dots for ultrasensitive fluorescence *in vivo* imaging in the second near-infrared window. *Chem.*

*Mat.* **28**:3041-3050.

Lambacher N.J., Bruel A.L., Van Dam T.J.P., Szymanska K., Slaats G.G., Kuhns S., McManus G.J., Kennedy J.E., Gaff K., Wu K.M*., et al.* (2016) TMEM107 recruits ciliopathy proteins to subdomains of the ciliary transition zone and causes Joubert syndrome. *Nat. Cell Biol.* **18**:122-131.

Lee C.Y., Reuillard B., Sokol K.P., Laftsoglou T., Lockwood C.W.J., Rowe S.F., Hwang E.T., Fontecilla-Camps J.C., Jeuken L.J.C., Butt J.N*., et al.* (2016) A decahaem cytochrome as an electron conduit in protein-enzyme redox processes. *Chem. Commun.* **52**:7390-7393.

Lee S.C., Knowles T.J., Postis V.L.G., Jamshad M., Parslow R.A., Lin Y.P., Goldman A., Sridhar P., Overduin M., Muench S.P*., et al.* (2016) A method for detergent-free isolation of membrane proteins in their local lipid environment. *Nat. Protoc.* **11**:1149-1162.

Lenton S., Walsh D.L., Rhys N.H., Soper A.K. & Dougan L. (2016) Structural evidence for solvent-stabilisation by aspartic acid as a mechanism for halophilic protein stability in high salt concentrations. *Phys. Chem. Chem. Phys.* **18**:18054-18062.

Li K.M., Wilkinson C., Kellosalo J., Tsai J.Y., Kajander T., Jeuken L.J.C., Sun Y.J. & Goldman A. (2016) Membrane pyrophosphatases from *Thermotoga maritima* and *Vigna radiata* suggest a conserved coupling mechanism. *Nat. Commun.* **7**:13596.

Li S.B., Gong X.Q., Mc Nally C.S., Zeng M.L., Gaule T., Anduix-Canto C., Kulak A.N., Bawazer L.A., McPherson M.J. & Meldrum F.C. (2016) Rapid preparation of highly reliable PDMS double emulsion microfluidic devices. *RSC Adv.* **6**:25927-25933.

Liu L.J., He B.Y., Miles J.A., Wang W.H., Mao Z.F., Che W.I., Lu J.J., Chen X.P., Wilson A.J., Ma D.L*., et al.* (2016) Inhibition of the p53/hDM2 protein-protein interaction by cyclometallated iridium(iii) compounds. *Oncotarget* **7**:13965-13975.

Loundras E.A., Herod M.R., Harris M. & Stonehouse N.J. (2016) Foot-and-Mouth disease virus genome replication is unaffected by inhibition of type iii phosphatidylinositol-4-kinases. *J. Gen. Virol.* **97**:2221-2230.

Ma P., Patching S.G., Ivanova E., Baldwin J.M., Sharpies D., Baldwin S.A. & Henderson P.J.F. (2016) Allantoin transport protein, Pucl, from *Bacillus subtilis*: Evolutionary relationships, amplified expression, activity and specificity. *Microbiology-(UK)* **162**:823-836.

Mankouri J., Walter C., Stewart H., Bentham M., Park W.S., Heo W.D., Fukuda M., Griffin S. & Harris M. (2016) Release of infectious hepatitis c virus from huh7 cells occurs via a trans-golgi network-to-endosome pathway independent of very-low-density lipoprotein secretion. *J. Virol.* **90**:7159-7170.

McLachlan D.H., Lan J., Geilfus C.M., Dodd A.N., Larson T., Baker A., Horak H., Kollist H., He Z.S., Graham I*., et al.* (2016) The breakdown of stored triacylglycerols is required during light-induced stomatal opening. *Curr. Biol.* **26**:707-712.

McLean T.C., Hoskisson P.A. & Seipke R.F. (2016) Coordinate regulation of antimycin and candicidin biosynthesis. *mSphere* **1**:e00305.

McPhillie M., Zhou Y., El Bissati K., Dubey J., Lorenzi H., Capper M., Lukens A., Hickman M., Muench S., Kumar Verma S., *et al*. (2016) New paradigms for understanding and step changes in treating active and chronic, persistent apicomplexan infections. *Sci. Rep.* **6**:29179.

Miles D.E., Mitchell E.A., Kapur N., Beales P.A. & Wilcox R.K. (2016) Peptide: Glycosaminoglycan hybrid hydrogels as an injectable intervention for spinal disc degeneration. *J. Mat. Chem. B* **4**:3225-3231.

Miles J.A., Yeo D.J., Rowell P., Rodriguez-Marin S., Pask C.M., Warriner S.L., Edwards T.A. & Wilson A.J. (2016) Hydrocarbon constrained peptides - understanding pre-organisation and binding affinity. *Chem. Sci.* **7**:3694-3702.

Mitcheson D.F., Bottrill A.R., Carr K., Coxon C.R., Cano C., Golding B.T., Griffin R.J., Fry A.M., Doerig C., Bayliss R.*, et al.* (2016) A new tool for the chemical genetic investigation of the *Plasmodium falciparum* Pfnek-2 NIMA-related kinase. *Malar. J.* **15**:1-12.

Mohl B.P., Bartlett C., Mankouri J. & Harris M. (2016) Early events in the generation of autophagosomes are required for the formation of membrane structures involved in hepatitis c virus genome replication. *J. Gen. Virol.* **97**:680-693.

Morra R., Fessl T., Wang Y.C., Mancini E.J. & Tuma R. (2016) Biophysical characterization of chromatin remodeling protein CHD4. *Methods Mol. Biol.* **1431**:175-193.

Morrison P.M., Balmforth M.R., Ness S.W., Williamson D.J., Rugen M.D., Turnbull W.B. & Webb M.E. (2016) Confirmation of a protein-protein interaction in the pantothenate biosynthetic pathway by using sortase-mediated labelling. *ChemBioChem* **17**:753-758.

Muench S.P. (2016) Single particle cryo-EM, from sample to reconstruction introduction. *Methods* **100**:1-2.

Naylor J., Minard A., Gaunt H.J., Amer M.S., Wilson L.A., Migliore M., Cheung S.Y., Rubaiy H.N., Blythe N.M., Musialowski K.E.*, et al.* (2016) Natural and synthetic flavonoid modulation of TRPC5 channels. *Br. J. Pharmacol.* **173**:562-574.

O'Connor M., Paci E., McIntosh-Smith S. & Glowacki D.R. (2016) Adaptive free energy sampling in multidimensional collective variable space using boxed molecular dynamics. *Faraday Discuss.* **195**:395-419.

Ooi N., Eady E.A., Cove J.H. & O'Neill A.J. (2016) Tert-butyl benzoquinone: Mechanism of biofilm eradication and potential for use as a topical antibiofilm agent. *J. Antimicrob. Chemother.* **71**:1841-1844.

Oram J. & Jeuken L.J.C. (2016) A re-evaluation of electron-transfer mechanisms in microbial electrochemistry: *Shewanella* releases iron that mediates extracellular electron transfer. *ChemElectroChem* **3**:829-835.

O'Sullivan D., Murray B.J., Ross J.F. & Webb M.E. (2016) The adsorption of fungal ice-nucleating proteins on mineral dusts: A terrestrial reservoir of atmospheric ice-nucleating particles. *Atmos. Chem. Phys.* **16**:7879-7887.

Palmer A.J., Baker A. & Muench S.P. (2016) The varied functions of aluminium-activated malate transporters-much more than aluminium resistance. *Biochem. Soc. Trans.* **44**:856-862.

Papachristos K., Muench S.P. & Paci E. (2016) Characterization of the flexibility of the peripheral stalk of prokaryotic rotary A-ATPases by atomistic simulations. *Proteins* **84**:1203-1212.

Parker F., White K., Phillips S. & Peckham M. (2016) Promoting differentiation of cultured

myoblasts using biomimetic surfaces that present alpha-laminin-2 peptides. *Cytotechnology* **68**:2159-2169.

Parmar M.J., Lousa C.D., Muench S.P., Goldman A. & Postis V.L.G. (2016) Artificial membranes for membrane protein purification, functionality and structure studies. *Biochem. Soc. Trans.* **44**:877-882.

Pashley C.L., Hewitt E.W. & Radford S.E. (2016) Comparison of the aggregation of homologous beta(2)-microglobulin variants reveals protein solubility as a key determinant of amyloid formation. *J. Mol. Biol.* **428**:631-643.

Patani H., Bunney T.D., Thiyagarajan N., Norman R.A., Ogg D., Breed J., Ashford P., Potterton A., Edwards M., Williams S.V., *et al.* (2016) Landscape of activating cancer mutations in FGFR kinases and their differential responses to inhibitors in clinical use. *Oncotarget* **7**:24252-24268.

Peckham M. (2016) How myosin organization of the actin cytoskeleton contributes to the cancer phenotype. *Biochem. Soc. Trans.* **44**:1026-1034.

Petrache A.I., Machin D.C., Williamson D.J., Webb M.E. & Beales P.A. (2016) Sortase-mediated labelling of lipid nanodiscs for cellular tracing. *Mol. Biosyst.* **12**:1760-1763.

Peyman S.A., McLaughlan J.R., Abou-Saleh R.H., Marston G., Johnson B.R.G., Freear S., Coletta P.L., Markham A.F. & Evans S.D. (2016) On-chip preparation of nanoscale contrast agents towards high-resolution ultrasound imaging. *Lab Chip* **16**:679-687.

Pouessel D., Neuzillet Y., Mertens L.S., Van Der Heijden M.S., De Jong J., Sanders J., Peters D., Leroy K., Manceau A., Maille P., *et al.* (2016) Tumor heterogeneity of fibroblast growth factor receptor 3 (FGFR3) mutations in invasive bladder cancer: Implications for perioperative anti-FGFR3 treatment. *Ann. Oncol.* **27**:1311-1316.

Poujois A., Devedjian J.C., Moreau C., Devos D., Chaine P., Woimant F. & Duce J.A. (2016) Bioavailable trace metals in neurological diseases. *Curr. Treat. Options Neurol.* **18**:46.

Qi W.J., Baldwin S.A., Muench S.P. & Baker A. (2016) Pi sensing and signalling: from prokaryotic to eukaryotic cells. *Biochem. Soc. Trans.* **44**:766-773.

Radu V., Frielingsdorf S., Lenz O. & Jeuken L.J.C. (2016) Reactivation from the Ni-B state in NiFe hydrogenase of *Ralstonia eutropha* is controlled by reduction of the superoxidised proximal cluster. *Chem. Commun.* **52**:2632-2635.

Rajasekar K.V., Lovering A.L., Dancea F., Scott D.J., Harris S.A., Bingle L.E.H., Roessle M., Thomas C.M., Hyde E.I. & White S.A. (2016) Flexibility of KorA, a plasmid-encoded, global transcription regulator, in the presence and the absence of its operator. *Nucleic Acids Res.* **44**:4947-4956.

Randall C.P., Rasina D., Jirgensons A. & O'Neill A.J. (2016) Targeting multiple aminoacyl-tRNA synthetases overcomes the resistance liabilities associated with antibacterial inhibitors acting on a single such enzyme. *Antimicrob. Agents Chemother.* **60**:6359-6361.

Rawson S., Davies S., Lippiat J.D. & Muench S.P. (2016) The changing landscape of membrane protein structural biology through developments in electron microscopy. *Mol. Membr. Biol.* **33**:12-22.

Rawson S., Harrison M.A. & Muench S.P. (2016) Rotating with the brakes on and other

unresolved features of the vacuolar ATPase. *Biochem. Soc. Trans.* **44**:851-855.

Rawson S., Iadanza M.G., Ranson N.A. & Muench S.P. (2016) Methods to account for movement and flexibility in cryo-EM data processing. *Methods* **100**:35-41.

Rennie Y.K., Mcintyre P.J., Akindele T., Bayliss R. & Jamieson A.G. (2016) A TPX2 proteomimetic has enhanced affinity for Aurora-A due to hydrocarbon stapling of a helix. *ACS Chem. Biol.* **11**:3383-3390.

Richards M.W., Burgess S.G., Poon E., Carstensen A., Eilers M., Chesler L. & Bayliss R. (2016) Structural basis of N-Myc binding by Aurora-A and its destabilization by kinase inhibitors. *Proc. Natl. Acad. Sci. USA.* **113**:13726-13731.

Rolfsson O., Middleton S., Manfield I.W., White S.J., Fan B.C., Vaughan R., Ranson N.A., Dykeman E., Twarock R., Ford J.*, et al.* (2016) Direct evidence for packaging signal-mediated assembly of bacteriophage MS2. *J. Mol. Biol.* **428**:431-448.

Samson A., Bentham M.J., Scott K., Nuovo G., Bloy A., Appleton E., Adair R.A., Dave R., Peckham-Cooper A., Toogood G., Nagamori S., Coffey M., Vile R., Harrington K., Selby P., Errington-Mais F., Melcher A.A. & Griffin S. (2016) Oncolytic viruses as combined anti-viral and anti-tumour agents for the treatment of liver cancer**.** *Gut* **doi:** 10.1136/gutjnl-2016-312009.

Saunders J.C., Young L.M., Mahood R.A., Jackson M.P., Revill C.H., Foster R.J., Smith D.A., Ashcroft A.E., Brockwell D.J. & Radford S.E. (2016) An *in vivo* platform for identifying inhibitors of protein aggregation. *Nat. Chem. Biol.* **12**:94-101.

Saundh B.K., Baker R., Harris M. & Hale A. (2016) A prospective study of renal transplant recipients reveals an absence of primary JC polyomavirus infections. *J. Clin. Virol.* **77**:101-105.

Scarff C.A., Ashcroft A.E. & Radford S.E. (2016) Characterization of amyloid oligomers by electrospray ionization-ion mobility spectrometry-mass spectrometry (ESI-IMS-MS). *Methods Mol. Biol.* 1345:115-132.

Schiffrin B., Calabrese A.N., Devine P.W.A., Harris S.A., Ashcroft A.E., Brockwell D.J. & Radford S.E. (2016) Skp is a multivalent chaperone of outer-membrane proteins. *Nat. Struct. Mol. Biol.* **23**:786-793.

Schumann S., Baquero-Perez B. & Whitehouse A. (2016) Interactions between KSHV ORF57 and the novel human TREX proteins, CHTOP and CIP29. *J. Gen. Virol.* **97**:1904-1910.

Shah N.R., Vidilaseris K., Xhaard H. & Goldman A. (2016) Integral membrane pyrophosphatases: A novel drug target for human pathogens? *AIMS Biophys.* **3**:171-194.

Shar N.A., Vijayabaskar M.S. & Westhead D.R. (2016) Cancer somatic mutations cluster in a subset of regulatory sites predicted from the encode data. *Mol. Cancer* **15**:76.

Sharkey L.K.R., Edwards T.A. & O'Neill A.J. (2016) ABC-F proteins mediate antibiotic resistance through ribosomal protection. *mBio* **7**:e01975-15.

Sharma R., Deacon S.E., Nowak D., George S.E., Szymonik M.P., Tang A.a.S., Tomlinson D.C., Davies A.G., McPherson M.J. & Walti C. (2016) Label-free electrochemical impedance biosensor to detect human interleukin-8 in serum with sub-pg/ml sensitivity. *Biosens. Bioelectron.* **80**:607-613.

Smith G.A., Fearnley G.W., Abdul-Zani I., Wheatcroft S.B., Tomlinson D.C., Harrison M.A. & Ponnambalam S. (2016) VEGFR2 trafficking, signaling and proteolysis is regulated by the ubiquitin isopeptidase USP8. *Traffic* **17**:53-65.

Smith G.A., Howell G.J., Phillips C., Muench S.P., Ponnambalam S. & Harrison M.A. (2016) Extracellular and luminal pH regulation by vacuolar $H^+$-ATPase isoform expression and targeting to the plasma membrane and endosomes. *J. Biol. Chem.* **291**:8500-8515.

Smith G.A., Tomlinson D.C., Harrison M.A. & Ponnambalam S. (2016) Ubiquitin-mediated regulation of cellular responses to vascular endothelial growth factors. *Prog. Mol. Biol. Transl. Sci.* **141**:313-338.

Stevenson S.R., Kamisugi Y., Trinh C.H., Schmutz J., Jenkins J.W., Grimwood J., Muchero W., Tuskan G.A., Rensing S.A., Lang D.*, et al.* (2016) Genetic analysis of *Physcomitrella patens* identifies abscisic acid non-responsive, a regulator of ABA responses unique to basal land plants and required for desiccation tolerance. *Plant Cell* **28**:1310-1327.

Stewart H., Bingham R.J., White S.J., Dykeman E.C., Zothner C., Tuplin A.K., Stockley P.G., Twarock R. & Harris M. (2016) Identification of novel RNA secondary structures within the hepatitis C virus genome reveals a cooperative involvement in genome packaging. *Sci. Rep.* **6**:22952.

Stewart K.L., Hughes E., Yates E.A., Akien G.R., Huang T.Y., Lima M.A., Rudd T.R., Guerrini M., Hung S.C., Radford S.E.*, et al.* (2016) Atomic details of the interactions of glycosaminoglycans with amyloid-beta fibrils. *J. Am. Chem. Soc.* **138**:8328-8331.

Stockwell J., Daniels A.D., Windle C.L., Harman T.A., Woodhall T., Lebl T., Trinh C.H., Mulholland K., Pearson A.R., Berry A.*, et al.* (2016) Evaluation of fluoropyruvate as nucleophile in reactions catalysed by N-acetyl neuraminic acid lyase variants: Scope, limitations and stereoselectivity. *Org. Biomol. Chem.* **14**:105-112.

Stull F., Koldewey P., Humes J.R., Radford S.E. & Bardwell J.C.A. (2016) Substrate protein folds while it is bound to the ATP-independent chaperone Spy. *Nat. Struct. Mol. Biol.* **23**:53-58.

Surtees R., Dowall S.D., Shaw A., Armstrong S., Hewson R., Carroll M.W., Mankouri J., Edwards T.A., Hiscox J.A. & Barr J.N. (2016) Heat shock protein 70 family members interact with Crimean-Congo hemorrhagic fever virus and Hazara virus nucleocapsid proteins and perform a functional role in the nairovirus replication cycle. *J. Virol.* **90**:9305-9316.

Sutthibutpong T., Matek C., Benham C., Slade G.G., Noy A., Laughton C., Doye J.P.K., Louis A.A. & Harris S.A. (2016) Long-range correlations in the mechanics of small DNA circles under topological stress revealed by multi-scale simulation. *Nucleic Acids Res.* **44**:9121-9130.

Theodoulou F.L., Carrier D.J., Schaedler T.A., Baldwin S.A. & Baker A. (2016) How to move an amphipathic molecule across a lipid bilayer: Different mechanisms for different ABC transporters? *Biochem. Soc. Trans.* **44**:774-782.

Thompson R.F., Walker M., Siebert C.A., Muench S.P. & Ranson N.A. (2016) An introduction to sample preparation and imaging by cryo-electron microscopy for structural biology. *Methods* **100**:3-15.

Timsah Z., Ahmed Z., Ivan C., Berrout J., Gagea M., Zhou Y., Pena G.N.A., Hu X., Vallien C., Kingsley C.V.*, et al.* (2016) Grb2 depletion under non-stimulated conditions inhibits PTEN,

promotes Akt-induced tumor formation and contributes to poor prognosis in ovarian cancer. *Oncogene* **35**:2186-2196.

Tomlinson J.H., Thompson G.S., Kalverda A.P., Zhuravleva A. & O'Neill A.J. (2016) A target-protection mechanism of antibiotic resistance at atomic resolution: Insights into FusB-type fusidic acid resistance. *Sci. Rep.* **6:**19524.

Towey J.J., Soper A.K. & Dougan L. (2016) Low-density water structure observed in a nanosegregated cryoprotectant solution at low temperatures from 285 to 238 K. *J. Phys. Chem. B* **120**:4439-4448.

Tych K.M., Batchelor M., Hoffmann T., Wilson M.C., Hughes M.L., Paci E., Brockwell D.J. & Dougan L. (2016) Differential effects of hydrophobic core packing residues for thermodynamic and mechanical stability of a hyperthermophilic protein. *Langmuir* **32**:7392-7402.

Tych K.M., Batchelor M., Hoffmann T., Wilson M.C., Paci E., Brockwell D.J. & Dougan L. (2016) Tuning protein mechanics through an ionic cluster graft from an extremophilic protein. *Soft Matter* **12**:2688-2699.

Vandelinder V., Adams P.G. & Bachand G.D. (2016) Mechanical splitting of microtubules into protofilament bundles by surface-bound kinesin-1. *Sci. Rep.* **6:**39408.

Vo U., Vajpai N., Flavell L., Bobby R., Breeze A.L., Embrey K.J. & Golovanov A.P. (2016) Monitoring ras interactions with the nucleotide exchange factor son of sevenless (sos) using site-specific NMR reporter signals and intrinsic fluorescence. *J. Biol. Chem.* **291**:1703-1718.

Walter S., Bollenbach A., Doerrbecker J., Pfaender S., Brown R.J.P., Vieyres G., Scott C., Foster R., Kumar A., Zitzmann N.*, et al.* (2016) Ion channel function and cross-species determinants in viral assembly of nonprimate hepacivirus p7. *J. Virol.* **90**:5075-5089.

Wang J.N., Wang F.H., Li F.Z., Zhang W.J., Shen Y.Y., Zhou D.J. & Guo S.R. (2016) A multifunctional poly(curcumin) nanomedicine for dual-modal targeted delivery, intracellular responsive release, dual-drug treatment and imaging of multidrug resistant cancer cells. *J. Mat. Chem. B* **4**:2954-2962.

Wang Y., Guo Y., Shen Y.Y., Chen R.J., Wang F.H., Zhou D.J. & Guo S.R. (2016) HCl-retarded gold nanorod growth for aspect ratio and shape tuning. *J. Nanosci. Nanotechnol.* **16**:1194-1201.

Watson M.R., Lin Y.F., Hollwey E., Dodds R.E., Meyer P. & McDowall K.J. (2016) An improved binary vector and *Escherichia coli* strain for *Agrobacterium tumefaciens*-mediated plant transformation. *G3-Genes Genomes Genet.* **6**:2195-2201.

Whyte C.S., Chernysh I.N., Domingues M.M., Connell S., Weisel J.W., Ariens R.a.S. & Mutch N.J. (2016) Polyphosphate delays fibrin polymerisation and alters the mechanical properties of the fibrin network. *Thromb. Haemost.* **116**:897-903.

Wiebalck S., Kozuch J., Forbrig E., Tzschucke C.C., Jeuken L.J.C. & Hildebrandt P. (2016) Monitoring the transmembrane proton gradient generated by cytochrome $bo_3$ in tethered bilayer lipid membranes using SEIRA spectroscopy. *J. Phys. Chem. B* **120**:2249-2256.

Wilson A.J. & Gunning P.T. (2016) Understanding protein-protein interactions: Essential players in (patho)physiology (part1). *ChemBioChem* **17**:644-645.

Wilson A.J. & Gunning P.T. (2016) Understanding protein-protein interactions: Essential

players in (patho)physiology (part2). *ChemMedChem* **11**:732-733.

Wood J.J., Boyne J.R., Paulus C., Jackson B.R., Nevels M.M., Whitehouse A. & Hughes D.J. (2016) ARID3B: A novel regulator of the Kaposi's sarcoma-associated herpesvirus lytic cycle. *J. Virol.* **90**:9543-9555.

Ye S.J., Benz F., Wheeler M.C., Oram J., Baumberg J.J., Cespedes O., Christenson H.K., Coletta P.L., Jeuken L.J.C., Markham A.F.*, et al.* (2016) One-step fabrication of hollow-channel gold nanoflowers with excellent catalytic performance and large single-particle SERS activity. *Nanoscale* **8**:14932-14942.

Young L.M., Saunders J.C., Mahood R.A., Revill C.H., Foster R.J., Ashcroft A.E. & Radford S.E. (2016) ESI-IMS-MS: A method for rapid analysis of protein aggregation and its inhibition by small molecules. *Methods* **95**:62-69.

**The Astbury Centre for**
**Structural Molecular Biology**
University of Leeds
Leeds
LS2 9JT
Tel: 0113 343 3086
astbury@leeds.ac.uk
www.astbury.leeds.ac.uk

**UNIVERSITY OF LEEDS**
University of Leeds
Leeds, United Kingdom
LS2 9JT
Tel: 0113 243 1751
www.leeds.ac.uk